UNIVERSITÀ DEGLI STUDI
DI MODENA E REGGIO EMILIA

Department of Biomedical, Metabolic and Neural Sciences
PhD course in Neuroscience
XXXV Cycle

Brain Morphometry in Temporal Lobe Epilepsy: cortical and subcortical patterns of atrophy and connectivity

Candidate: Alice Ballerini

Supervisor: Prof. Stefano Meletti

Co-supervisor: Dr. Anna Elisabetta Vaudano
Dr. Carrie R. McDonald

Director: Prof. Sandro Rubichi

Abstract

Temporal Lobe Epilepsy (TLE) is the most common form of focal epilepsy. It is recognized as a network disease, involving subcortical volume loss, cortical atrophy, and loss of white matter integrity. When the seizure focus involves the medial temporal lobe structures, we refer to medial temporal lobe epilepsy (MTLE). The commonest MTLE is characterized by a hippocampal volume loss called hippocampal sclerosis (HS). Electroencephalography (EEG) is certainly the most widely used tool for diagnosing epilepsy. However, neuroimaging is also essential for detecting structural, functional, or metabolic abnormalities.

The aims of this doctoral thesis are to explore different structural patterns underlying TLE, with regarding to different etiologies. To explore the structural alteration in TLE we adopted a subfield of morphometry and brain sciences called "brain morphometry". This methodology concerns with the measurement of brain structures and changes of these during development, aging, learning, disease, and evolution. It mainly uses structural neuroimaging data: T_1-weighted sequences and diffusion-weighted sequences and allows to quantify many anatomical features of the brain, like grey matter cortical thickness, cortical and subcortical volumes, and white matter connectivity. The thesis is articulated in two main sections: the first section (i.e., chapter 2 and 3) is focused on the exploration of the subcortical structures involved in TLE, in the second part (i.e., chapter 4) we seek to determine the different biological processes underlying cortical grey and white matter injury in TLE.

Thus, our first studies have been focused on the role of the amygdala and its nuclei in different types of TLE. Recently, an increase in amygdala volumes (i.e., amygdala enlargement) has been proposed as morphological biomarker of a subtype of TLE patients without MRI lesions and/or alteration on clinical diagnostic imaging exams. However, previous studies treated the amygdala as a single entity, while instead it is composed by different nuclei, each with peculiar function and connection. Hence, a first study was conducted on a well-selected TLE population with a symptomatic hippocampal sclerosis and with non-lesional TLE, to explore the different features of amygdala substructures, and map specific amygdala nuclei structural changes in patients with or without lesions detected by the MRI scans. To our knowledge, this was the first study on amygdalae substructures in a TLE population. Lately, we explored the role of the amygdala and its substructures in TLE patients with Ictal Central Apnea (ICA) manifestations. ICAs has been recently considered a localizing sign in

TLE and we hypnotized a possible amygdala involvement in the epileptogenic network of these patients.

The second part of this doctoral thesis has been conducted in collaboration with Dr. McDonald's lab at the University of California, San Diego (UCSD). This study aims to extend our knowledge about the processes underlying grey and white matter atrophy in TLE patients. There is evidence that cortical atrophy and white matter injury follow different spatial patterns in TLE, thus, we examined the patterns of subcortical and cortical grey matter atrophy and the white matter microstructural damage, and we tried to characterize how these pathologies spatially correlate across tissue type. Finally, we explore how these relationships vary across different ages of seizures onset.

In summary, this thesis aims to investigate brain morphometry changes in TLE compared to healthy controls. Particularly, most of our research had been focused on the different etiologies characterized TLE and the potential clinical yields of the structural changes across disease classifications.

List of scientific papers

This doctoral thesis is based on the five scientific papers listed below.

1. **Amygdala subnuclear volumes in temporal lobe epilepsy with hippocampal sclerosis and in non-lesional patients**
   Ballerini A, Tondelli M, Talami F, Molinari MA, Micalizzi E, Giovannini G, Turchi G, Malagoli M, Genovese M, Meletti S, Vaudano AE
   In *Brain Communications* 2022, 4(5): fcac225.
2. **Ictal apnea: A prospective monocentric study in patients with epilepsy**
   Micalizzi E, Vaudano AE, Ballerini A, Talami F, Giovannini G, Turchi G, Cioclu MC, Giunta L, Meletti S
   In *European Journal of Neurology* 2022, 29(12): 3701-3710.
3. **The role of the amygdala in Ictal Central Apnea: insights from brain MRI structural morphometry**
   Micalizzi E, Ballerini A, Giovannini G, Cioclu MC, Scolastico S, Pugnaghi M, Orlandi N, Malagoli M, Genovese M, Todeschini A, Giunta L, Villani F, Meletti S, Vaudano AE
   Under review in *Neurology*
4. **Spatial patterns of gray and white matter compromise relate to age of seizure onset in temporal lobe epilepsy**
   Ballerini A, Arienzo D, Stasenko A, Schadler A, Vaudano AE, Meletti S, Kaestner E, McDonald CR
   Under review in *NeuroImage: Clinical*
5. **Evaluation of the recommended HARNESS-MRI protocol for focal epilepsy: a monocentric prospective study**
   Vaudano AE, Ballerini A, Zucchini F, Micalizzi E, Scolastico S, Talami F, Giovannini G, Pugnaghi M, Orlandi N, Biagioli N, Cioclu MC, Vallone S, Genovese M, Todeschini A, Cavalleri F, Malagoli M, Meletti S
   In *Epileptic Disorders* 2023, 00: 1-12.

Other scientific contributes

ENIGMA-Epilepsy

Our group is part of the **ENIGMA-Epilepsy Consortium**, an international worldwide effort to brings together researchers all over the world to improving our understanding of in vivo neuroanatomical networks in people with epilepsy compared to healthy individuals.

List of ENIGMA-Epilepsy scientific paper

- **Cerebellar grey and white matter volume alterations across epilepsy syndromes: an ENIGMA-Epilepsy study**

  Kerestes R, Perry A, Vivash L, O'Brien TJ, Bargalló N, Arienzo D, Aventurato I, Ballerini A, João RB, Ferri Baltazar G, Bender B, Brioschi R, Bürkle E, Caligiuri ME, Cendes F, de Tisi J, Ives-Deliperi V, Duncan JS, Engelle Jr JP, Foley S, Fortunato F, Fried I, Gambardella A, Giacomini T, Hall G, Keller SS, Khalid KH, Kleiser B, Alvim MKM, Labate A, Lenge M, Guerrini R, Marotta C, Martin P, Mascalchi M, Meletti S, Owens-Walton C, Pascual-Diaz S, Parodi CB, Powell D, Rebsamen M, Reiter J, Riva A, Rüber T, Rummel C, Salamon N, Silva LS, Scheffler F, Severino M, Staba RJ, Striano P, Taylor PN, Thomopoulos SI, Thompson PM, Tortora D, Vaudano AE, Weber B, Wiest R, Winston GP, Yasuda CL, Zheng H, McDonald CR, Sisodiya SM and Harding IH for the ENIGMA-Epilepsy working group

  Under review in *Neurology*

ENIGMA-Epilepsy Secondary Proposals

We recently submitted a secondary proposal to the working group entitled: **"Examining the spatial concordance of grey and white matter patterns across epilepsy syndromes"**. This proposal is in collaboration with Dr. McDonald from University of California, San Diego. Our aims are to evaluate the spatial correspondence between cortical thinning and alteration in superficial white matter in patients with different epilepsy syndromes at the whole brain level.

Conference contributions

- *The role of amygdala subnuclei in cognitive performances of patients with temporal lobe epilepsy*
  Ballerini A, Tondelli M, Talami F, Molinari MA, Giovannini G, Turchi G, Meletti S, Vaudano AE
  Presented as poster at 34th International Epilepsy Congress (2021)
- *Il ruolo dei sotto-nuclei dell'amigdala nelle performance cognitive di pazienti con epilessia del lobo temporale*
  Ballerini A, Tondelli M, Talami F, Molinari MA, Giovannini G, Turchi G, Meletti S, Vaudano AE
  Presented as poster at 44th Italian ILAE Chapter, LICE National Congress (2021)
- *Distinct Spatial Patterns of Cortical Atrophy and White Matter Compromise Associated with Temporal Lobe Epilepsy*
  Ballerini A, Arienzo D, Vaudano AE, Stasenko A, Schadler A, McDonald CR, Kaestner E
  Presented as poster and oral communication at American Epilepsy Society (2022)

Table of Contents

Chapter 1

Introduction

Epilepsy is a neurological disorder, including many different syndromes and conditions, that affects 0.6-1.5% of the worldwide population (G. S. Bell et al., 2014). It has been defined as a *"brain disorder characterized predominantly by recurrent and unpredictable interruptions of normal brain function, the epileptic seizures"* (Fisher et al., 2005). Epilepsy is not a singular disease entity but a variety of disorders reflecting underlying brain dysfunction that may result from many different causes (Fisher et al., 2005). The epilepsy classification has been subjected to continuous revisions and changes over the past years, in 2017 the International League Against Epilepsy (ILAE) proposed a new classification of epilepsies as a multilevel classification (**Fig. 1.1**), designed to classify epilepsy in different clinical environments (Scheffer et al., 2017).

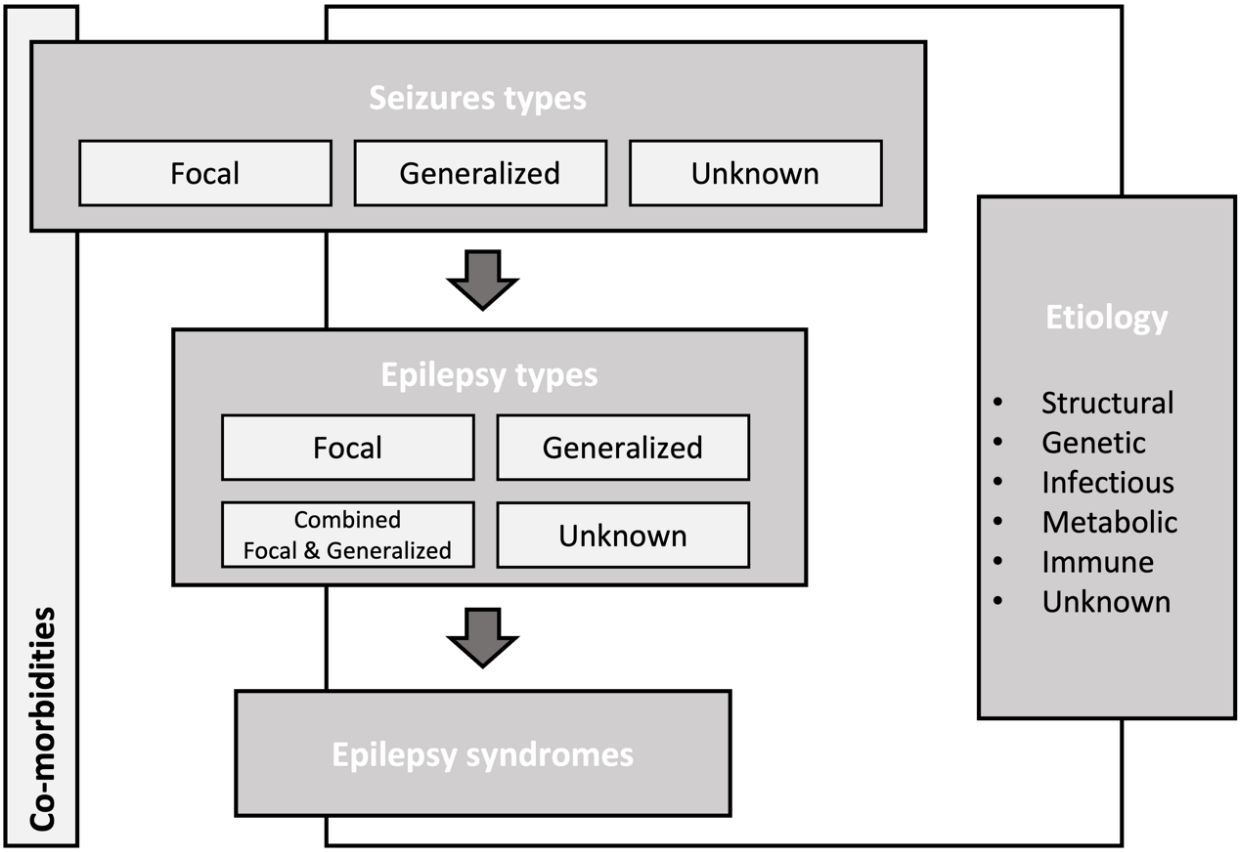

Figure 1.1. ILAE epilepsies' classification from Scheffer et al., 2017.

Seizure has been defined as *"a transient occurrence of signs and/or symptoms due to abnormal excessive or synchronous neuronal activity in the brain"* (Fisher et al., 2005), and it could have a focal onset, a generalized onset, or an unknown onset (**Fig. 1.2**). Focal seizures are the most common type of seizure, accounting for up to 60% of the incident and prevalent epilepsy cases (Wiebe, 2000). Focal epilepsy is characterized by the onset within a neural network limited to a hemisphere. However, it may spread to other areas of the brain, and sometimes it can evolve into bilateral tonic-clonic seizure (GTC). Focal seizures can be further divided into non-impaired or impaired awareness. In the first form, the person is fully aware of what is happening around them but may not be able to talk or respond to stimuli. When the focal seizure is characterized by impaired awareness, the person may appear confused, vague, and/or disorientated. Generalized onset means that the seizure affects the whole brain, thus both hemispheres are involved. This type of seizure usually affects awareness in some way; therefore, the patient may lose consciousness at the start of the seizure. It can be classified as motor or non-motor seizure (i.e., absence).

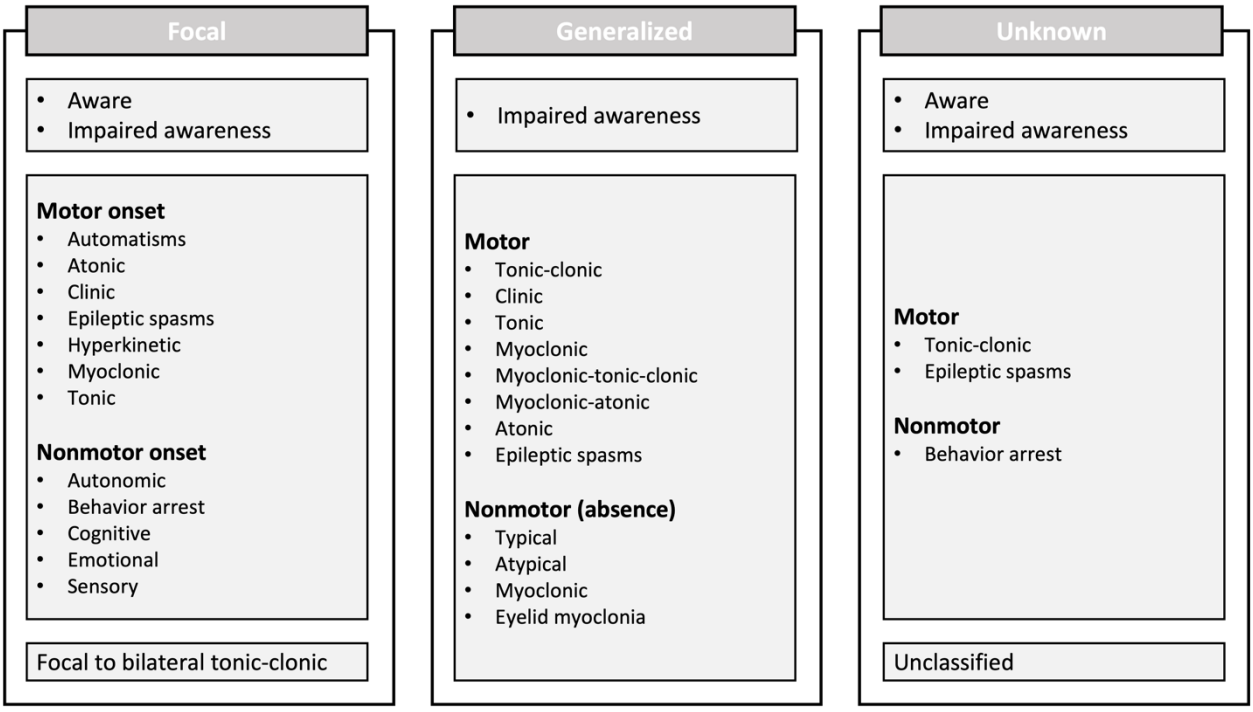

Figure 1.2. ILAE seizures' classification from Scheffer et al., 2017.

The EEG is certainly the most wide test used for diagnosing epilepsy, it helps determine seizure type and epilepsy syndrome, and thereby choice of antiepileptic medication and prediction of

prognosis (S. Smith, 2005). Interictal Epileptiform Discharges (IEDs) are typically EEG patterns commonly found in patients with epilepsy (Engel, 1984; Pillai & Sperling, 2006; Hoppe et al., 2009; Tatum et al., 2018). Most epileptic patients show characteristic IEDs termed spike (<70 μsec duration), spike and wave, or sharp-wave (70–200 μsec duration) discharges (St. Louis & Frey, 2016) (**Fig. 1.3A**). EEG findings contribute to the multi-axial diagnosis of epilepsy, in terms of whether the seizure disorder is focal or generalized (S. Smith, 2005). With respect to focal epilepsies, the EEG typically shows localized epileptiform abnormalities in specific electrodes on the scalps corresponding to definite brain regions (**Fig. 1.3B**). The characteristic morphology of a focal IED is a very sharp rise time, a complex waveform often with several phases or baseline crossings, and an after-going slow wave discharge that disturbs or disrupts the continuity of the background rhythm at least momentarily (St. Louis & Frey, 2016). Generalized epilepsies' EEG typically shows generalized spike-wave or polyspike discharges, polyspikewave discharges, or both (St. Louis & Frey, 2016) all over the brain (**Fig. 1.3C**).

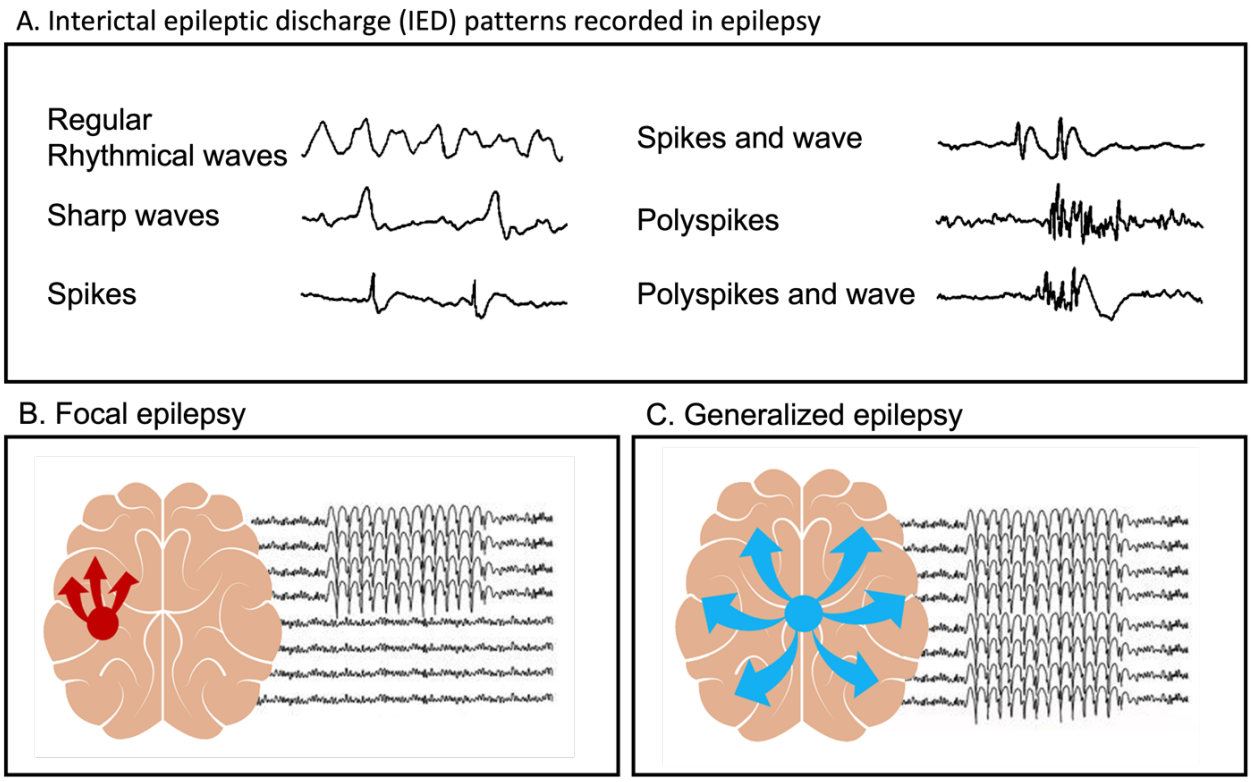

Figure 1.3. Panel A shows the different pattern of IEDs frequently common in epilepsy. Panel B and Panel C represents respectively an EEG pattern in focal and generalized epilepsies.

Despite the central role of the EEG methodology to diagnose epilepsy, neuroimaging methodologies are also essential for detecting the different etiologies that cause epilepsy disease. Ideally, the MRI is the first investigation carried out that allows the clinician to decide if there is a structural etiology (Scheffer et al., 2017). When epilepsy is due to structural causes it means that is due to acquired factors, like cortical and/or subcortical lesions, cerebrovascular events, and tumors. However, there are many other reasons why people could develop epilepsy, like chromosomal or genetic abnormalities, infections, and metabolic or immune disorders as well. Some patients suffer from a kind of epilepsy with no obvious cause, in those cases there are no brain lesions, genetic abnormalities, or other causes. In epilepsy, a structural etiology refers to abnormalities visible on structural neuroimaging, and its identification requires appropriate MRI protocols (Gaillard et al., 2009; Bernasconi et al., 2019). In 2019, the ILAE's Neuroimaging Task Force published the official recommendation of structural MRI for epilepsy, the "Harmonized neuroimaging of epilepsy structural sequences – HARNESS" (Bernasconi et al., 2019). The following sequences were recommended as the minimum required protocol: (I) 3D millimetric T_1-weighted images, (II) 3D millimetric fluid-attenuated inversion recovery (FLAIR) images, and (III) 2D sub-millimetric coronal T_2-weighted images acquired perpendicular to the long axis of the hippocampus (**Fig. 1.4**). The HARNESS protocol has been developed with the idea to standardize the best-practice neuroimaging of epilepsy in outpatient clinics and specialized surgery centers. Technical differences in MRI acquisition protocol (e.g., slice thickness, interslice gaps) could indeed potentially impact the lesions' detection (Friedman, 2014; von Oertzen, 2002; Wellmer et al., 2013). So far, the diagnostic yield of the HARNESS protocol has been verified mostly throughout the single case descriptions (Clavijo Prado et al., 2022; Federico et al., 2020; Larivière, Federico, et al., 2021) while prospective studies on a larger cohort of patients are missed.

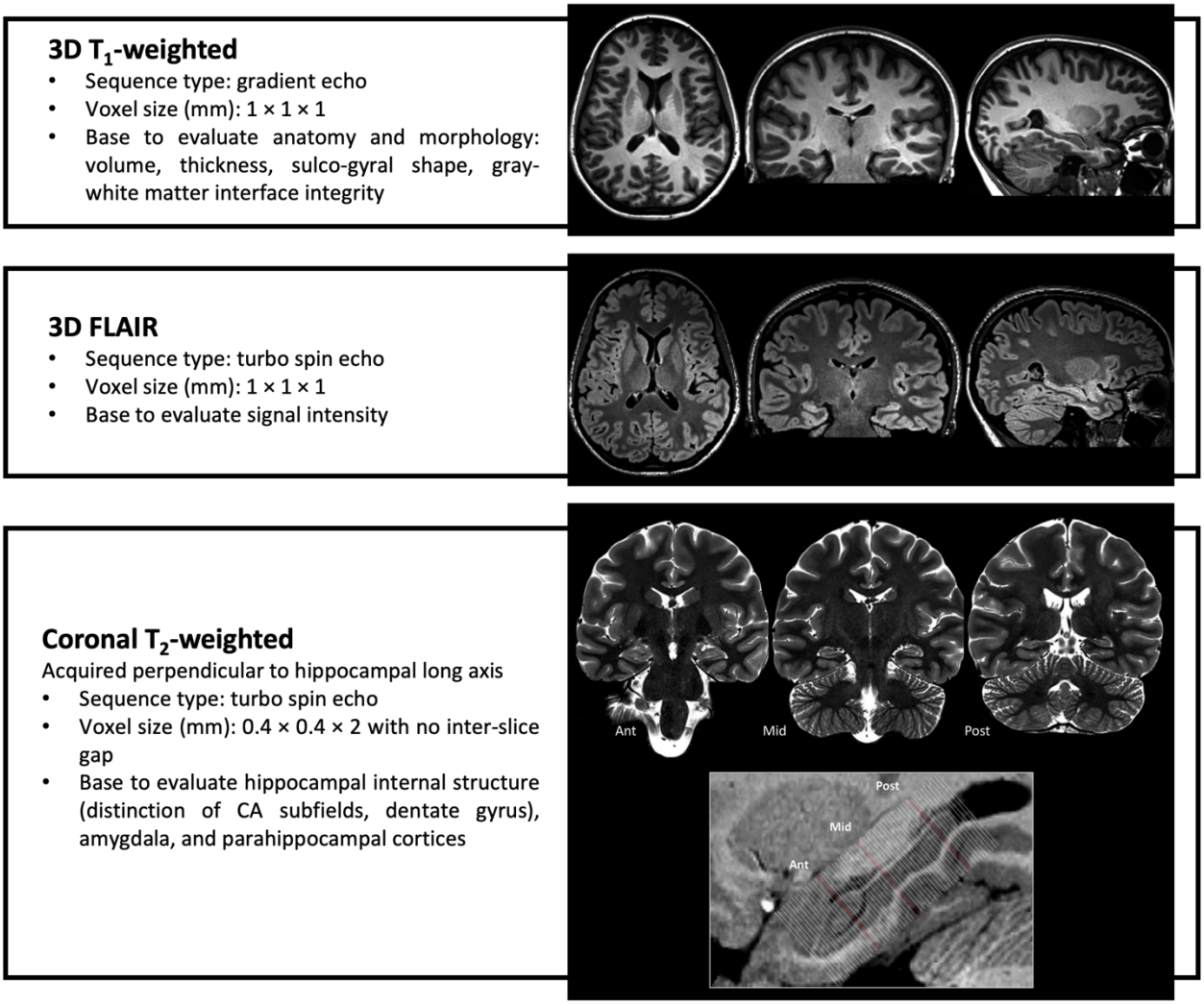

Figure 1.4. HARNESS-MRI (Harmonized Neuroimaging of Epilepsy Structural Sequences) protocol proposed by Bernasconi and colleagues, from the ILAE's Neuroimaging Task Force in 2019.

In a recent study from our laboratory (Vaudano et al., 2023), we aimed to fill this gap by assessing the clinical utility of the HARNESS protocol in a prospective cohort of patients with focal epilepsy who underwent a structural MRI for diagnostic purposes between 2020-2021 at Baggiovara Hospital (Modena, Italy). Our aim was to investigate whether the adoption of this standardized and optimized protocol, together with relevant clinical information, would increase the detection of epileptogenic lesions thus improving the clinical management of patients with focal epilepsy enrolled in a presurgical evaluation process. By comparing the radiological outcome of the MRI acquired with the HARNESS protocol versus the ones without in the same patients, we demonstrated a significant increase in focal cortical dysplasia (FCD) diagnosis when the protocol was adopted. Our results while supporting previous observations that a dedicated MRI protocol significantly improves the diagnosis

of focal epilepsy (Rados et al., 2022), expand the available knowledge, and show that it might be particularly helpful for the search for FCD. The increase in FCD detection seems independent of the neuroradiologists' expertise and the scanner's field strength. Considering the feasibility and short time of imaging acquisition of the core sequences of the HARNESS protocol, the findings of the present study are important for patients being assessed for epilepsy surgery even in resource-poor locations where access to MRI scanners is limited.

1.1. Temporal Lobe Epilepsy

Temporal lobe epilepsy (TLE) is the most common type of focal epilepsy (Wiebe, 2000). TLE refers to a syndrome that encompasses all epilepsy with seizures arising anywhere in the temporal lobe, irrespective of the location or the pathology. However, is important to distinguish the seizures that originate from the neocortex from those that onset from the medial temporal structures. We call lateral TLE (LTLE) the TLE that has its onset in the temporal cortex. LTLE accounts only for about 10% of all TLEs (Michelucci et al., 2009) and is distinguished from medial temporal lobe epilepsies (MTLEs) especially because of its specific seizure characteristic, including auditory auras, aphasic seizures, and the propensity to generalize (Florindo et al., 2006). Seizures arising in the mesial temporal structures determine what is called MTLE, the structures involved are the hippocampus, the amygdala, the entorhinal cortex, and the parahippocampal cortex (Querol Pascual, 2007). The clinical features reported by patients with MTLE are epigastric or substernal rising sensation, or a sensation that is difficult to describe, sudden fear or anxiety, a sense of familiarity, autonomic symptoms, and – less often – olfactory or gustatory sensations (Thom & Bertram, 2012). Auras are not experienced by all patients, however, with or without alteration of awareness there is typically a behavior arrest. The automatisms seen mostly are oral, with lip smacking or chewing. Motor symptoms and convulsions are uncommon, especially in those patients who respond to anti-seizures medications (Thom & Bertram, 2012). MTLE is the most common form of TLE, however, it's not a single disorder but a collection of different syndromes with variations in pathology and etiology although with a likely common feature of involvement of one or more of the mesial limbic structures at seizure onset (Thom & Bertram, 2012; Blümcke et al., 2013). The most common histopathologic abnormality that characterized adults with drug-resistant MTLE is the Hippocampal Sclerosis (HS) (Cavanagh & Meyer, 1956; Blümcke et al., 2002; De Lanerolle et al., 2003; Blümcke et al., 2012). Surgical resection offers postoperative seizure freedom in 60–80% of cases and leads to clinical, psychological, and social improvements (Engel, 1993; Arruda et al., 1996; Bien et al., 2001; Wiebe et al., 2001; H. G. Wieser et

al., 2003; Janszky, 2004; von Lehe et al., 2006). The main surgical treatment of TLE associated with HS is the Anteromedial Temporal Lobectomy (ATL), although, over the past years, different surgical techniques have been successfully performed on these patients, like Selective Amygdalohippocampectomy (SAH) (Asadi-Pooya & Rostami, 2017). Clinical-related factors such as years of duration, age at epilepsy onset, and the presence of an early preceding event, especially complex and prolonged febrile seizures (Davies et al., 1996; Blümcke et al., 1999; Janszky, 2004; Janszky et al., 2004; von Lehe et al., 2006), are likely to influence the degree of HS. Moreover, seizure frequency and severity, as well as genetic susceptibility, could also affect the development of the HS (Blümcke et al., 2013). However, the exact causes of HS associated with MTLE are still unknown (Thom & Bertram, 2012).

Due to the heterogeneous of the disease, cognitive and psychiatric (e.g., anxiety, depression, and/or interictal dysphoria) dysfunctions are highly prevalent and debilitating comorbidity in TLE patients (Saling, 2009; B. Bell et al., 2011; Vinti et al., 2021). About 80% of TLE patients demonstrate cognitive impairment in, at least, one cognitive domain, frequently in language and/or memory (Helmstaedter et al., 2003, 2006). It is not surprising that TLE is associated with memory impairment, due to the involvement of temporal lobes' structures. Memory impairment tends to be material specific: verbal memory is impaired if the TLE is lateralized in the language-dominant hemisphere, and vice-versa visuospatial memory is impaired if TLE is lateralized in the nondominant hemisphere (Helmstaedter & Kockelmann, 2006). Despite the seizures arising from temporal lobe regions, there is variability in the nature and severity of cognitive impairment observed across TLE patients; some demonstrate generalized impairment, some show a profile of focal cognitive deficits, and others show relatively intact cognitive profiles (Elverman et al., 2019; Reyes et al., 2019; Hermann et al., 2020). Moreover, some focal cognitive impairment that involves executive function and low intelligence levels are also quite often observed (Hermann et al., 1997). In addition, the association of cognitive abnormalities with other epilepsy characteristics (e.g., age of onset, seizure frequency/severity, duration of disorder) further clarified the presence, nature, and severity of associated cognitive morbidity (Dodrill, 1992; Baxendale & Thompson, 2010; Rudzinski & Meador, 2013). In order to explain the heterogeneity of cognitive impairment in TLE, studies have shifted from examining patients with TLE in the aggregate to identifying different cognitive phenotypes (Hermann et al., 2007; Elverman et al., 2019; Kaestner et al., 2019; Reyes et al., 2019). From the first study – by Hermann et al., 2007 – to nowadays, has been identified three distinct cognitive phenotypes in TLE: (I) patients with memory and language impairment; (II) patients with minimal or no impairment, and (III) patients

with a generalized and pervasive impairment (Hermann et al., 2007, 2020; Reyes et al., 2019, 2020). Patients with generalized impairment are characterized by longer disease duration, while patients with no impairment have more years of education. However, patients demonstrating the classic TLE profile (i.e., both language and memory impairment) seem not more likely to have an earlier age at onset and/or HS compared to other groups (Reyes et al., 2020).

1.2. Brain Morphometry

Brain morphometry is a subfield of both morphometry and brain sciences, whose main goal is to obtain quantitative biomarkers, and provide a measurement of brain structures and their changes during development, aging, learning, disease, and evolution.

Neuroimaging has accelerated our knowledge of the brain and plays an important role in the diagnosis and treatment of patients with epilepsy (van Vliet et al., 2017). Magnetic resonance imaging (MRI) is the choicest method for non-invasive assessments of brain structure, it is used for disease monitoring, and therapy control in a wide range of neurological and neurogenerative disorders, which are often associated with structural changes of the brain (Alexander-Bloch et al., 2013). Due to the high complexity of the human brain, MRI has allowed researchers to quantify *in vivo* structural and functional information related to neurodevelopment, brain aging, and diseases' progressions. The most frequent MRI images employed in brain morphometry are 3D conventional structural MRI T_1-weighted (T_1), and Diffusion-weighted imaging (DWI), like the Diffusion tensor imaging (DTI) sequences. Through these sequences, a variety of anatomical features can be quantified with brain morphometry methodologies. While T_1s are more likely used to explore the grey matter (GM) changes, damages, and differences between healthy subjects and pathology processes, DTI sequences are dedicated to the study of the *in vivo* tissue microstructure of the white matter (WM). DTI provides measures of diffusivity (i.e., mean diffusivity, MD) and directionality of diffusion (i.e., fractional anisotropy, FA) (O'Donnell & Westin, 2011). Diffusion-based tractography enables the graphical reconstruction of the WM pathways in the brain. This technique has many potential clinical applications and is fundamental to studying structural connectivity brain patterns.

In the present chapter, a brief introduction focused on 3D T_1-weighted MRI morphometry methodologies is presented. Voxel-based morphometry (Ashburner & Friston, 2000) and Surface-based morphometry (Dale et al., 1999; Fischl et al., 1999) are the principal methodologies used for estimating cortical morphology measures starting from 3D T_1 sequences. These two techniques share common processes, both starting with 3D T_1 MRI preprocessing and conclude with statistical analysis.

However, the middle steps are different in those pipelines, and different factors influence their reliability (**Fig. 1.5**).

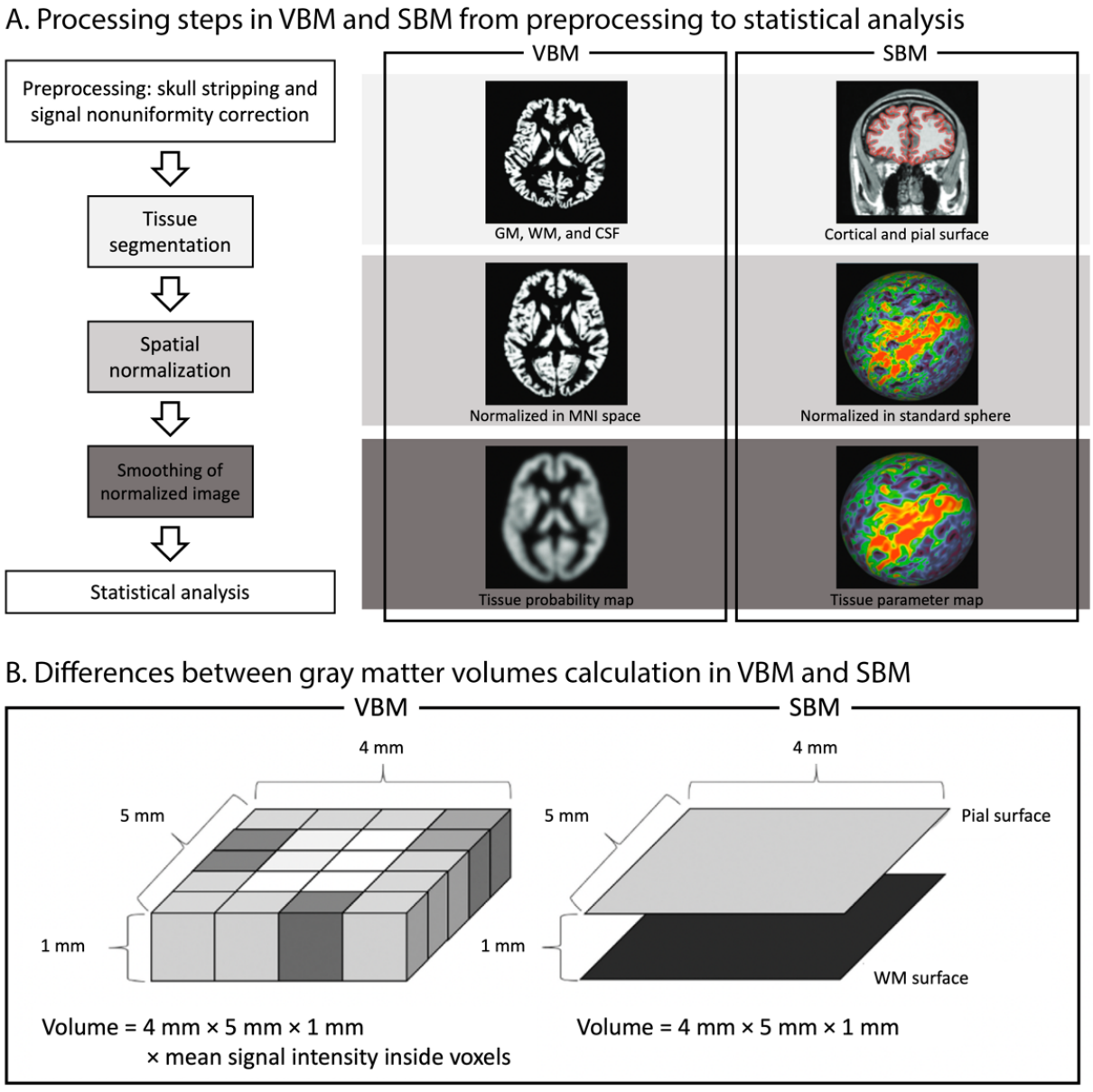

Figure 1.5. Differences in data processing steps in VBM and SBM taken from Goto et al., 2022. Figure **A** shows the processes for each method, which are both initiated by preprocessing and finished by statistical analysis. Major points of difference between VBM and SBM processing are highlighted with three boxes in the middle between preprocessing and statistical analysis. Figure **B** shows the difference in the measurement of grey matter volume in VBM and SBM. In VBM the GM volume is calculated from voxel size and signal intensity on a segmented grey matter image used as a tissue probability map. In SBM the GM volume is calculated from area size and grey matter thickness. CSF: cerebrospinal fluid; GM: grey matter; SBM, surface-based morphometry; VBM, voxel-based morphometry; WM: white matter.

1.2.1. Voxel-based morphometry

Voxel-based morphometry (VBM) is a neuroimaging technique commonly used to estimate the differences in brain tissue concentrations through a voxel-wise comparison of multiple brain images (Ashburner & Friston, 2000). Voxel-based methods establish voxel-for-voxel correspondence across subjects through nonlinear registration of multiple subjects' brain images to a standard anatomical template (Memarian et al., 2013), using the following equation: *signal intensity inside voxel* × *volume of voxel* (Goto et al., 2022). The preprocessing is composed of three steps: (I) tissue classification, (II) spatial normalization, and (III) spatial smoothing (Kurth et al., 2015). The final step of VBM involves voxel-wise statistical analysis that commonly includes group comparisons or correlations with covariates of interest (**Fig. 1.6**; Mechelli et al., 2005; Keller & Roberts, 2008).

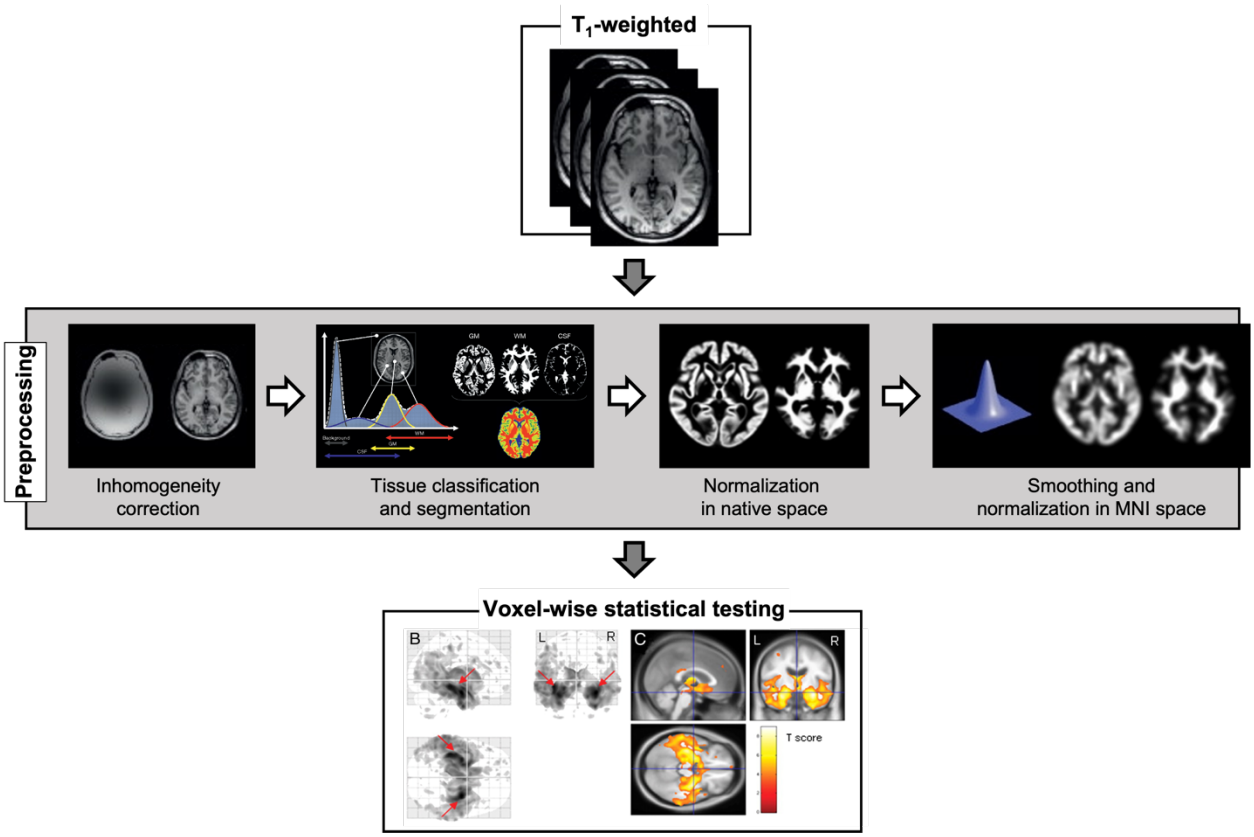

Figure 1.6. Graphical representation of the VBM steps from preprocessing to statistical analysis.

The main value of VBM is the possibility to perform the analysis all over the brain volumes, thus is not necessary to establish a prior spatial hypothesis. However, it can be sensitive to various artifacts, which include misalignment of brain structures, misclassification of tissue types, differences in folding

patterns, and in cortical thickness (Ashburner, 2009). These artifacts may confound the statistical analysis, could decrease the sensitivity, and increase the chance of false positives. Finally, the major limitation of VBM is the interpretation of the results, because this methodology is not capable to distinguish whether the volumes change is related to a change in cortical thickness or in cortical surface area (Voets et al., 2008; Winkler et al., 2010).

1.2.2. Surface-based morphometry

Surface-based morphometry (SBM) is a brain morphometric technique used to reconstruct and analyze surfaces that represent structural boundaries within the brain (Memarian et al., 2013). While VBM is primally used to estimate the GM volume, SBM can estimate a variety of features, like cortical thickness, cortical and subcortical volumes, surface area, and gyrification (**Fig. 1.7**; Mills & Tamnes, 2014). These morphometric measures are derived from geometric models of the cortical surface or surface-based models of subcortical structures (Memarian et al., 2013).

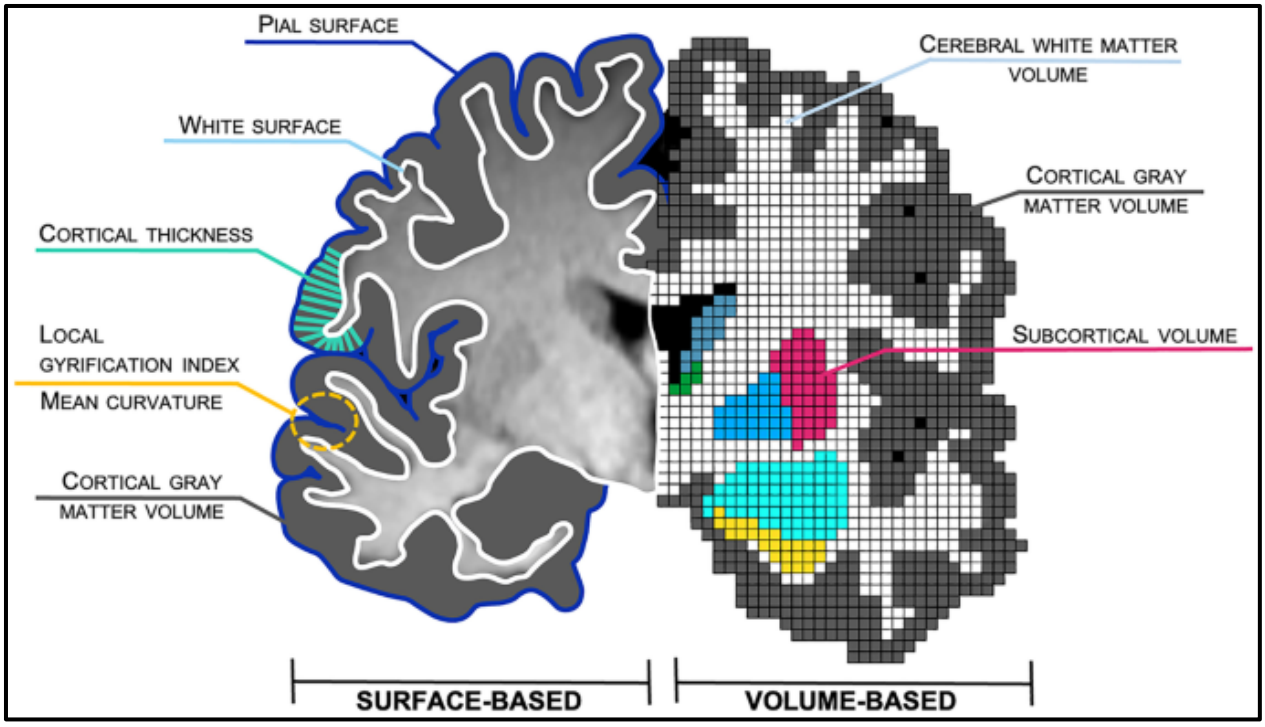

Figure 1.7. Graphical representation of the features acquirable with surface-based morphometry techniques. On the left, the variety of features is measurable with a surface-based approach. On the right, the volume is measurable with a volume-based approach.

The preprocessing steps involved in SBM of the brain are similar to the VBM's ones (i.e., skull stripping, signal nonuniformity correction as the preprocessing step, and tissue segmentation, spatial normalization, smoothing of the normalized image, and statistical analysis) (Goto et al., 2022). The most popular software packages to perform SBM are (I) FreeSurfer (Martinos Center for Biomedical Imaging, Boston, USA), (II) CIVET (McConnell Brain Imaging Center, Montreal, Canada), and (III) Computational Anatomy Toolbox 12 (CAT12) (Structural Brain Mapping Group, Jena, Germany). These methods use different approaches in cortex segmentation: FreeSurfer uses a model-based deformation approach, CIVET uses a skeleton-based reconstruction approach, and CAT12 uses a projection-based thickness approach (Redolfi et al., 2015; Righart et al., 2017). The most popular package to perform SBM, and the one used for all the studies included in this doctoral thesis, is FreeSurfer (Fischl, 2012; https://surfer.nmr.mgh.harvard.edu). Thus, the following SBM computational steps described are referring to the FreeSurfer pipeline and are illustrated in **Figure 1.8**.

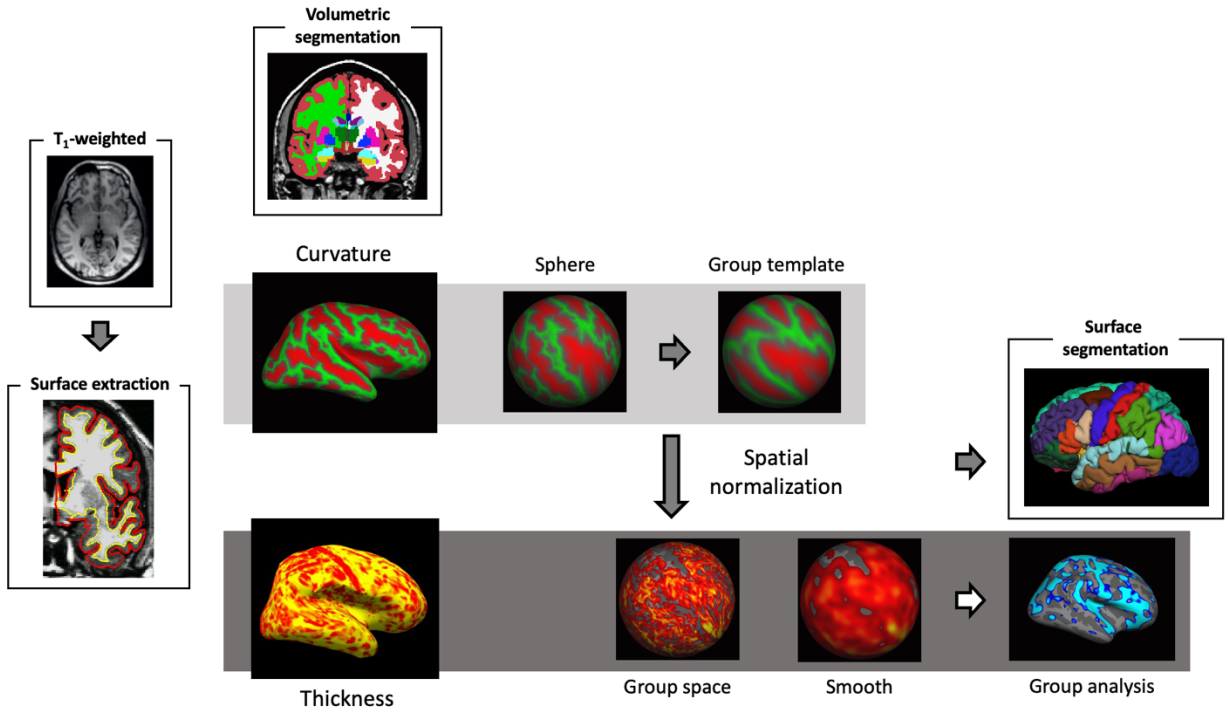

Figure 1.8. Graphical representation of FreeSurfer pipeline.

First, the WM surface and the pial surface are extracted and used to create the segmented tissue images (Dale et al., 1999). The two boundaries are determined based on voxel intensity information. Thus,

two boards are created: the first border divides the WM and the GM, and the second divide the GM and CSF. WM is divided between the two cortical hemispheres, and surface tessellation is performed for each hemisphere at each border voxel. This process is a determination of a square consisting of two triangles to separate WM from GM. The surfaces' vertices are used to estimate the indexes of cortical morphology – thickness, area, volume, and gyrification (**Fig. 1.7**) – as follows.

I. The cortical thickness is defined at each WM vertex as the shortest distance to the pial surface.
II. The cortical area at each vertex can be computed as the average area of all the triangles which include the vertex.
III. The GM volume is measured as the product of cortical thickness and surface area at each ROI.
IV. The whole brain gyrification index is defined as the ratio of the total pial surface over the total perimeter of the brain.

While with a VBM approach the normalization is performed in 3D, in SBM the spatial normalization from the native space to a standard surface space is performed on the 2D cortical sheet (**Fig. 1.5**; Fischl et al., 1999, 1999). Thus, identifying corresponding points on different cortical surfaces requires the establishment of a uniform surface-based coordinate system. For this aim, the patient's WM surface is going to get "inflated" to the shape of a sphere, and the geometric quantification of the WM surface is transferred to the sphere (**Fig. 1.8**; Greve & Fischl, 2018). The registration is performed in a spherical space, and the folding pattern quantification technique is used to drive a nonlinear, surface-based, inter-subject registration procedure that aligns the cortical folding patterns of each subject to a standard surface space. This technique is similar to the normalization on the MNI space used by VBM (Greve & Fischl, 2018). As for the VBM, the smoothing process is performed before statistical analysis. However, in SBM, the spatial smoothing is performed in parameter maps of factors (e.g., cortical thickness) on the spherical surface by the Gaussian smoothing kernel (Greve & Fischl, 2018) for a reduction in inter-individual variation. After smoothing, various indices like cortical thickness, area, and volume, are obtained at each vertex. Then, statistical analysis (i.e., group analysis) is performed vertex by vertex and allows the comparison between two groups with spatially smoothed index images. To estimate the morphology with the atlas-based method, FreeSurfer uses a non-smoothed index image. With this method, is possible to demonstrate the absolute index values (Zheng et al., 2019). The possibility to explore different GM features (i.e., cortical thickness, volume and/or surface) and the atlas-based method make SBM more precise than VBM, allowing a better interpretability of the results thank to the parcellation in well-defined brain atlas (Desikan et al., 2006; Destrieux et al., 2010). However, this procedure is very computational demanding (Rebsamen et al.,

2020). Moreover, the good quality of the results needs a manual inspection, or dedicated quality control pipeline, sometimes manual edits are required.

1.2.3. Brain morphometry in epilepsy

The use of brain morphometry methodologies to study brain MRIs is strongly related to the concept of imaging biomarkers. Biomarkers are quantitative biological measurements that provide information about a disease or a treatment response. Some biomarkers are commonly used to identify people at risk for a condition, others are used to diagnose disease, assess its progression, and/or predict disease outcome (Davis et al., 2008). The Biomarkers Definitions Working Group – an NIH-convened working group – in 2001 defined a biomarker as *"a characteristic that is objectively measured and evaluated as an indicator of normal biologic processes, pathogenic processes, or pharmacological responses to a therapeutic intervention"* (Atkinson et al., 2001).

Epilepsy is recognized as a network disease, characterized by a widespread structural alteration beyond the epileptogenic focus (Bernhardt et al., 2015; Vaughan et al., 2016). Although, HS is the most common pathological substrate of MTLE, is frequently observed extrahippocampal abnormalities, especially in the thalami, but even in the neocortex as well (Keller & Roberts, 2008; Bernhardt, Worsley, et al., 2009; Blanc et al., 2011; Labate et al., 2011; Vaughan et al., 2016). Even in generalized epilepsies – Idiopathic Generalized Epilepsy (IGE) and childhood syndromes – are often reported neocortical abnormalities (Bernhardt, Rozen, et al., 2009; O'Muircheartaigh et al., 2011; Vollmar et al., 2011; Ronan et al., 2012; Overvliet et al., 2013). Thus, cortico-subcortical networks' disturbances seem to characterize many common epilepsies (Berg et al., 2010), however, the causes and the patterns underlying these disturbances are still unknown, as well as their relation to functional declines (Vlooswijk et al., 2010; N. Bernasconi, 2016; Nickels et al., 2016). The identification of biological patterns common underlying focal and generalized epilepsy syndromes may be used as biomarkers and therapeutic targets which could optimize treatment strategies (Pitkänen et al., 2016). To address these aims, MRI has been fundamental in our understanding of brain processes underlying epilepsy. Still, large samples seize are needed to report consistent MRI findings and hypothetical imaging biomarkers.

Enhancing Neuro Imaging Genetics through Meta-Analysis (ENIGMA) is a global initiative combining samples from studies all over the world into a large-scale sample with coordinated image processing, integrating phenotypic, genomic, and MRI imaging data from research centers worldwide (Thompson et al., 2020). ENIGMA-Epilepsy is a working group of ENIGMA aiming to: (I) create a

worldwide network of epilepsy neuroimaging centers; (II) collect summary statistics on brain shape, brain volume, and white matter connectivity from people with epilepsy and neurologically healthy controls; (III) compare and contrast these measures in affected/unaffected groups and, accordingly, illustrate possible differences between the two; (IV) identify structural differences between the primary forms of epilepsy and major types of seizure; (V) develop collaborations and infrastructure for future analyses (Sisodiya et al., 2020). The first projects of the ENIGMA-Epilepsy working group explored the structural and diffusion MRI patterns using advanced brain morphometry techniques across epilepsy syndromes in large and heterogenous sample sizes from centers worldwide (Whelan et al., 2018; Hatton et al., 2020). Whelan and colleagues used ROI-based morphometry to explore the sharing and differential biological cortico-subcortical patterns across different epilepsy syndromes. Their results suggested a common neuroanatomical signature shared by all epilepsies, regardless of the specific syndromes, characterized by local atrophy in the thalamus formation, pallidum, precentral gyrus, paracentral gyrus, and superior frontal cortices. Both left and right MTLEs showed an ipsilateral HS, as expected, without any significant results regarding the contralateral hippocampus. Moreover, this study confirmed previously suggested; MTLE seems to be a network disease, that involves extrahippocampal subcortical abnormalities (i.e., ipsilateral atrophy of thalamus and pallidum) and widespread atrophy in cortical thickness in many extratemporal regions. This result will be replicated a few years later in another ENIGMA-Epilepsy study by Larivière et al. (2020). These authors confirmed profound atrophy in the bilateral precuneus, bilateral precentral and paracentral gyri, and superior temporal cortices, as well as the ipsilateral hippocampus and ipsilateral thalamus in patients with TLE. IGE is typically associated with "normal" or negative MRI (Woermann et al., 1998), however, both these ENIGMA-Epilepsy studies highlighted a central involvement of the thalamus formation and precentral gyri (Whelan et al., 2018; Larivière et al., 2020). These studies contributed to determining a robust brain structural GM pattern within and between epilepsy syndromes, moreover, these findings may provide a neuroanatomical map of common epilepsies and may support future neuropathological work, animal mode, and gene expression studies (Whelan et al., 2018). Once epilepsy was considered primarily a GM disease, however, studies employed diffusion MRI revealed that both focal and generalized epilepsies are characterized by widespread WM alterations, even in the absence of visible MRI lesions (Engel et al., 2013). While TLE-HS patients exhibited WM abnormalities both proximal to and distant from the epileptogenic focus (Focke et al., 2008; Ahmadi et al., 2009; Labate et al., 2015; Caligiuri et al., 2016), IGE patients have demonstrated microstructural compromise in bilateral frontal and parietal regions, and in thalamocortical pathways (Keller et al.,

2011; C.-Y. Lee et al., 2014; Szaflarski et al., 2016). WM disruption in epilepsy is widely important, especially because of its link to cognitive performances (C. R. McDonald, Ahmadi, et al., 2008; Yogarajah et al., 2008, 2010) and its role in postsurgical seizure outcomes (Bonilha et al., 2015; Keller et al., 2015; Gleichgerrcht et al., 2018). The second project from ENIGMA-Epilepsy aimed to map the WM disruption in common epilepsy syndromes compared to a control population (Hatton et al., 2020). This was the first study that investigated WM in a large sample of patients composed of different epilepsy syndromes. The alteration found were more robust in the frontal regions' tracts and in the external capsule, these results mirroring the structural findings by Whelan and colleagues. According to previous literature (Slinger et al., 2016), Hatton and colleagues confirmed a pronounced and wide spreader WM injury in TLE compared to other epilepsy syndromes. Moreover, their results highlighted a stronger pattern in TLE with HS pathology, especially ipsilateral to the seizure focus, and in those WM tracts afferent and efferent to the hippocampal formation. The same pattern of WM disruption was found in TLE with a negative MRI, however, this kind of TLE seemed to be milder compared to TLE-HS. IGE patients reported modest alteration compared to focal epilepsy patients. Confirming previous results by Slinger et al., IGE seemed to be characterized by disruption in commissural, projection, and cortico-cortical pathways, supporting the hypothesis of a fronto-thalamic pathology underlying this epileptic syndrome.

Chapter 2

Amygdala subnuclear volumes in temporal lobe epilepsy with hippocampal sclerosis and in non-lesional patients

Alice Ballerini[1], Manuela Tondelli[2], Francesca Talami[1], Maria Angela Molinari[3], Elisa Micalizzi[4], Giada Giovannini[3,4], Giulia Turchi[3], Marcella Malagoli[5], Maurilio Genovese[5], Stefano Meletti[1,3], & Anna Elisabetta Vaudano[1,3]

[1]*Department of Biomedical, Metabolic and Neural Sciences, University of Modena and Reggio Emilia, Modena, Italy*

[2]*Azienda USL, Modena, Italy*

[3]*Neurology Unit, OCB Hospital, AOU Modena, Modena, Italy*

[4]*PhD Program in Clinical and Experimental Medicine, University of Modena and Reggio Emilia, Modena, Italy*

[5]*Neuroradiology Unit, OCB Hospital, AOU Modena, Modena, Italy*

2.1. Introduction

The amygdalar nuclear complex and hippocampal/parahippocampal region are key components of the limbic system that play a critical role in emotion, learning and memory, and complex behavior . In Temporal Lobe Epilepsy (TLE) the greatest attention has been focused on the hippocampus as hippocampal sclerosis (HS) is recognized as the most common cause of TLE (Coan, Morita, Campos, et al., 2013; H.-G. Wieser, 2004). However, accumulating evidence suggests the amygdala as a key component in TLE in association or independent from HS (Na et al., 2020). In patients with MRI-negative TLE (TLE-MRIneg), the absence of obvious epileptogenic lesions on routine visual assessment carries delays in surgical referral and in many cases the need for intracranial recordings before surgery. Advanced MRI morphometric approaches might contribute to reveal subtle structural abnormalities linked to the epileptogenic process (Morita-Sherman et al., 2021). Recently, different studies described an increased amygdala volume (named amygdala enlargement, AE) in patients with TLE-MRIneg. Evaluation of AE differed between studies: while in some studies the increased amygdala's volume was observed by qualitative visual assessment (Kim et al., 2012; Lv et al., 2014; Minami et al., 2015; Mitsueda-Ono et al., 2011), in others it was revealed after post-processing MRI approaches (Coan, Morita, Campos, et al., 2013; Coan, Morita, de Campos, et al., 2013; Reyes et al., 2017). Overall, AE is reported on MRI in patients with non-lesional TLE at rates that range from 12% to 63% (Bower, 2003; Coan, Morita, de Campos, et al., 2013; Minami et al., 2015), leading to the hypothesis that AE represents a distinct subtype of TLE (Lv et al., 2014) with specific nosological

characteristics. This scenario however is complicated by the observation of AE also in patients with MRI-negative Extra temporal lobe epilepsy, thus suggesting that AE can be a feature associated to "non-lesional" focal epilepsy (Reyes et al., 2017) but not specific to TLE. The amygdala formation is commonly treated as a single entity in structural MRI; however, it is composed of multiple nuclei, each exhibiting different connectivity and histochemical profiles (Janak & Tye, 2015). Due to the small size of the amygdala, no prior studies focused on changes of amygdala subnuclei in patients with TLE. Thanks to recent advances in parcellation methods, it is possible to label amygdala subnuclei and automatically provide volumetric information for each one based on an in vivo atlas (Saygin et al., 2017). The amygdala subnuclei might be further organized in groups or complexes based on their reciprocal connections and specific functions (Sah et al., 2003). These approaches have been successfully applied in patients with psychiatric conditions (Armio et al., 2020; Asami et al., 2018; Cui et al., 2020) but up to date not in the epilepsy field.

In the present work, by investigating the morphometric characteristics of the amygdala substructures, we aim to map specific amygdala subnuclei participation in TLE-HS and TLE-MRIneg thus providing increased knowledge about the pathophysiological networks that mediate the amygdalar involvement in temporal lobe epilepsies.

2.2. Methods and Materials

2.2.1. Study population

We retrospectively reviewed a cohort of consecutive patients with diagnosis of TLE who underwent a structural brain MRI study for diagnostic purposes at a 3 Tesla MRI scan between April 2016 and April 2021 at the Neurology Unit, OCB Hospital (Modena, Italy). The inclusion criteria were: (I) age older than 18 years; (II) a brain MRI protocol encompassing at least a three-dimensional (3D) high-resolution T_1-weighted (T1-3D) sequence. We excluded patients with: (I) abnormalities on the MRI scan except for hippocampal sclerosis; (II) patients older than 65 years old; (III) patients with progressive diseases (e.g., neurodegenerative disorders, encephalopathies); (IV) patients with previous neurosurgery; (V) patients in whom the diagnostic work-up (including cerebrospinal fluid analysis, CSF) suggested an autoimmune etiology; (VI) patients with bilateral seizures' onset zone based on clinical investigations; (VII) patients with reported seizures in the 48 hours before the MRI scan. This latter criterion is motivated by the intention to avoid any bias in amygdala volume estimation temporally related to the occurrence of ictal activity (Lv et al., 2014; Mariajoseph et al., 2021). TLE patients were divided in TLE-MRIneg, if no focal lesion was observed on the MRI, and TLE-HS if

the structural MRI scan showed an alteration consistent with hippocampal sclerosis (HS). A population of patients with focal epilepsy rather than TLE (Extra-TLE) was included as an epilepsy control population. Inclusion and exclusion criteria were the same as TLE groups, except for the presence of focal cortical dysplasia (FCD) on the clinical MRI scan after expert evaluation. All the recruited patients underwent a comprehensive diagnostic evaluation protocol which included the clinical history with seizures' semiology, neurological examination, prolonged scalp Video-EEG monitoring, and structural MRI scan. Interictal FDG-PET was performed when indicated. Epilepsy patients' classification in this study was determined by board-certified neurologists (S.M., G.G., G.T., E.M., and A.E.V.) with expertise in epileptology and in accordance with criteria defined by the International League Against Epilepsy (Fisher et al., 2017; Scheffer et al., 2017). Specifically, a diagnosis of TLE was performed in presence of at least one Video-EEG recorded seizure arising from the temporal lobe. Neuroradiological diagnosis and classification of patients were done on visual inspection by two neuroradiologists (M.M., and M.G.) with experience in epilepsy. In case of discordance, the final classification was reached after a thorough discussion with a neurologist (S.M., and A.E.V.). From each patient recruited, we collected clinical information regarding gender, age, handedness, side of the epileptic focus, age of seizure onset, duration of epilepsy, the drug-response to antiseizures medications (ASMs), and type of ASM at the time of MRI scan. A patient was defined as drug-responder if she/he had sustained seizure-freedom during the last 12 months before the MRI scan (Kwan et al., 2010). Psychiatric comorbidity was defined as a history of documented psychiatric and/or psychological therapy and/or previous psychiatric hospitalization. Finally, the volume measurements of subcortical and amygdala nuclei in all the patients' groups were compared with MRI data collected from 30 health controls (HC) matched in age and gender studied with the same MRI protocol and analysis.

2.2.2. MRI data and segmentation protocol

MRI was performed on two different 3T scanners adopting an epilepsy-dedicated protocol: a 3.0 Tesla Philips Intera MRI scanner (Best, The Netherlands) (for patients recruited between 2016-2017), and a 3.0 Tesla GE Healthcare MRI scanner (Chicago, United States of America) (for patients recruited after 2018). As common sequences, the protocols included a 3D T_1-weighted sequence, a 3D fluid-attenuated inversion recovery (FLAIR), and a bidimensional coronal T_2-weighted image acquired perpendicular to the long axis of the hippocampus. Of note, patients (both TLE and Extra-TLE) with an increased signal on T_2-weighted images on the amygdala, mono or bilaterally, were

excluded from further analysis, after expert visual evaluation. This procedure was applied as changes in the amygdala signal at MRI (particularly increased in T2/FLAIR signal) might be secondary to recurrent seizures instead of reflecting structural modifications (Duncan, 2002; Na et al., 2020). T_1-weighted images were analyzed using a standardized image toolbox (FreeSurfer, version 6.0, https://surfer.nmr.mgh.harvard.edu), quality assurance (outlier detection based on interquartile of 1.5 standard deviations along with visual inspection of segmentation), and statistical methods. Visual inspections of subcortical segmentations were conducted following standardized ENIGMA protocols (http://enigma.usc.edu), used in prior genetic studies of brain structure (Hibar et al., 2018; Stein et al., 2014), large-scale case-control studies of epilepsy (B. Park et al., 2022; Whelan et al., 2018) and neuropsychiatric illnesses (Boedhoe et al., 2018; Schmaal et al., 2016). The amygdala subnuclei segmentation module, which is only present in the FreeSurfer dev version (ftp://surfer.nmr.mgh.harvard.edu/pub/dist/freesurfer/dev), was used to parcellate the amygdala in nine nuclei for each side: anterior amygdaloid area (AAA), cortico-amygdaloid transition area (CAT), basal (Ba), lateral (La), accessory basal (AB), central (Ce), cortical (Co), medial (Me), and paralaminar (PL) nuclei (Saygin et al., 2017) (**Fig. 2.1**).

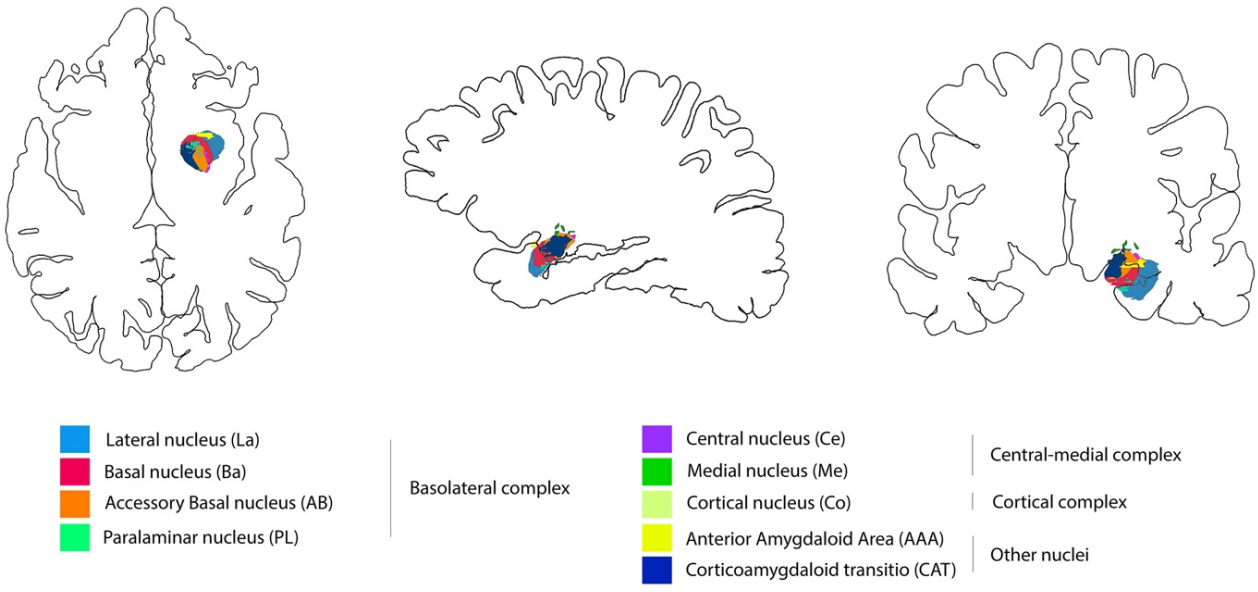

Figure 2.1. Amygdala subnuclei segmentation module based on Saygin & Kliemann, 2017 pipeline.

To account for correct subfield delineations, segmentations were visually inspected after processing. Analysts (A.B., M.T., and F.T.) were blind to participant diagnoses. Moreover, based on their

cytoarchitectonics, histochemistry, and connections(Price et al., 1987), the different nuclei of amygdala were subdivided into three main regions or complexes: (I) the deep group represented by the basolateral complex (BLA), which includes the lateral nucleus, the basal nucleus, the accessory basal nucleus, and the paralaminar nucleus; (II) the superficial group named cortical complex (CC), which include the cortical nucleus; (III) and the central-medial complex (CMC) composed by the medial and the central nuclei (**Fig. 2.1**). In separate analyses, we also performed the segmentation of hippocampal subfields (Iglesias, Augustinack, et al., 2015) and thalamic structures (Iglesias et al., 2018) as implemented in the FreeSurfer dev version (ftp://surfer.nmr.mgh.harvard.edu/pub/dist/freesurfer/dev). These additional segmentations were required because of the strict anatomical and functional relationships between the hippocampus, thalamus, and amygdala. As far as the hippocampal subfields we obtained the volumes of the following structures bilaterally: hippocampal body, hippocampal head, hippocampal tail, hippocampal fissure, subiculum, presubiculum, parasubiculum, CA1, CA2/3, CA4, molecular layer, granule cell and molecular layer of the dentate gyrus (GC-ML-GD), fimbria, and hippocampal-amygdala transition area (HATA). We also calculated the volumes of 25 individual thalamic nuclei for each side, including the anteroventral nuclei in the anterior group; the laterodorsal and lateral posterior nuclei in the lateral group; the ventral anterior, ventral anterior magnocellular, ventral lateral anterior, ventral lateral posterior, ventromedial, and ventral posterolateral nuclei in the ventral group; the central medial, central lateral, paracentral, centromedian, and parafascicular nuclei in the intralaminar group; the paratenial, medial ventral, mediodorsal medial magnocellular, and mediodorsal lateral parvocellular nuclei in the medial group; and the lateral geniculate, medial geniculate, suprageniculate, pulvinar anterior, pulvinar inferior, pulvinar lateral, and pulvinar medial nuclei in the posterior group.

2.2.3. Statistical analysis

One-way ANOVAs were used to assess differences in demographic and clinical variables among groups when distributed normally, Kruskal-Wallis tests were performed otherwise. Fisher's exact tests were performed on categorical variables. Volume measurements across the two different MRI scanners were harmonized using the "neuroCombat" (Fortin et al., 2018; Johnson et al., 2007) package for R (https://cran.r-project.org/). After harmonization, the volumes of all subcortical structures and the volumes of amygdala subnuclei and complexes were converted into z-scores based on the mean and standard deviation (SD) of HC population. To confirm the success of the scanner harmonization, we performed an independent sample t-test between the z-scored volumes of the

whole left and right amygdala obtained after ComBat harmonization in all patients' groups. The statistical significance of differences in mean volumes between left and right amygdala sub-structures in HC population was assessed using paired t-tests to check for asymmetries. To account for the side of the epileptic focus, subcortical measurements of right TLE and Extra-TLE patients were flipped in order to have all the morphometric data of the epileptic focus on the left hemisphere. All morphometric subcortical analyses are then reported as ipsilateral or contralateral respect with the epilepsy focus. After testing the normality of morphometric data with Shapiro-Wilks test, group differences for subcortical, hippocampal subfields, thalamus, and amygdala substructures volumes were examined using multivariate analyses of covariance (MANCOVAs) with one between-subjects grouping factor (groups: TLE-HS, TLE-MRIneg, Extra-TLE, and HC) with age, gender, and estimated total intracranial volume (eTIV) as covariates. The eTIV is a reliable indirect measure of the head size (Hansen et al., 2015) and is used as a covariate in most large-scale ENIGMA collaborations studies in epilepsy (Larivière et al., 2020; B. Park et al., 2022; Sisodiya et al., 2020; Whelan et al., 2018). All the analyses were followed by Bonferroni post-hoc correction. To estimate the effect size, independent two-sample t-tests were performed between the studied populations, and Cohen's d value was reported. Logistic regression was performed to test the relationship between the not flipped volumes of the amygdala structures that resulted significantly different across groups and the clinical diagnosis. Additionally, the accuracy of these models was assessed by areas under the curve (AUCs) with 95% confidence intervals obtained by the receiver operating characteristic (ROC) curve. Finally, correlation analyses between the flipped amygdala volumes and clinical variables (age of epilepsy onset, duration of illness, and number of ASMs) were performed for the TLE patients. In the correlations age, gender, and eTIV were included as confounding factors. Independent sample t-tests were used to determine whether there were group differences in drug-response and psychiatric comorbidity in relation to the volume of amygdala subnuclei. All statistical analyses were performed using SPSS software 27 (IBM, Chicago, IL). Statistical significance for all tests was set at $p<.05$.

2.3. Results

2.3.1. Patients' population demographic and clinical characteristics

Out of an original pool of 116 TLE patients, 48 were recruited. The remaining 68 patients were excluded for lack of T1-3D sequence in the MRI protocol (n=13), progressive neurological diseases (e.g., AD, encephalopathies, n=5), age older than 65 years old (n=5), previous neurosurgery (n=3), structural lesions different from HS (e.g., LEAT "Long-term Epilepsy Associated Tumors",

FCD, amygdala signal changes, n=33) and segmentation errors after the FreeSurfer post-processing process (n=9). Among the TLE group, 24 patients were classified as TLE-HS and 24 as TLE-MRIneg. Demographic and clinical characteristics are summarized in **Table 2.1**. The Extra-TLE group was constituted by 20 patients, 14 (70%) with Frontal Lobe Epilepsy (FLE) and 6 (30%) with Parietal Lobe Epilepsy (PLE). 12/20 Extra-TLE patients (60%) had cryptogenic epilepsy, 6/20 (30%) a frontal focal cortical dysplasia (FCD), 2/20 (10%) a FCD in the parietal lobe. Interictal FDG-PET was available in 15 TLE and 7 Extra-TLE patients and the revealed hypometabolism confirmed the electro-clinical hypotheses in all cases. Out of all patients' cohort, seven patients underwent epilepsy surgery: five TLE-HS and two Extra-TLE. Histology confirmed the hippocampal sclerosis in all TLE-HS, and two FCD type Ia were reported in Extra-TLE. In two TLE-HS postsurgical specimens, an amygdala gliosis was documented by the pathologist. Mean follow-up after surgery was 34 months and all patients are in Engel Class Ia (Engel, 1993). No statistical differences were observed between groups in age, gender distribution, and eTIV. Across epilepsy groups there were no statistical differences in the side of the epileptic focus, age at epilepsy onset, and epilepsy's duration. Despite the greater number of drug-resistant patients in the TLE-HS group, the drug-response status did not show a significant difference between the epilepsy groups. There was a statistically significant difference in the number of antiseizure meds between groups: Extra-TLE were on polytherapy more frequently compared with TLE-MRIneg ($p_{Bonferroni}$=.011). Psychiatric comorbidity was documented in 11 patients mainly represented by TLE: the reported symptoms in all patients were compatible with a mixed anxiety-depressive disorder (MADD) (Kara et al., 2000).

Table 2.1. Demographic and clinical characteristics of the studied populations

	TLE-MRIneg (N=24)	TLE-HS (N=24)	Extra-TLE (N=20)	HC (N=30)	p-value	Pairwise comparison#
Gender, M/F	8/16	9/15	11/9	11/19	0.498[F]	
Age, y	36.54(13.97)	40.46(12.13)	34.75(13.63)	35.27(5.82)	0.366[K-W]	
Age of onset, y	29.21(14.63)	25.25(14.54)	21.80(15.42)	-	0.117[K-W]	
Epilepsy duration, y	7.50(8.27)	15.29(12.10)	12.50(10.89)	-	0.725[K-W]	
Side, L/R	14/10	15/9	10/10	-	0.748[F]	
ASMs-respondents, Yes/No	14/10	6/18	7/13	-	0.054[F]	
N° of ASMs	1.92(0.88)	2.38(0.71)	2.55(0.76)	-	0.031[K-W]*	Extra-TLE > TLE-MRIneg (p = .011)
Psychiatric comorbidity, Yes/No	3/21	5/19	3/17	-	0.780[F]	
eTIV, mm^3	1422561 (144470)	1446261 (180209)	1521645 (173721)	1457345 (213170)	0.334[A]	

Data are presented in means, standard deviations (SDs) are presented in the parentheses. [F]: Fisher's exact test, [K-W]: Kruskal-Wallis test, [A]: one-way ANOVA, [#]: significant p-value of pairwise comparisons between groups using Bonferroni method. *: p<.05, **: p<.01, ***: p<.001.

2.3.2. Subcortical structures

The MANCOVAs analyses highlighted a decreased volume in the hippocampus ipsilateral to the epileptic focus in TLE-HS compared to all the other groups [TLE-MRIneg, Extra-TLE, and HC: $F(3,91)=12.498$, $p<.000$] and an increased lateral ventricular volume bilaterally [$F(3,91)=5.561$, $p=.002$ for the left ventricle; $F(3,91)=4.838$, $p=.004$ for the right ventricle]. An independent sample t-test between TLE-HS and HC showed also a significant atrophy of the bilateral thalamus in TLE-HS group compared to HC [left thalamus: $t(52)=-2.381$, $p=.021$, $d=-.652$; right thalamus: $t(52)=-2.189$, $p=.033$, $d=-.599$], while no significant differences were observed for basal ganglia and accumbens nucleus. There were no significant differences in subcortical structures between TLE-MRIneg and HC, between Extra-TLE and HC, and between TLE-MRIneg and Extra-TLE groups (**Fig. 2.2**).

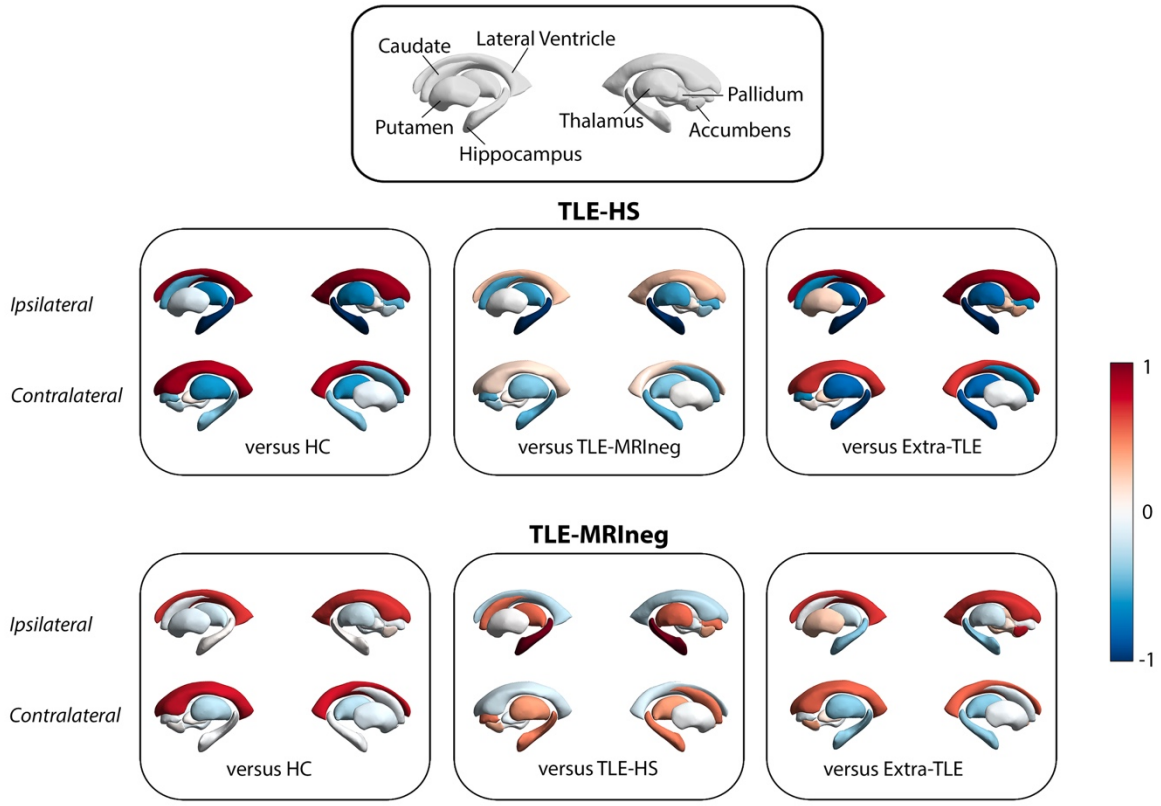

Figure 2.2. Graphic representations of subcortical comparison between patients' groups and HC, and within patients' populations. The comparison between TLE-HS and the other groups, and TLE-MRIneg and the other groups are represented with Cohen's d effect size value starting from absolute z-score volumes. Blue colors indicate a decrease of volume in subcortical structures, red colors indicate an increase in volume of subcortical structures. In the box on the top is presented the legend of subcortical structures examined. The present images were created by using the ENIGMA-Toolbox by Larivière et al., 2021.

As far as the hippocampus subfield's parcellation, the MANCOVA analysis did not find any differences in the volumes of hippocampal structures between TLE-MRIneg, Extra-TLE, and HC populations. As expected, TLE-HS patients showed overall atrophy of hippocampal subfields ipsilateral to HS compared to all other patients and HC. Few ipsilateral subfields appeared unimpaired by HS: the hippocampal fissure, parasubiculum, fimbria, and HATA. The CA4 and dentate gyrus head appeared atrophic even contralaterally. Regarding the thalamus segmentation, the MANCOVA analysis demonstrated isolated atrophy of the ipsilateral mediodorsal magnocellular nucleus in TLE-HS patients compared to all populations (versus HC: $p_{Bonferroni}$=.024, versus TLE-MRIneg: $p_{Bonferroni}$=.025, versus Extra-TLE: $p_{Bonferroni}$=.038), and of the ipsilateral anterior portion of the pulvinar compared to HC ($p_{Bonferroni}$=.005). No differences were observed between TLE-MRIneg, Extra-TLE, and HC. An independent sample t-test between TLE-HS and HC groups showed a generalized atrophy of whole ipsilateral thalamus [t(52)=-2.181, p=.034, d=-.597] and, particularly, of nuclei

belonging to the anterior [anteroventral: t(52)=-2.373, p=.021, d=-.650], intralaminar [central medial: t(52)=-2.622, p=.011, d=-.718; and paracentral: t(52)=-2.270, p=.027, d=-.622], medial group [medial ventral: t(52)=-2.308, p=.025, d=-.631, mediodorsal medial magnocellular: t(52)=-3.449, p=.001, d=-.945, and mediodorsal lateral parvocellular: t(52)=-2.697, p=.009, d=-.739], the whole pulvinar [t(52)=-2.341, p=.023, d=-.641], particularly the anterior [t(52)=-3.388, p=.001, d=-.928] and medial [t(52)=-2.471, p=.017, d=-.677] portions. The same nuclei of the intralaminar and medial group as well as the anterior and medial pulvinar nuclei were atrophic also contralaterally to the HS. Regarding the amygdala subnuclei and complexes, results are summarized in **Table 2.2** and in **Fig. 2.3** and **2.4**. There were no differences in the amygdala volumes between left and right hemispheres in HC.

Table 2.2. Morphometric comparison of amygdala substructures between patients' groups and HC

		TLE-MRIneg	TLE-HS	Extra-TLE	HC	F	p-value	Pairwise comparison#
Ipsilateral	Whole amygdala	1821.383 (202.543)*	1657.693 (264.616)*	1902.373 (272.393)*	1799.279 (209.579)*	4.639	0.005**	TLE-HS < HC (p=.040) TLE-HS < TLE-MRIneg (p=.010) TLE-HS < exTLE (p=.018)
	Lateral nucleus	670.808 (68.034)*	619.674 (93.304)*	711.153 (106.522)*	673.051 (77.678)	4.064	0.009**	TLE-HS < TLE-MRIneg (p=:044) TLE-HS < exTLE (p=.016)
	Basal nucleus	461.260 (49.973)*	418.723 (70.350)*	481.192 (68.681)*	456.974 (58.518)*	4.320	0.007**	TLE-HS < HC (p=.042) TLE-HS < TLE-MRIneg (p=.015) TLE-HS < exTLE (p=.027)
	AB nucleus	283.686 (41.460)*	256.723 (43.831)*	290.711 (44.443)	276.833 (34.705)	3.833	0.012*	TLE-HS < TLE-MRIneg (p=.012)
	Paralaminar nucleus	50.994 (4.904)*	45.889 (8.131)*	53.368 (7.486)*	51.643 (6.789)	4.728	0.004**	TLE-HS < HC (p=.011) TLE-HS < TLE-MRIneg (p=.016) TLE-HS < exTLE (p=.024)
	Central nucleus	49.967 (10.638)*	43.936 (8.812)*	49.536 (9.803)	47.455 (7.999)	3.142	0.029*	TLE-HS < TLE-MRIneg (p=.023)
	Medial nucleus	26.562 (7.952)*	21.313 (6.552)*	26.077 (6.758)	20.747 (4.284)*	5.093	0.003**	TLE-HS < TLE-MRIneg (p=.009) HC < TLE-MRIneg (p=.012)
	Cortical nucleus	28.540 (5.278)*	24.819 (5.309)*	28.716 (4.767)	26.837 (4.074)	3.618	0.016*	TLE-HS < TLE-MRIneg (p=.010)
	AAA	57.656 (7.266)	53.203 (11.486)	62.079 (10.311)	55.937 (7.980)	2.524	0.063	
	CAT	191.825 (23.878)*	174 (32.102)*	198.751 (28.111)	189.961 (27.599)*	3.290	0.024*	TLE-HS < TLE-MRIneg (p=.037)
	Basolateral complex	366.687 (39.304)*	335.252 (52.614)*	384.106 (55.194)*	364.625 (41.753)*	4.559	0.005**	TLE-HS < HC (p=.033) TLE-HS < TLE-MRIneg (p=.013) TLE-HS < exTLE (p=.018)
	Cortical complex	28.540 (5.278)*	24.819 (5.309)*	28.716 (4.767)	26.837 (4.074)	3.618	0.016*	TLE-HS < TLE-MRIneg (p=.010)
	Central-medial complex	38.264 (8.744)*	32.625 (7.227)*	37.807 (7.579)	34.101 (5.490)	4.195	0.008**	TLE-HS < TLE-MRIneg (p=.005)
Contralateral	Whole amygdala	1806.576 (278.917)	1720.756 (164.209)	1878.866 (274.433)	1821.415 (334.747)	1.326	0.271	
	Lateral nucleus	665.074 (97.899)	645.940 (67.732)	692.898 (105.466)	672.753 (120.093)	0.802	0.496	
	Basal nucleus	459.111 (72.231)	438.850 (42.867)	477.929 (72.681)	463.525 (85.591)	1.142	0.336	
	AB nucleus	280.271 (47.547)	262.683 (29.166)	291.781 (44.518)	282.866 (58.423)	1.644	0.185	

Paralaminar nucleus	51.239 (7.478)	48.679 (5.400)	53.009 (7.730)	51.717 (9.462)	1.648	0.184	
Central nucleus	50.127 (11.536)	46.674 (6.130)	49.957 (11.332)	49.663 (14.428)	0.637	0.593	
Medial nucleus	25.694 (7.866)	20.897 (4.043)*	26.702 (6.241)*	22.502 (7.397)*	5.095	0.003**	TLE-HS < exTLE (p=.017) HC < exTLE (p=.037)
Cortical nucleus	28.400 (4.773)	25.096 (4.427)	29.719 (5.141)	27.773 (6.982)	2.962	0.036*	
AAA	55.857 (9.450)	55.197 (6.812)	59.703 (9.067)	56.643 (10.189)	0.270	0.847	
CAT	191.219 (33.856)	176.041 (18.329)	196.265 (27.886)	193.981 (34.985)	2.504	0.064	
Basolateral complex	363.924 (52.249)	349.038 (34.039)	378.904 (56.331)	367.715 (67.395)	1.158	0.330	
Cortical complex	28.400 (4.773)	25.096 (4.427)	29.719 (5.141)	27.773 (6.982)	2.961	0.036*	
Central-medial complex	37.911 (8.800)	33.831 (4.426)	38.330 (8.160)	36.083 (10.405)	1.575	0.201	

Data (in mm^3) are presented in means; Standard Deviations (SDs) are presented in the parentheses. Age, gender, and eTIV as covariates. F: MANCOVA's F-test value. *: p<.05, **: p<.01, ***: p<.001. #: significant p-value of pairwise comparisons between groups using post-hoc Bonferroni correction (p<.05). AAA: anterior amygdaloid area, CAT: corticoamygdaloid transition area.

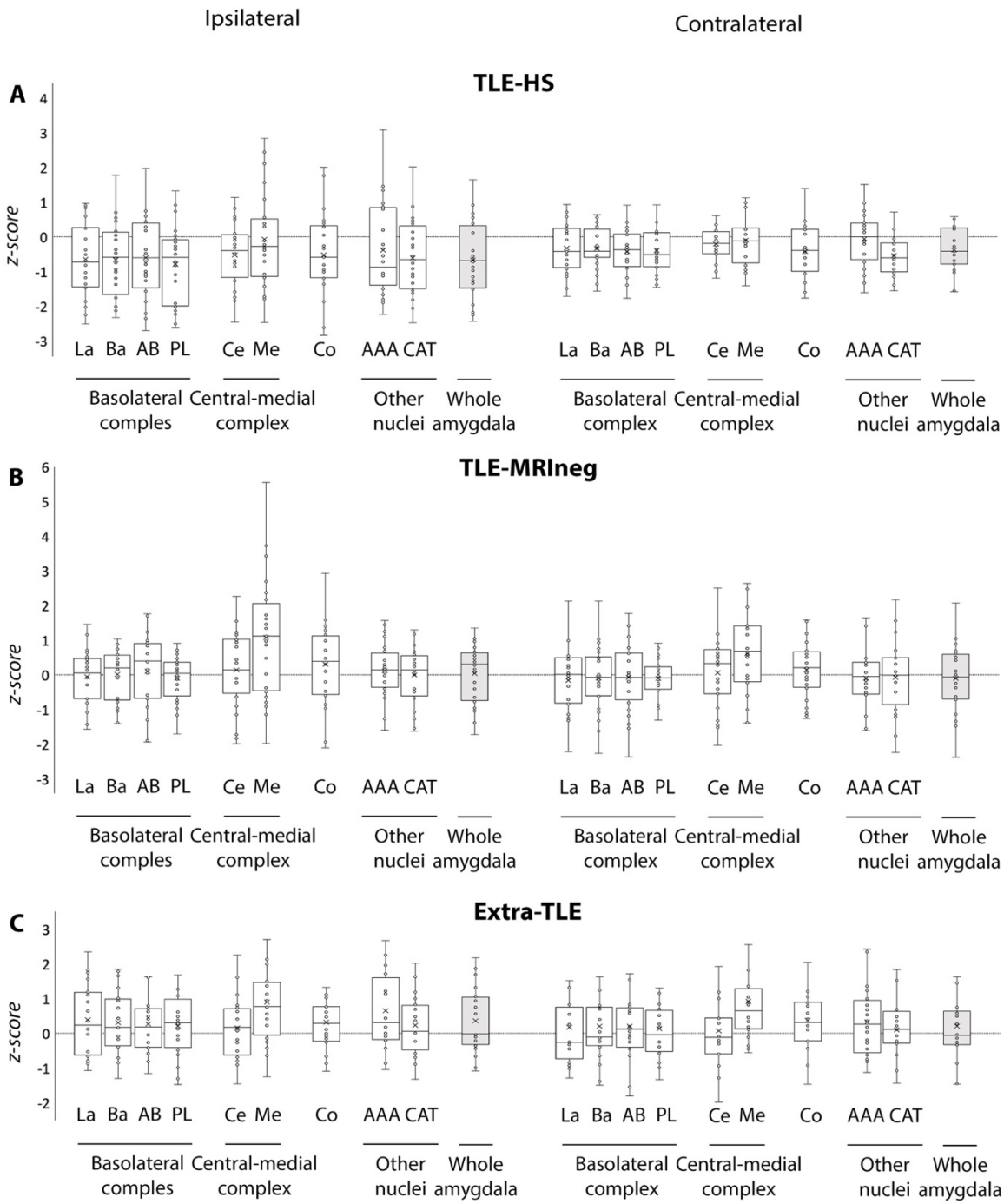

Figure 2.3. Amygdalar subnuclei comparisons between patients' groups and HC. Box-and-whisker plots of volumes of amygdalar structures ipsilateral and contralateral to the epileptic focus in patients with TLE-HS (a), TLE-MRIneg (b), and Extra-TLE (c) standardized relative to HC. The central horizontal line of the boxes marks the median of the sample, the upper and lower edges of the box (the hinges) mark the 25th and 75th percentiles (the central 50% of the values fall within the box). The open circles represent individual patients. The dashed line on value 0 designates the mean volume of HC. The "x" in the middle of each box marks the mean volume for every nucleus. The "*" on the box and/or on the complexes name indicates the significant results of the MANCOVA analysis ($p<.05$) of the volume differences between each patients' group and HC. La: lateral nucleus, Ba: basal nucleus, AB: accessory basal nucleus, PL: paralaminar nucleus, Ce: central nucleus, Me: medial nucleus, Co: cortical nucleus, AAA: anterior amygdaloid area, CAT: corticoamygdaloid transition area.

An overall atrophy of the whole amygdala, ipsilateral to the epileptic focus, was observed in the TLE-HS versus HC ($p_{Bonferroni}$=.040, d=-.613), TLE-MRIneg ($p_{Bonferroni}$=.010, d=-.708) and Extra-TLE ($p_{Bonferroni}$=.018, d=-.958). The atrophy involved particularly the BLA (TLE-HS versus HC, $p_{Bonferroni}$=.033, d=-.629; TLE-HS versus TLE-MRIneg, $p_{Bonferroni}$=.013, d=-.693; TLE-HS versus Extra-TLE, $p_{Bonferroni}$=.018, d=-.953) and all its constituent nuclei especially the basal nucleus (TLE-HS versus HC, $p_{Bonferroni}$=.042, d=-.620; TLE-HS versus TLE-MRIneg, $p_{Bonferroni}$=.015, d=-.723; TLE-HS versus Extra-TLE, $p_{Bonferroni}$=.027, d=-.942) and the paralaminar nucleus (TLE-HS versus HC, $p_{Bonferroni}$=.011, d=-.739; TLE-HS versus TLE-MRIneg, $p_{Bonferroni}$=.016, d=-.762; TLE-HS versus Extra-TLE, $p_{Bonferroni}$=.018, d=-.968). The cortical complex and its subnuclei were atrophic in the TLE-HS population versus TLE-MRIneg ($p_{Bonferroni}$=.010, d=-.698) ipsilateral to the epileptic focus. TLE-MRIneg demonstrated a significant increased volume of the medial nucleus ipsilateral to the epilepsy focus versus HC ($p_{Bonferroni}$=.012, d=.792) and versus TLE-HS ($p_{Bonferroni}$=.009, d=.733). Finally, Extra-TLE showed a statistically significant increase of the medial nucleus volume contralateral to the epilepsy focus compared to HC ($p_{Bonferroni}$=.037, d=.839) and TLE-HS ($p_{Bonferroni}$=.017, d=1.014). Although not significant, it must be noted the whole amygdala volume of TLE-MRIneg and Extra-TLE is greater than HC, especially the one ipsilateral to the epileptic focus. Given the results of MANCOVAs analyses, we explored the behavior of the BLA and the medial nucleus in all the patients' groups at individual level to isolate the patients in whom the abnormalities were observed. We thus considered abnormal values that were ±2 SD from the mean of normal controls. The BLA, ipsilateral to the epileptic focus, was reduced in its volume in 5 out of 24 TLE-HS (21%), no TLE-HS patients showed BLA enlargement. In TLE-MRIneg group, 6 out of 24 (25%) patients presented a larger medial nucleus ipsilateral to the epileptic focus, while the same nucleus resulted enlarged in 3 Extra-TLE patients (15%), contralateral to the epileptic onset. The medial nucleus was never reduced in its volume in any TLE-MRIneg and Extra-TLE patients.

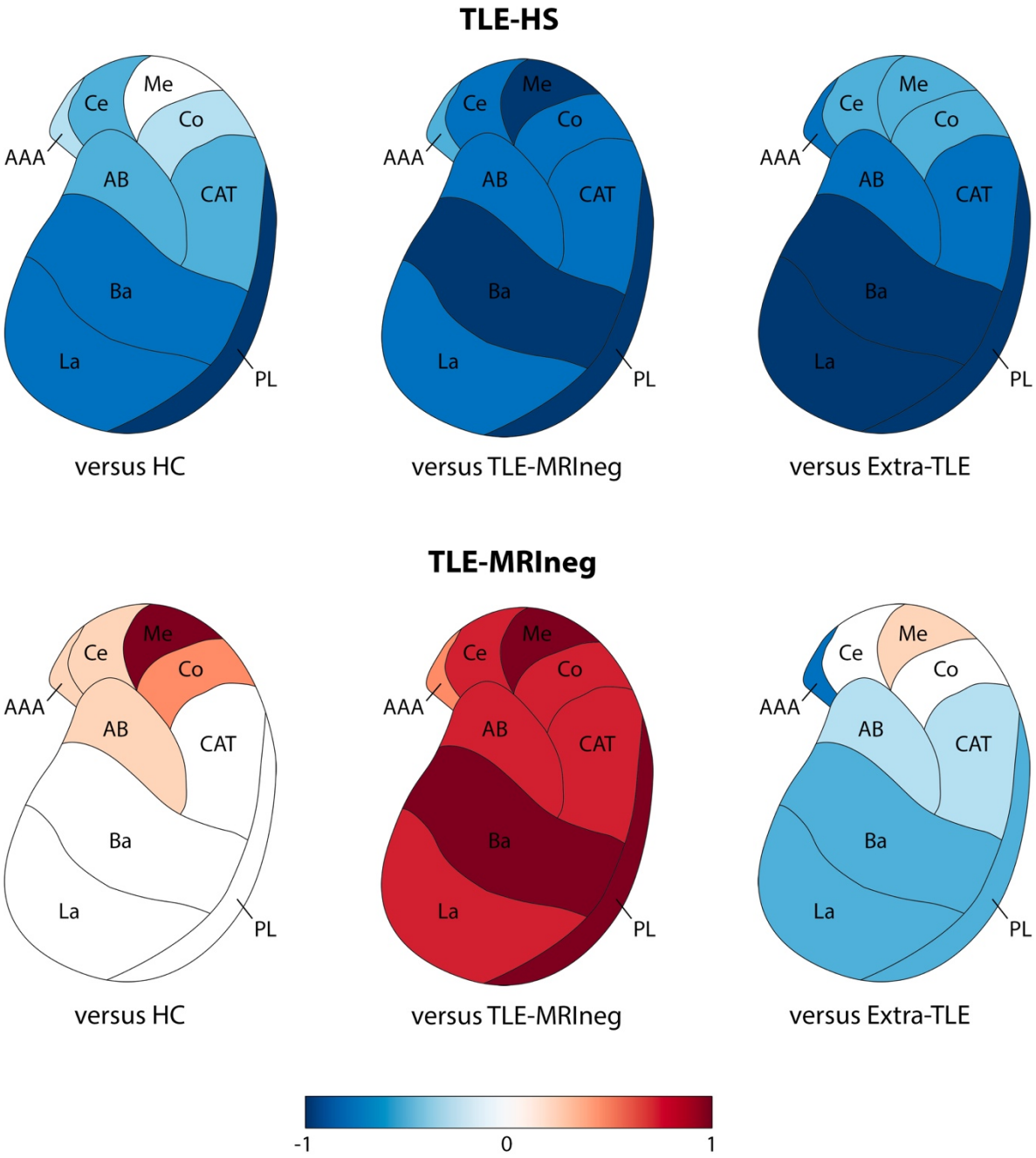

Figure 2.4. Graphic representations of amygdalar subnuclei comparisons between patients' groups and HC, and within patients' populations. Only the amygdala ipsilateral to the epileptic focus is presented. The comparison between TLE-HS and the other groups, and TLE-MRIneg and the other groups are represented with Cohen's d effect size value. Blue colors indicate a decrease of volume in amygdala subnuclei, red colors indicate an increase in volume of amygdala substructures. La: lateral nucleus, Ba: basal nucleus, AB: accessory basal nucleus, PL: paralaminar nucleus, Ce: central nucleus, Me: medial nucleus, Co: cortical nucleus, AAA: anterior amygdaloid area, CAT: corticoamygdaloid transition area. See text for details.

Logistic regression analysis

A multinomial logistic regression analysis showed that the BLA differentiated TLE-HS versus HC (β=.780, SE=.297, p=.009). Sensitivity and specificity of this model were 77% and 71% respectively (AUC=.704), the positive predictive value (PPV) was 77% and the negative predictive value (NPV) was 71%. In TLE-MRIneg, the logistic regression analysis showed the medial nucleus of the amygdala was able to discriminate this group from HC (β=.620, SE=.221, p=.005) with a sensitivity and a specificity of 53% and 93% respectively (AUC=.714, PPV=87%, NPV=72%). In both situations, the AUC measure suggests an acceptable, although not excellent, ability of the BLA and medial nucleus volumes to discriminate between patients (TLE-HS and TLE-MRIneg respectively) and controls. By counterpart, the volumes of both amygdala's subregions were not able to discriminate between TLE-HS and TLE-MRIneg [medial nucleus (β=.530, SE=.276, p=.054), basolateral complex (β=.133, SE=.380, p=.726)].

2.3.3. Correlation analyses

Age of epilepsy onset, epilepsy duration, number of ASMs, and drug-resistance were not correlated with the amygdala morphometric measures in both TLE-HS and TLE-MRIneg. Although limited by the small number of patients, we tested any significant relation between the presence of psychiatric comorbidity and amygdala volume measures. A significantly increased volume of the ipsilateral lateral nucleus [t(22)=2.117, p=.046, d=1.307] was observed in TLE-MRIneg patients with psychiatric comorbidity with respect to those without psychiatric disorders. No relations were observed in the entire TLE population between the amygdala subnuclei's volume and the presence of psychiatric comorbidity.

2.4. Discussion

To the best of our knowledge, this cross-sectional study is the first which utilizes automated neuroanatomical quantification to evaluate in vivo amygdala subnuclei volumetric differences in epilepsy patients. The main findings of the present study are (I) a significant atrophy of the whole amygdala, particularly the basolateral complex (BLA) in TLE-HS compared to HC and other epilepsy populations, and (II) a significant increased volume the medial nucleus (which is part of the central-medial complex) but not the whole amygdala in TLE-MRIneg group compared to HC. In both scenarios the involved amygdala's structure is ipsilateral to the epileptic focus. Additionally, we observed that the BLA and the medial nucleus of amygdala volumes can be differentiated TLE-HS

and TLE-MRIneg, respectively, versus HC, with a good performance. Overall, our findings, while confirming the involvement of the amygdala in TLE particularly in patients with mesial TLE with HS, expand previous knowledge as they suggest specific amygdala subnuclei as possible morphological biomarkers of TLE. Indeed, amygdala pathology is of great relevance in view of the importance of this region in the production of a full spectrum of experiential symptoms typical of temporal lobe seizures (Gloor et al., 1982), the sensitivity of the amygdala to kindling protocols in animal studies (Goddard, 1969), and its role in emotional/behavioral alteration in TLE (Bonora et al., 2011; Meletti et al., 2003; Monti & Meletti, 2015).

The involvement of the amygdala in mesial temporal lobe epilepsy is well recognized especially in association with HS. Histological reports from TLE patients with HS demonstrated in a large proportion the presence of amygdaloid damage represented mainly by neuronal loss and gliosis most often ipsilateral to the HS (Hudson et al., 1993). Previous volumetric studies have largely documented an amygdala atrophy in TLE-HS patients on the same side of the sclerotic hippocampus (N. Bernasconi, 2003; Cendes et al., 1993; Graebenitz et al., 2011), leading to hypothesize the smallest amygdala as a characteristic report of TLE due to HS (Cendes et al., 1993). Our analyses support these observations as a substantial decrease in volume of all the amygdala structures was observed in the TLE-HS population (**Fig. 2.3** and **2.4**) compared to HC. Additionally, the present morphometric data show that the volumes' reductions were ipsilateral to the epileptic focus for all the amygdala nuclei thus sustaining that the volumetric measurements of mesial temporal regions including the amygdala might be useful to the lateralization of the site of seizure onset in TLE (Cendes et al., 1993). In our population of TLE-HS patients, the amygdala's volumes were significantly different not only from HC but even when compared with TLE-MRIneg patients and, for some nuclei belonging to the BLA (see **Fig. 2.3** and **2.4**), to Extra-TLE subjects. The directionality of this difference is always versus an atrophy in TLE-HS patients. In line with our results, an increase in amygdala's volume has almost never been documented ipsilaterally to the TLE-HS (Mitsueda-Ono et al., 2011) while a recent study provided evidence of an amygdala enlargement contralateral to the HS in a proportion of patients with mesial TLE (Coan, Morita, Campos, et al., 2013). As far as the other subcortical structures, in line to what expected, hippocampal subfields were almost all atrophic ipsilaterally to the epileptic focus, thus supporting previous morphometric data in TLE-HS using the same methodological approach (Costa et al., 2019; Ono et al., 2021; Riederer et al., 2021). Atrophy was particularly pronounced in CA1-CA4 and dentate gyrus regions as already reported (Costa et al., 2019; Sadler, 2006). In our TLE-HS population, CA4 and the dentate gyrus appeared reduced in volume even contralaterally to the HS

when compared to controls. Neuronal loss in CA1, CA3, CA4, and in the dentate gyrus has been reported to be typically bilateral in mesial temporal sclerosis, although the atrophy is greater on the side of the epileptic focus (Sadler, 2006). Beyond the hippocampus, we demonstrated a bilateral thalamic atrophy coupled with a bilateral lateral ventricle enlargement. These data are in line with a growing body of literature (Bonilha et al., 2004; de Campos et al., 2016; Keller et al., 2014; Whelan et al., 2018) indicating that TLE-HS is an example of network disease in which atrophy extends beyond the mesial temporal regions. Additionally, the thalamic nuclei's segmentation demonstrated that the volumetric changes are mostly homolateral to the HS, in agreement with post-mortem anatomic-pathology evidence (H.-J. Lee et al., 2020; Sinjab et al., 2013). Intriguingly, our analysis shown that in HS patients, the nuclei belonging to the so-called "limbic thalamus" were mainly involved (Vertes et al., 2015). Wrist the pulvinar is not formally part of the limbic network, its involvement has been reported in mesial TLE epilepsies by intracerebral electrophysiological recordings (Guye et al., 2006; Rosenberg et al., 2006, 2009), imaging studies (Barron et al., 2015), and the entity of its atrophy linked to the resistance to epilepsy surgery (Keller et al., 2014). Since hippocampus and thalamus in TLE patients present specific morphometric patterns that have been largely documented (H.-J. Lee et al., 2020; K. M. Park et al., 2018; Riederer et al., 2021; Whelan et al., 2018; Wu et al., 2020), the results obtained by these additional analyses on hippocampus' subfields and thalamus' subnuclei reinforce the assumption that our TLE sample is representative of the general TLE population, and the amygdala subnuclei analyses are consequently reliable.

TLE-MRI negative patients represent a clinical challenge especially within the presurgical work-up. An increased volume of amygdala (i.e., AE) was found in MRI negative TLE in several reports and interpreted as possible epileptogenic focus (Coan, Morita, de Campos, et al., 2013; Lv et al., 2014; Mitsueda-Ono et al., 2011). By contrast, in our analysis the whole amygdala's volumes, while appearing greater in TLE-MRIneg and Extra-TLE with respect to controls, did not reach the statistical significance except for the medial nucleus of amygdala which resulted hypertrophic in both populations. It must be noted that the mean age at seizure's onset in our population were lower compared to previous studies (Beh et al., 2016). This is not trivial, as it has been shown by others a relationship between AE and a later epilepsy onset (Beh et al., 2016; Bower, 2003). In addition, AE in older age is more likely to be associated with a faster resolution of the amygdala enlargement at follow-up thus possibly reflecting inflammatory/encephalitis processes or seizures-induced changes (Na et al., 2020). The individual level analysis confirmed the hypertrophy of the medial nucleus in 25% of TLE-MRIneg and in 15% of Extra-TLE patients, while this nucleus was never atrophic in both

populations. These rates of amygdala volume changes, although limited to single subnuclei/complexes, are in line with previously reported percentage of AE in non-lesional TLE patients (Coan, Morita, Campos, et al., 2013; Coan, Morita, de Campos, et al., 2013; Reyes et al., 2017). Overall, the present analyses support and expand previous observations in patients with non-lesional focal epilepsy (Reyes et al., 2017), by confirming that the increased volume of amygdala represents an unspecific finding common across different epilepsy syndromes, probably not limited to MRI negative cases.

2.4.1. Different amygdala subnuclei involvement in TLE

Among the various nuclei of amygdala, the lateral and the BLA have been demonstrated to display the greatest histochemical (Yilmazer-Hanke et al., 2000) and pathological alterations (Aliashkevich et al., 2003) in patients with mesial TLE. The BLA is constituted of the lateral nucleus, the basal nucleus, the accessory basal nucleus, and the paralaminar nucleus, and it comprises 69% of the total amygdala volume in humans (LeDoux, 2007). This complex of the amygdala (i.e., BLA) receives strong sensory input from multiple cortical and thalamic sources (Aggleton et al., 1980; A. J. McDonald, 1998), which terminate primarily in the lateral nucleus, and has reciprocal interactions with the hippocampal formation (Benarroch, 2015), including the entorhinal cortex, perirhinal cortex and parahippocampal cortex. According to a recent study (Yang & Wang, 2017), the BLA and hippocampus generate a circuit of information, and the connection area of BLA with the hippocampus is typically the CA1 subregion which is one of the most vulnerable fields for gliosis and neuronal loss as observed in the HS (Dutra et al., 2015; Yang & Wang, 2017). Our results of a pronounced basolateral atrophy in TLE-HS ipsilateral to the epileptic focus support previous described electrophysiological and histochemical studies. The exact mechanism by which the amygdala activity can interplay with the atrophic hippocampus and contribute to seizures generation/maintenance is not completely clear, but evidence suggests an excitation-inhibition unbalance toward a disinhibited state (Kullmann, 2011; Yilmazer-Hanke et al., 2000) of the amygdala substructures. In the TLE-MRIneg group the medial nucleus was increased in its volume, ipsilateral to the epileptic focus. This nucleus belongs to the central-medial complex (CMC) and represents the main output of the amygdala to the brainstem and hypothalamus (Benarroch, 2015). Human neuroimaging studies support a role of the CMC in motor behavior and response preparation and throughout its connections with the hypothalamus and brainstem mediates the visceral and autonomic reactions to fear (Petrulis, 2020). Additionally, recent resting state fMRI studies provided evidence about its involvement also in the

emotional processing, social behavior and executive control process mediated by direct connection with the ventromedial frontal cortex (Kerestes et al., 2017). Future studies must integrate neuropsychological data and amygdala morphometric analysis to better understand if the involvement of different amygdala nuclear complexes is related to specific cognitive-behavioral impairments in larger cohorts of patients (see **Appendix A**). As an interesting and speculative observation, the medial nucleus appeared hypertrophic even in Extra-TLE patients, although contralateral to the epilepsy focus. The observation of an amygdala involvement ipsilateral to the epileptic focus in TLE while contralateral to Extra-TLE deserve further investigations, on higher number of subjects, and correlations with epilepsy and behavioral patients' phenotypes.

2.4.2. Relationship between amygdala subnuclear volumes and clinical variables

Correlation analyses did not disclose any significant relationship between the amygdala's subnuclei volumes and the clinical variables including age of epilepsy onset, duration of epilepsy, drug response status in the last 12 months, and ASMs load in TLE-HS and TLE-MRIneg. Similar findings have been observed by others in a larger cohort of patients with AE (Coan, Morita, de Campos, et al., 2013; Reyes et al., 2017). A remarkable result of this study was the correlation between the increased volume of the ipsilateral lateral nucleus (which is part of the BLA), in those patients with TLE-MRIneg and MADD symptoms. Despite the caution due to the small number of patients, this finding is of interest being consistent with previous volumetric studies in TLE patients with psychosis and dysthymia symptoms (Tebartz van Elst et al., 1999; Tebartz Van Elst et al., 2002). Patients with psychosis and epilepsy showed indeed an amygdala enlargement compared to TLE without psychiatric symptoms (Tebartz Van Elst et al., 2002). The basolateral amygdala integrates inputs from sensory and other limbic structures and has been theorized to function as "gatekeeper" by assessing incoming sensory information and assigning emotional saliency to appropriate stimuli. In addition, alteration of the BLA might affect downstream pathways involved in social cognition and decision-making processes throughout its communication with the prefrontal and orbitofrontal cortex (Sinha et al., 2015). Morphometric alterations of BLA have been documented in vivo in different psychiatric conditions (Aghamohammadi-Sereshki et al., 2021; Asami et al., 2018; Cui et al., 2020; L. Zhang et al., 2020). Particularly, in patients with psychosis, the basolateral amygdala, and particularly the lateral nucleus, resulted affected, confirming the role of this structure in schizophrenia patients, and highlighting an alteration of its volume as a biomarker even in unaffected but high-risk subjects (Armio et al., 2020). An interesting experiment in animals' models documented that BLA is selectively affected

by chronic stress and present microstructural alterations including dendritic hypertrophy and spine enlargement; these changes in turn correlated to the anxiety-like behaviors of the animals (Zhang et al., 2019). Recently, an enlargement of the BLA was positively correlated with social and communication impairments in adolescents with autism (Seguin et al., n.d.) and the deep brain stimulation of the BLA has been proposed as a possible treatment for social anxiety (Sinha et al., 2015).

2.4.3. Study Limitations

We are aware that this study has limitations. Firstly, we recognize the limited sample of patients studied in the TLE and Extra-TLE subgroups. However, this limitation is justified by the strict inclusion criteria adopted. We explored indeed the amygdala subnuclei volumes being careful to exclude patients with any sign of amygdala abnormalities on structural MRI, both in terms of altered volume and/or signal. MRI scans, including the oldest ones, were acquired using dedicated epilepsy protocols and inspected by expert neuroradiologists. Compatibly with the limitation of visual inspection, we are thus confident to have collected real "negative MRI" TLE cases. Secondly, the amygdala subnuclei segmentation adopted here has not previously been used in the epilepsy contest which raises concerns about the reliability of the approach adopted. Segmentation of amygdala nuclei is challenging due to small regional volumes and limited availability of a clear ground truth. The amygdala atlas was developed by manually segmenting amygdala in post-mortem samples using high resolution 7T MRI. Since its introduction (Saygin et al., 2017), the algorithm has been validated in different contests including psychiatric disorders (Armio et al., 2020; Asami et al., 2018; Cui et al., 2020) and premature born adults (Schmitz-Koep et al., 2021). Recently, Buser and colleagues (Buser et al., 2020) explored specifically the spatial and numerical reliability for the segmentation of amygdala and hippocampal nuclei in FreeSurfer. The numerical reliability was mostly high within all the amygdala subnuclei except for a few regions including the anterior amygdaloid area and the paralaminar nucleus, which demonstrated only moderate spatial reliability. Thirdly, medication could influence the amygdala and subnuclei volumes of TLE and Extra-TLE patients. In this study, all the patients were taking at least one ASM and mostly more than one, so we could not rule out drug effects on the results. However, correlation analysis did not disclose any relationship between the amygdala subnuclear volumes and the ASM drug-load. Fourth, this study is a cross-sectional study. Future studies would benefit from longitudinal monitoring to determine whether the amygdala and subnuclei volumes change during the individual's clinical progression. Different studies indeed reported a

decreased volume of enlarged amygdala at follow-up visits in parallel with achieving seizures' freedom, suggesting that at least in some patients, amygdala hypertrophy can be linked to seizures' recurrence (Na et al., 2020; Peedicail et al., 2020).

Chapter 3

The role of the amygdala in Ictal Central Apnea: insights from brain MRI structural morphometry

Elisa Micalizzi[1,2], Alice Ballerini[3], Giada Giovannini[4], Maria Cristina Cioclu[3], Simona Scolastico[3], Matteo Pugnaghi[4], Nicolò Orlandi[3], Marcella Malagoli[5], Maurilio Genovese[5], Alessandra Todeschini[5], Leandra Giunta[4], Flavio Villani[1], Stefano Meletti[3,4], Anna Elisabetta Vaudano[3,4]

[1]*Neurophysiology Unit, Epilepsy Center, IRCCS San Martino Hospital, Genoa, Italy*

[2]*PhD Program in Clinical and Experimental Medicine, University of Modena and Reggio Emilia, Modena, Italy*

[3]*Department of Biomedical, Metabolic and Neural Sciences, University of Modena and Reggio Emilia, Modena, Italy*

[4]*Neurology Unit, OCB Hospital, AOU Modena, Modena, Italy*

[5]*Neuroradiology Unit, OCB Hospital, AOU Modena, Modena 41126, Italy*

3.1. Introduction

Ictal central apnea (ICA) is a frequent clinical correlate of focal seizures, being observed in 40-43% of patients with focal epilepsy admitted to Epilepsy Monitoring Units (EMU) (Lacuey et al., 2018; Vilella et al., 2019). ICA is regarded as a potential electroclinical biomarker of sudden unexpected death in epilepsy (SUDEP), since ictal respiratory disruption has been demonstrated to be a relevant mechanism leading to a fatal outcome (Ryvlin et al., 2013; Vilella et al., 2019). Recent evidence supports ICA as a distinctive ictal semiological feature of TLE, in particular as a hint of the limbic network involvement (Lacuey et al., 2018; Micalizzi et al., 2021, 2022; Vilella et al., 2019). Data suggesting a functional connection between the amygdala and the neural respiratory networks in the brainstem derive from experimental studies conducted on animals (Bailey & Sweet, 1940; Hoffman & Rasmussen, 1953; Kaada et al., 1949; W. K. Smith, 1945). In humans, evidence of the relevance of the limbic network in the respiratory network can be found in electroclinical and invasive neurophysiological studies carried out for surgical purposes (Kaada et al., 1949; Penfield & Jasper, 1954). More recently, researchers' attention has focused on the role of the amygdala in generating the seizure-related central apneic response (Dlouhy et al., 2015; Lacuey et al., 2019; Nelson & Ray, 1968; Nobis et al., 2020). As demonstrated by studies that utilized stereo-EEG combined with video-EEG and cardiorespiratory polygraphy, both the primary and secondary involvement of the amygdala, especially of the basolateral complex (Dlouhy et al., 2015)(Dlouhy et al., 2015), throughout the

epileptic discharge, were strongly associated with ICA (Dlouhy et al., 2015; Lacuey et al., 2019; Nobis et al., 2020). Although ictal respiratory modifications are considered to be associated with a higher risk of SUDEP, data regarding morphometric modifications of subcortical structures in relation to ICA occurrence are scarce. Herein, we aim to investigate subtle morphometric changes of subcortical structures in ICA patients, specifically of the amygdala, thalamic and brainstem subnuclei, and to find valuable neuroimaging biomarkers of ICA in patients with focal epilepsy.

3.2. Methods and Materials

3.2.1. Study population

Patients were prospectively recruited among patients with epilepsy admitted to the Epilepsy Monitoring Unit (EMU) at the Ospedale Civile of Baggiovara, Modena Academic Hospital (Modena, Italy) from April 2020 to September 2022. Each patient underwent a Video-EEG Long-Term Monitoring (VLTM) with a 10-20 EEG system (Nihon Kohden Neurofax EEG-1200, Mod JE-120) integrated with a standard precordial single-channel electrocardiogram (EKG), pulse-oximetry for SpO2 measurement, and thoracoabdominal belt for respiratory inductance plethysmography. Patients were included according to the following criteria: (I) age over 14 at the time of hospitalization; (II) having a diagnosis of focal epilepsy; (III) having at least one focal seizure recorded during VLTM with cardiorespiratory polygraphy (EKG, pulse-oximetry and thoracoabdominal respiratory inductance plethysmography); (IV) having performed a high-resolution 3D T_1-weighted brain MRI scan. Patients were excluded if (I) they had a large brain lesion involving the subcortical structures and/or underwent neurosurgical procedures; (II) poor quality of MRI scans. According to published criteria, apnea was considered as a respiratory arrest of five or more seconds visible on the pneumographic channel, preceded and followed by stable breathing for at least five seconds, and confirmed by visual inspection of the recorded video (Kanth et al., 2020; Lacuey et al., 2018; Micalizzi et al., 2021, 2022; Vilella et al., 2019). Post-ictal apnea was defined as a respiratory arrest starting within five seconds after ictal discharge termination. For each patient, the following electroclinical data were collected: age at the time of admission, sex, age at 3D T_1-weighted brain MRI, age of epilepsy onset, disease duration, the hemisphere of the epileptogenic zone (EZ), family history of epilepsy, febrile seizures in past medical history, number of antiseizure medications (ASMs) at the time of brain MRI, ASMs response according to ILAE definition of drug-resistance (Kwan et al., 2010). As regards the ICA patients, further electroclinical information was collected: apnea duration, hypoxemia duration and nadir.

Patients meeting the inclusion criteria were subdivided into two groups: ICA and noICA patients in relation to ICA occurrence during the VLTM. A further analysis was performed considering only the patients with TLE subdivided in ICA-TLE and noICA-TLE. A pool of 30 healthy controls matched by age and sex was collected.

3.2.2. Magnetic resonance imaging (MRI) acquisition

All the included patients and controls underwent a 3T brain MRI for clinical purposes, adopting an epilepsy-dedicated standardized protocol which included a 3D T_1-weighted volumetric image (Bernasconi et al., 2019). MRIs were performed on a 3T scanner (3.0 Tesla GE Healthcare, Chicago, United States of America). Each patient was interviewed before the MRI scan to check for seizures occurring in the 48 hours before the exam and no patient reported seizures in this time window. Healthy controls underwent a structural MRI scan on the same scanner and with the identical protocol of patients. Quality check (QC) on images was twofold: (I) a qualitative QC taking into account the main common artifacts, including motion, ringing, and susceptibility. This visual-performed quality check ended with the judgment of "pass" for images with good quality or "fail" otherwise, following previous published workflow (Backhausen et al., 2016); (II) a quality assurance process (outlier detection based on interquartile of 1.5 standard deviations along with visual inspection of segmentations), was performed adopting a standardized ENIGMA (http://enigma.usc.edu), protocols as implemented in previous large-scale case-control studies of epilepsy (Larivière et al., 2020; B. Park et al., 2022; Whelan et al., 2018).

3.2.3. MRI post-processing

3.2.3.1. Voxel-based morphometry

For the voxel-based morphometry (VBM) analysis, 3D T_1-weighted images were utilized. Pre-processing and statistical analysis were performed using the computational anatomy toolbox (CAT12) and SPM12 (Statistical Parametric Mapping; http://www.fil.ion.ucl.ac.uk/spm) on Matlab 2020b (MathWorks, USA). First, the original NIfTI files were flipped to account for the side of the epileptic focus using SPM12 The X-axis was turned negative for all the right-sided patients in order to have the epileptic hemisphere on the left side for all the patients enrolled. Next, the scans were normalized according to the Montreal Neurological Institute (MNI) template using the high-dimensional DARTEL algorithm and modulated by multiplying the Jacobian determinant for each voxel in SPM12.

Images were segmented into GM, WM, and cerebrospinal fluid (CSF) in CAT12, and finally, the derived GM images were smoothed using 8-mm full-width-half-maximum Gaussian smoothing in SPM12. To search for subcortical volume differences across groups, two-sample t-tests ($p<0.001$, minimum threshold cluster of 30 voxels) were performed in SPM12 between ICA vs. noICA, ICA vs. controls, and noICA vs. controls. The same statistical analyses were carried out for the TLE subgroups (i.e., ICA-TLE, noICA-TLE, and controls).

3.2.3.2. Surface-based morphometry

The 3D T_1-weighted images were analyzed using a standardized image toolbox (FreeSurfer, v7.1, https://surfer.nmr.mgh.harvard.edu). Furthermore, the amygdala, hippocampus, thalamus, and brainstem were parcellated using FreeSurfer dev version (ftp://surfer.nmr.mgh.harvard.edu/pub/dist/freesurfer/dev) according to their respective pipelines (Saygin et al., 2017; Iglesias, Augustinack, et al., 2015; Iglesias et al., 2018; Iglesias, Van Leemput, et al., 2015). Specifically, for the amygdala, the extracted nuclei were the anterior amygdaloid area (AAA), cortico-amygdaloid transition area (CAT), and the basal (Ba), lateral (La), accessory basal (AB), central (Ce), cortical (Co), medial (Me), and paralaminar (PL) nuclei (**Fig. 3.1A**). These nuclei were also clustered in three major complexes adopting the pipeline already published by our group (Ballerini et al., 2022): (I) the basolateral amygdala (BLA), who included the basal, lateral, accessory-basal, and paralaminar nuclei; (II) the central-medial complex- (CMC), composed by the central and the medial nuclei; (III) the cortical complex (CO), who included just the cortical nucleus. The AAA and the CAT were considered "other nuclei". For the hippocampus, the following subfields were obtained: CA1, CA3, CA4, subiculum, presubiculum, parasubiculum, the molecular and granule cell layers of the dentate gyrus (GCMLDG), the molecular layer, hippocampal tail, and the hippocampal amygdala transition area (HATA) (**Fig. 3.1B**). For the purpose of the present work, we considered the volumes of the hippocampal body, head, and tail, as well as the whole hippocampal volume. For the thalamic segmentation, the volume of 25 individual thalamic nuclei was calculated for each side. The nuclei were clustered into 6 groups according to Iglesias et al. (2018) as follow: (I) the anteroventral nuclei in the anterior group; (II) the laterodorsal and lateral posterior nuclei in the lateral group; (III) the ventral anterior, ventral anterior magnocellular, ventral lateral anterior, ventral lateral posterior, ventromedial, and ventral posterolateral nuclei in the ventral group; (IV) the central medial, central lateral, paracentral, centromedian, and parafascicular nuclei in the intralaminar group; (V) the paratenial, medial ventral, mediodorsal medial magnocellular, and mediodorsal lateral parvocellular

nuclei in the medial group; (VI) and the lateral geniculate, medial geniculate, suprageniculate, pulvinar anterior, pulvinar inferior, pulvinar lateral, and pulvinar medial nuclei in the posterior group (**Fig. 3.1C**). Finally, the brainstem was segmented into four regions: medulla, pons, midbrain, and superior cerebellar peduncle (**Fig. 3.1D**).

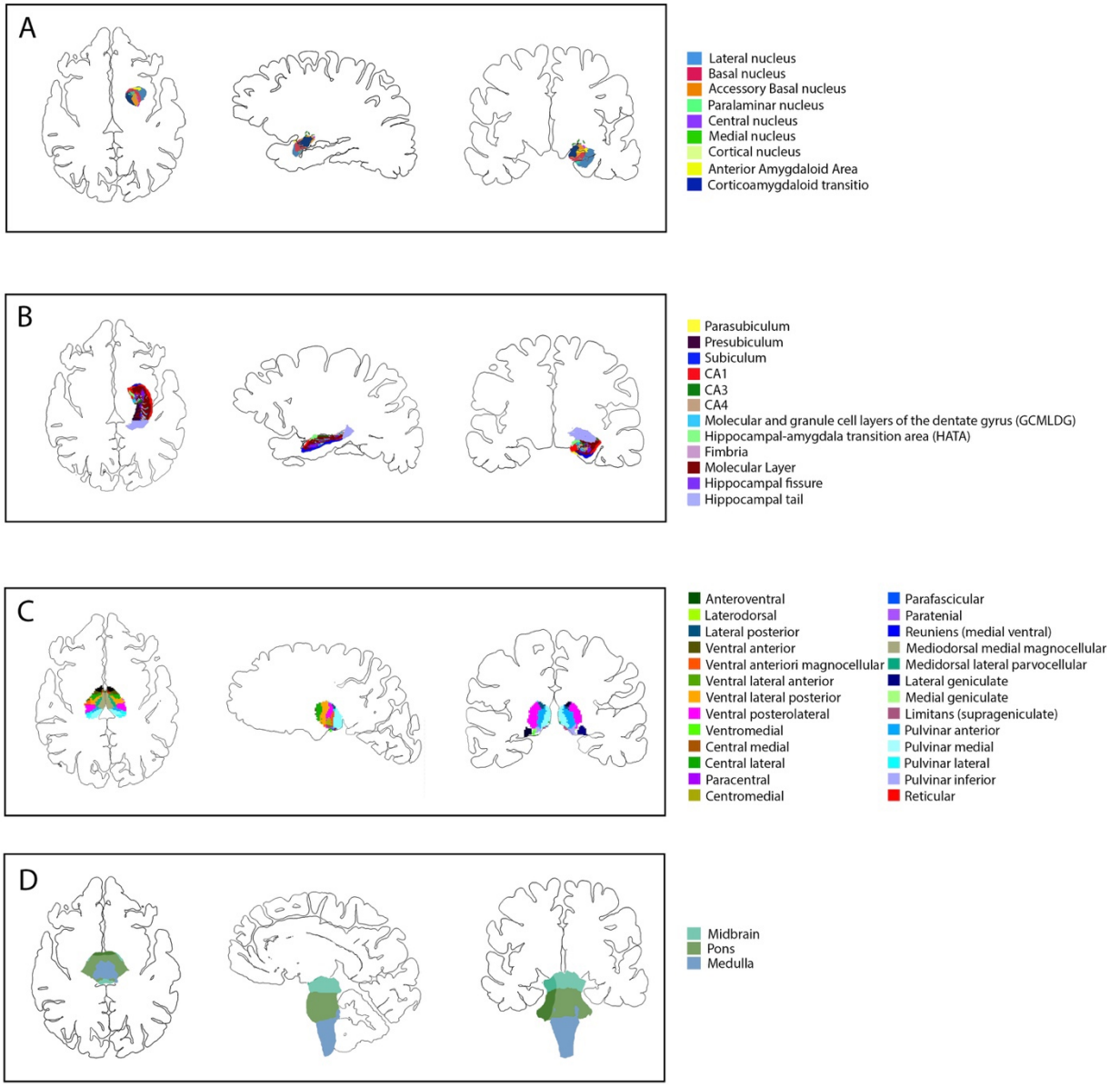

Figure 3.1. Parcellation of A. amygdala subnuclei, B. hippocampal subfield, C. thalamus nuclei, F. brainstem subregions based on relatives pipelines *(Saygin et al., 2017; Iglesias, Augustinack, et al., 2015; Iglesias et al., 2018; Iglesias, Van Leemput, et al., 2015).*

3.2.4. Surface-based statistical analyses

After testing for the normality distribution of the data with Shapiro-Wilks test, one-way ANOVAs and Chi-squared tests were used to assess differences in demographic and clinical variables among groups and between the patients' groups, and the control group. All subcortical volumes, their sub-parcellations, and the clustered complexes and groups were converted in z-scored based on the mean and the standard deviation (SD) of the control population. To account for the side of the EZ, all the subcortical measurements of right-sided patients were flipped to have all the morphometric data of the EZ on the left side. Thus, all morphometric values and results were reported as ipsilateral and contralateral with respect to the EF. Moreover, to assess for biological brain asymmetry, a pair sample t-test was performed for each subcortical volume in the control group. First, the group differences have been tested for all the morphometric subcortical values using two multivariate analyses of covariance (MANCOVAs): the first tested the volume differences across all ICA, noICA, and control groups; the second explored the differences only in the TLE sub-population (i.e., ICA-TLE, noICA-TLE, control). For each MANCOVA age, gender, and estimated total intracranial volume (eTIV) were included as covariates (Whelan et al., 2018). Finally, partial correlation analyses were performed between the regions of interest (ROIs) resulting significantly in the MANCOVAs and the clinical variables only in the ICA groups (i.e., all ICA and ICA-TLE). The following ICA-related variables were considered: apnea duration (in sec), desaturation's duration and nadir of desaturation (when present), whether there were group differences in drug-respondent and drug-resistant patients. The analyses were performed using SPSS software 28 (IBM, Chicago, IL), and statistical significance for all tests was set at $p<.05$. Significant p-values were considered when surviving a 5% FDR correction (Benjamini & Hochberg, 1995).

3.3. Results

In the study period, 46 patients met the inclusion criteria: 16 ICA and 30 noICA (**Table 3.1**). Among the ICA group, 12 patients were affected by TLE, 3 by frontal lobe epilepsy (FLE) and one by insular epilepsy (ILE). Fifteen participants out of the 30 noICA patients had a diagnosis of TLE, while the other 15 of FLE. A pool of 30 healthy controls, matched by age and sex, was collected. Statistical analyses did not highlight differences between patient groups and controls in age, sex, distribution, eTIV, age of onset, epilepsy duration, ASMs, and drug responsiveness (**Table 3.1**).

Table 3.1. Clinical and demographic differences between patients (ICA and noICA) and healthy controls.

	ICA (N=16)	noICA (N=30)	Control (N=30)	Stat.	p
TLE (y/n)	12/4	15/15			
Age	35.06(±12.234)#	37.20(±14.944)#	32.20(±12.234)	1.041^{F}#	.358#
	36.17(±13.037)*	39.47(±12.755)*		1.737^{F}*	.186*
Gender (F/M)	7/9#	13/17#	15/15	$.312^{X}$#	.856#
	5/7*	7/8*		$.243^{X}$*	.886*
eTIV	1.55^{E+06}(±1.38^{E+05})#	1.58^{E+06}(±1.80^{E+05})#	1.56^{E+06}(±1.41^{E+05})	$.186^{F}$#	.831#
	1.54^{E+06}(±1.58^{E+05})*	1.54^{E+06}(±1.54^{E+05})*		$.149^{F}$*	.862*
Age of onset	21.87(±14.678)#	22.53(±13.198)#	-	$.024^{F}$#	.878#
	24(±13.678)*	27.07(±13.477)*		$.341^{F}$*	.565*
Epilepsy duration	13.36(±15.028)#	14.72(±14.660)#	-	$.089^{F}$#	.767#
	12.37(±15.796)*	12.47(±13.376)*		$.000^{F}$*	.987*
ASM	2.50(±1.506)#	2.30(±1.317)#	-	$.218^{F}$#	.643#
	2.42(±1.240)*	1.60(±0.986)*		3.643^{F}*	.068*
Drug-respondent (y/n)	15/11#	10/20#	-	$.021^{X}$#	.886#
	4/8*	8/7*		1.080^{X}*	.299*

Data are presented in mean(±standard deviations). TLE=temporal lobe epilepsy, #=indicate the descriptive analyses and statistics regarding the entire population, *=indicate the descriptive analysis and statistics regarding the TLE subgroup only, eTIV=estimated intracranial volume, ASM=antiseizure medication, ^{F}=ANOVA, ^{X}=Chi-squared.

3.3.1. Electroclinical data

The detailed electroclinical data of the ICA patients are reported in **Table 3.2**. The etiology was either structural (11/16 patients) with a predominance of focal cortical dysplasias (FCDs), or unknown (5/16). Among the ICA patients, we recorded 87 seizures, 42 of which (48.3%) with seizure-related central apnea. Ten patients had hypoxemia as a consequence of ictal apnea, with an oxygen nadir ranging from 89 to 71%. No patient was aware of apnea occurrence. **Figure 3.2** displays the ictal EEG of one representative ICA patient. Regarding noICA cohort, 18 patients had structural etiology (mainly FCD) while in eight, it was not possible to find the underlying cause of epilepsy; two patients had an autoimmune cause and two a genetic etiology. The majority of patients (11/16 in the ICA group and 20/30 among the noICA) had drug-resistant epilepsy (Kwan et al., 2010). Four ICA patients underwent epilepsy surgery, but only for one patient (pt#9) the pathology of the amygdala was available and reported as gliosis.

Table 3.2. Electroclinical data in the ICA population

PtID/Age/Sex	Side/Epilepsy syndrome	Suspected etiology	Epilepsy duration	N° ASM/DR	Seizure frequency	Seizure occurrence	Surgery/ Histology	Follow Up#	N° seizures with ICA/ apnea duration	Oxygen desaturation (Nadir %)
1/32/ F	L/TLE	Unknown	7	1/no	>1/month	W/NREM	No	N/A	3/71.7(±10.7)	Yes (74%)
2/32/M	R/TLE	FCD	9	1/no	<1/month	W/NREM	Yes/FCD Ia	Ia	5/25.5(±23.4)	No
3/25/F	L/TLE	Unknown	10	3/yes	<1/month	W	No	N/A	1/16	Yes (89%)
4/51/M	R/TLE	B P calcifications	43	3/yes	<1/month	NREM	No	N/A	1/13	Yes (87%)
5/20/ M	L/TLE	Encephalocele	1	3/yes	>1/month	W	Yes/gliosis	Ib	2/31(±12.73)	Yes (76%)
6/55/F	L/TLE	HS	13	4/yes	>1/week	W	No	N/A	3/46.7(±47.2)	Yes (85%)
7/38/M	L/TLE	FCD	0.5	2/yes	>1/week	W	Yes/FCDIb*	Ia	1/11	No
8/41/F	R/TLE	FCD	10	3/yes	>1/week	NREM	No	N/A	1/30	No
9/50/M	L/TLE	Unknown	2	2/no	>1/week	W/NREM	No	N/A	10/37.7(±44.3)	Yes (87%)
10/21/M	R/TLE	Tumor (parieto-temporal LEAT)	4	3/yes	>1/month	W	Yes/ LEAT**	Ia	1/20	Yes (83%)
11/49/M	L/TLE	MCD	47	4/yes	>1/week	W	No	N/A	1/57	Yes (72%)
12/20/F	L/TLE	FCD	2	0/no	<1/month	W	No	N/A	1/23	No
13/42/M	R/FLE	Unknown	0.25	1/yes	>1/month	NREM	No	N/A	5/20.4(±20.4)	Yes (80%)
14/43/M	L/FLE	FCD	34	6/yes	>1/week	NREM	No	N/A	2/6.5(±2.8)	No
15/22/F	L/ILE	FCD	19	3/yes	>1/week	NREM	No	N/A	4/31.5(±2.6)	Yes (71%)
16/20/F	R/FLE	Unknown	12	1/yes	>1/month	W	No	N/A	1/12	No

Age and epilepsy duration are expressed in years. M=Male; F=female; L=Left; R=Right; B=Bilateral; TLE=Temporal Lobe Epilepsy; FLE=Frontal Lobe Epilepsy; ILE=Insular Lobe Epilepsy; P=Parietal; FCD=Focal Cortical Dysplasia; HS=Hippocampal Sclerosis; LEAT=Long term Epilepsy Associated Tumors; MCD=Malformation of Cortical Development; DR=Drug Resistance; ASM=Antiseizures Medications; W=Wakefulness. Apnea duration is expressed in seconds, if more than one apnea is recorded, the average length is displayed (± SD). Oxygen desaturation is expressed in %. (*)=histological report described an amygdala gliosis beyond the FCD in the temporal pole; (**)=the detail histology reports a glioneural lesion IDH1R132 wild type. #=Follow-up have been reported at 12 months from surgery according to Engel 1993 (Engel, 1993).

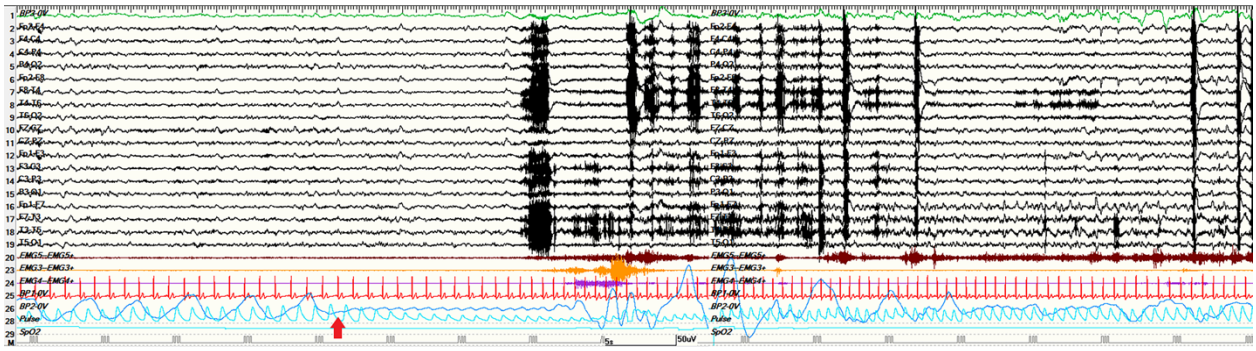

Figure 3.2. A 2-minute view of a left temporal seizure occurring during N2 sleep in a representative ICA patient (pt#9). ICA onset is indicated by the red arrow and precedes the appearance of the electrographic discharge over the left fronto-temporal regions. No hypoxemia was recorded during this seizure. Red channel: EKG; light blue channel: pulse-oxymetry; blue channel: thoracoabdominal respirogram.

3.3.2. Voxel-based morphometry results

The VBM whole-brain analysis showed an increased grey matter volume of the amygdala ipsilateral to the EZ in the ICA group with respect to noICA patients (MNI coordinates: X -19.50, Y -9, Z -13.50, T maximum = 3.24; number of contiguous voxels: K 181, $p < 0.190$). Moreover, the sub-analysis in the TLE group demonstrated a greater grey matter volume of the ipsilateral amygdala in the ICA-TLE patients compared with both noICA-TLE group (MNI coordinates: X -21, Y -3, Z -18; T maximum = 4.21; number of contiguous voxels: K 901, $p < 0.006$) and controls (MNI coordinates: X -19.5, Y 3, Z -27; T maximum = 4.01; number of contiguous voxels: K 138 $p < 0.234$) (**Fig. 3.3**).

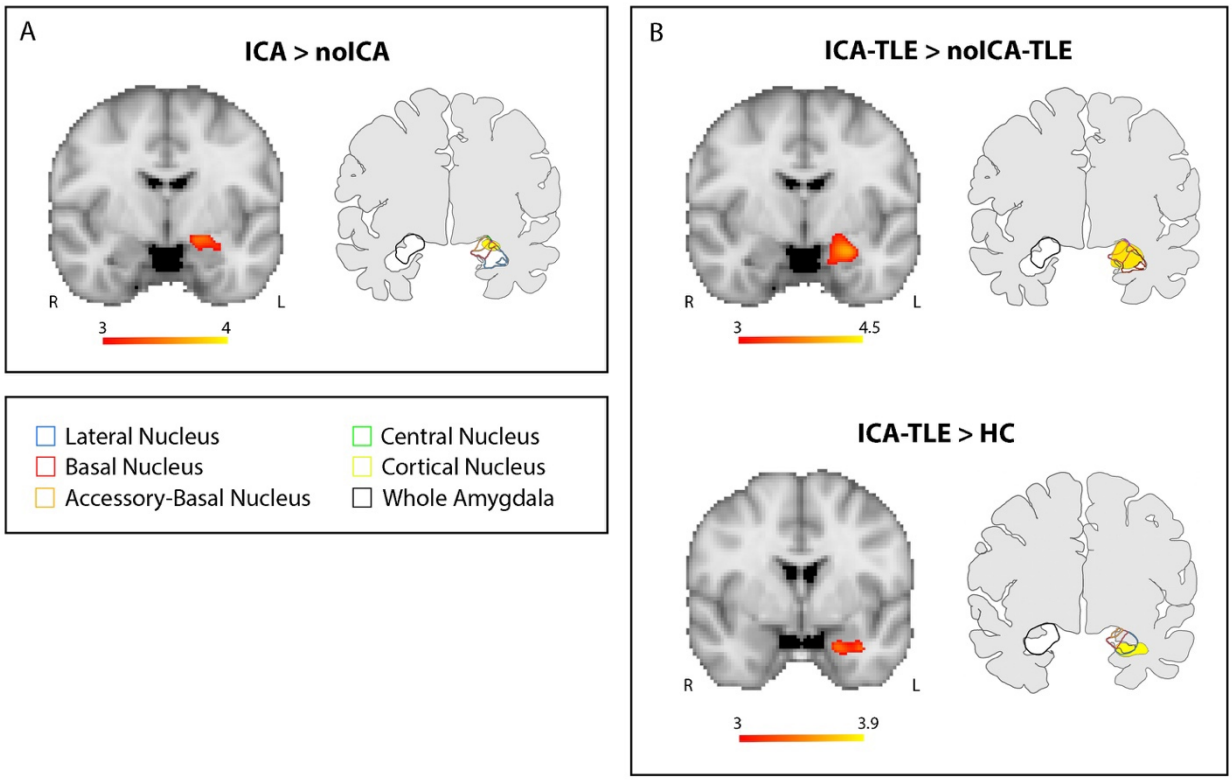

Figure 3.3. Voxel-based morphometry (VBM) results. Panel A: VBM analysis looking for grey matter volume increase in ICA compared to noICA patients. Panel B: VBM analysis exploring grey matter volume increases in ICA-TLE compared to noICA-TLE patients (upper images) and ICA-TLE compared to HC (lower images). For each Panel, left images show significant amygdala enlargement on the left side. Results are displayed on the coronal Montreal Neurological Institute (MNI) template image (MNI152-T1-2 mm). Color bar reflects T scores. Right images of each panel display the overlap of the VBM results and the amygdala subnuclei segmentation as provided by Saygin et al. (2017) 22. R=right; L=Left.

3.3.3. Surface-based morphometry results

The statistical analyses of subcortical volumes revealed significant volumetric differences only for the amygdala ipsilateral to the EZ, and its nuclei and complexes. The whole amygdala ipsilateral to the EZ was found to have a greater volume in ICA versus HC and ICA versus noICA, specifically the BLA (**Table 3.3 and Figure 3.4A**). The sub-analysis of single amygdalar nuclei showed an increase in the volume of the lateral nucleus in the comparison ICA versus HC (**Table 3.3**). The other amygdala nuclei did not show any differences in volume in ICA versus other populations and similarly, no significant differences were noted in the comparison between noICA and controls for any amygdala nuclei. When focusing on TLE patients, the ipsilateral whole amygdala volume was greater for the ICA-TLE group compared to controls, with the BLA appearing to be greater in volume (**Table 3.3** and **Figure 3.4B**, left panel). Moreover, the ICA-TLE patients compared to the noICA group, showed a larger ipsilateral BLA complex (**Table 3.3** and **Figure 3.4B**, right panel). Notably, no differences

were found when comparing noICA-TLE patients versus healthy controls. No other statistically relevant modifications were observed for the other subcortical structures including hippocampal, thalamic and brainstem subfields. Statistical correlation between ICA-related variables and amygdala volumes did not show any significant association.

Table 3.3. Significant structural morphometric comparison of ipsilateral amygdala complexes and subnuclei among patients' groups and controls.

Structure	ICA	noICA	Control	F	p	Pairwise comparisons°
Whole amy	1987.231(±214.919)# 2016.651(±231.994)*	1863.597(±292.128)# 1846.685(±338.526)*	1800.712(±183.124)# 1800.712(±183.124)*	5.383# 5.658*	.007# .006*	ICA > HC: p=.043# ICA > noICA: p=.038# ICA-TLE > HC: p=.022*
BLA	1611.857(±178,427)# 1640.033(±192.793)*	1511.947(±232.534)# 1497.260(±267.605)*	1452.557(±152.766)# 1452.557(±152.766)*	5.121# 6.742*	.008# .003*	ICA > HC: p=.026# ICA > noICA: p=.034# ICA-TLE > HC: p=.005* ICA-TLE > noICA-TLE: p=.035*
Lateral	743.436(±91.861)# 760.645(±99.570)*	695.239(±98.912)# 688.131(±109.486)*	668.163(±76.014)# 668.163(±76.014)*	6.160# 8.045*	.003# .001*	ICA > HC: p=.037# ICA-TLE > HC: p=.006*
Basal	516.310(±60.513)*	470.823(±92.370)*	457.621(±49.988)*	5.446*	.007*	ICA-TLE > HC: p=.017*

Data are presented in mean(±standard deviations). Amy=amygdala, BLA=Basolateral Complex, #=indicates the descriptive analyses and statistics regarding the entire population, *=indicates the descriptive analysis and statistics regarding the TLE subgroup only, °=P-value of pairwise comparisons between groups using FDR (False Discovery Rate) correction.

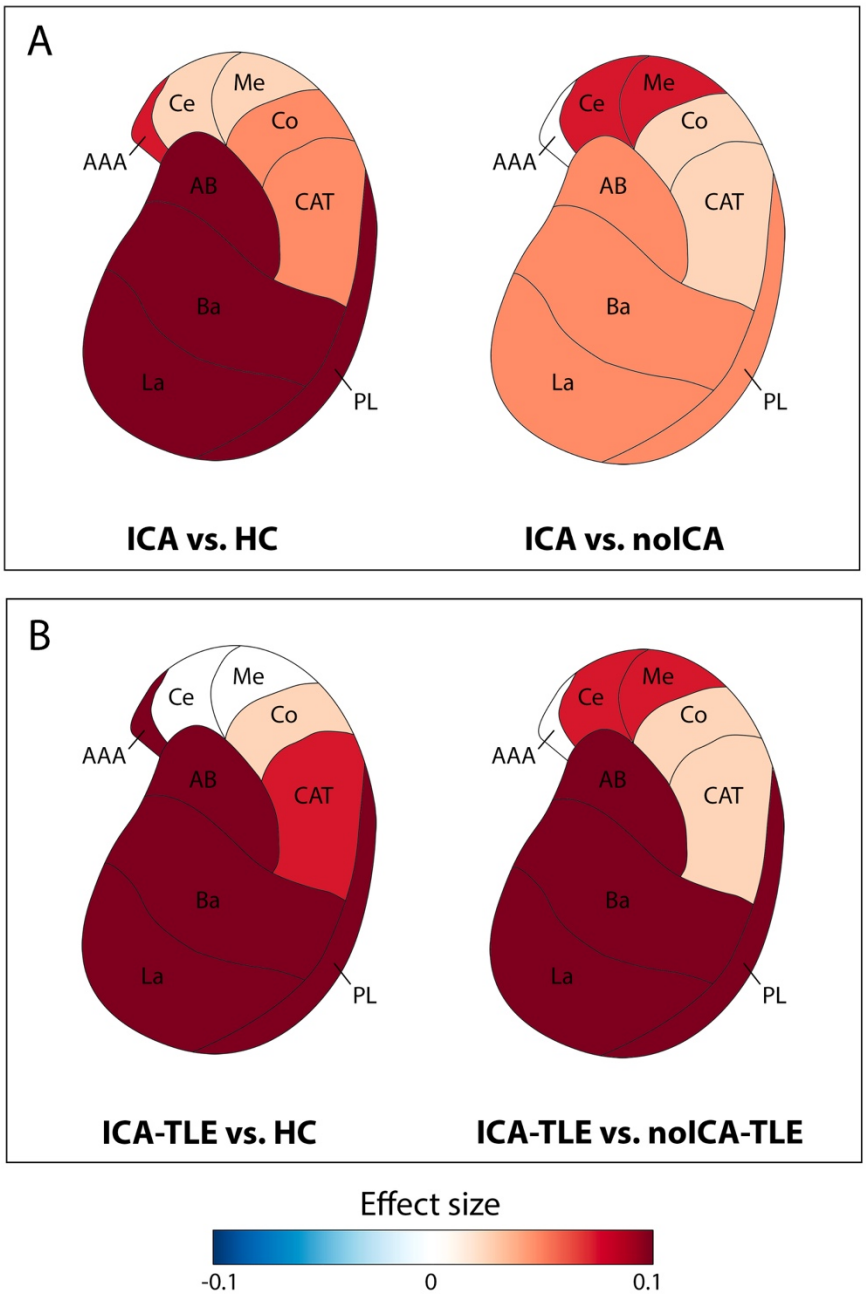

Figure 3.4. Amygdalar subnuclei comparisons between ICA, noICA, and HC in the whole population and in TLE subgroups. The comparisons between ICA and the other groups (i.e., HC and noICA) are represented using η^2 effect size value. Red colors indicate an increase in volumes of amygdala substructures, blue colors indicate a decrease. Only the amygdala ipsilateral to the epileptic focus is presented. Panel A shows the comparison between all ICA versus HC (left image) and noICA (right image). Panel B shows the comparison between the subgroups of ICA-TLE compared to HC (left image), and noICA-TLE (right image). La: lateral nucleus, Ba: basal nucleus, AB: accessory basal nucleus, PL: paralaminar nucleus, Ce: central nucleus, Me: medial nucleus, Co: cortical nucleus, AAA: anterior amygdaloid area, CAT: corticoamygdaloid transition area. See text for details.

3.4. Discussion

This study provides evidence that subtle structural volume changes can be found in patients presenting with focal seizures and ICA by means of advanced neuroimaging techniques. ICA is a quite frequent ictal phenomenon, especially, but not exclusively (Micalizzi et al., 2022), among patients with focal epilepsy. Indeed, the incidence of ictal autonomic manifestations and ictal respiratory changes is considered to be higher in temporal lobe seizures (Lacuey et al., 2018; Micalizzi et al., 2022; Tio et al., 2020). This study offers a specific insight on the physiopathological mechanisms of ictal central apnea, which is also regarded as a possible risk factor for SUDEP (Schuele et al., 2011; Vilella et al., 2019).

3.4.1. ICA and the basolateral complex

Previous invasive neurophysiological studies (Dlouhy et al., 2015; Lacuey et al., 2019; Nobis et al., 2020) reported that the direct electrical stimulation of the amygdala was sufficient to induce a transient respiratory arrest, both in relation to ictal activity and as a physiological response. Within the amygdala, the implicated nuclei seem to be the basal, lateral, and central. Specifically, one study (Dlouhy et al., 2015) identified the lateral and basal nuclei to be the most implicated in generating the apneic response, while other authors (Nobis et al., 2018) pointed out that only the direct stimulation of the central nucleus could lead to central apnea. Later, Lacuey et al., (2019) found that low- and high-frequency stimulation of basal and central nuclei induced apnea, while only high-frequency stimulation of the lateral nucleus was needed to obtain the apneic phenomenon. According to this evidence, our advanced neuroimaging findings showed that the whole amygdala ipsilateral to the EZ is increased in volume in patients with ICA, with the BLA being the most involved when considering the amygdala subnuclei. This volumetric increase confirms and expand previous suggestions regarding the involvement of the amygdala and specifically of the BLA in the epileptic network of patients with ictal central apnea. In the ICA group, the BLA was significantly greater in volume in comparison to both noICA patients and healthy controls. This observation could lead to the hypothesis that the BLA enlargement on advanced neuroimaging might be a biomarker for ICA occurrence in patients with focal epilepsy. This finding was supported by even stronger statistical significance when considering only the TLE patients. Thus, the ictal central apneic phenomenon may be reasonably a distinctive hallmark of temporal lobe epilepsy rather than extra-temporal seizures, as already reported (Lacuey et al., 2018; Micalizzi et al., 2022; Tio et al., 2020). Nevertheless, we already showed that even an ictal discharge that originates from extra-temporal cortical areas may secondarily involve the temporal regions causing the ictal respiratory arrest (Micalizzi et al., 2022; see **Appendix B**). Of note,

considering the presence of hippocampal sclerosis, only one ICA-TLE patient presented with this radiological finding, while this was evident in 5 noICA-TLE patients. As already reported in the literature, it was demonstrated that HS was significantly associated with volumetric reduction of the ipsilateral amygdala and, in particular, of the BLA (Ballerini et al., 2022). It could be argued that amygdalar atrophy could partially explain the volumetric differences between these two groups. However, the comparison against the healthy control group corroborates our main hypothesis that the volumetric changes may be more likely related to the apnea occurrence. We could also speculate that HS could be somehow protective against ictal respiratory arrest, but further evidence is warranted. As for the anatomo-physiological aspects, the BLA is constituted of the lateral nucleus, the basal nucleus, the accessory basal nucleus, and the paralaminar nucleus and comprises the majority of the total amygdala volume in humans (LeDoux, 2007). This complex of the amygdala receives strong sensory input from multiple cortical and thalamic sources which terminate primarily in the lateral nucleus, and has reciprocal interactions with the hippocampal formation, including the entorhinal cortex, perirhinal cortex, and parahippocampal cortex (Aggleton et al., 1980; Benarroch, 2015). The BLA is composed of neurons that resemble the pyramidal neurons of the cortex, leading to the hypothesis that for some TLE cases the primary epileptogenic focus in mesial TLE might be the amygdala itself and, specifically, the BLA (Benarroch, 2015; Lacuey et al., 2019). While the lateral nucleus does not directly project to the brainstem, it might influence the apneic response through intrinsic connections to amygdala nuclei or through hippocampal and thalamic projections.

3.4.2. The amygdala increased volume and SUDEP risk

Previous studies investigated the cortical and subcortical morphometric modifications in SUDEP patients and in patients with epilepsy considered to be at higher risk for SUDEP (L. A. Allen, Harper, et al., 2019; L. A. Allen, Vos, et al., 2019; Wandschneider et al., 2015). Different morphometric alterations were found in terms of cortical thickness and volume of brain structures, in the direction of tissue gain as well as atrophy. Specifically, in a previous study, the right amygdala appeared to have an increased volume in cases of SUDEP and those at high risk compared with low-risk and healthy controls (Wandschneider et al., 2015). Other authors observed a volumetric increase of the amygdala bilaterally in SUDEP patients versus healthy controls and of the right amygdala in high-risk patients compared to controls (L. A. Allen, Vos, et al., 2019). It is well known that peri-ictal respiratory impairment represents a risk factor for SUDEP. Our data provide an "imaging" link between ICA and SUDEP and confirm the key role of the amygdala in the pathophysiology of both phenomena.

The hypertrophy of the amygdala might be due to structural rearrangements, possibly secondary to the long-standing epileptic activity (Minami et al., 2015). As a consequence, the tissue gain of the amygdala might correspond to a gain of function, therefore leading to more chances that ictal apnea/SUDEP to occur.

3.4.3. Study limitations

Despite our novel findings, this study presents some limitations. Firstly, the number of participants is limited which could be due to the relatively short study-period and to strict inclusion criteria for patient recruitment. In particular, the number of extra-TLE patients with ICA is limited, thus preventing us from performing a thorough electro-clinical and imaging characterization of this population. In this scenario, our findings of a greater amygdala volumes in ICA-TLE patients need to be verified by further studies including a higher number of extra-TLE patients. Secondly, the absence of correlation with clinical variables needs to be interpreted with caution given the small study population. Of note, however, this finding could be of interest to better understand the pathophysiology of apnea phenomena. The amygdala volume increases can represent indeed a biomarker *per se* independently of any other clinical factor and, in particular, of apnea severity. Overall, our data support the need of larger multi-center studies to overcome these limitations and provide further evidence supporting these novel results.

3.5. Conclusion

ICA is a frequent clinical correlate of focal seizures, particularly involving the temporal lobe and limbic network. According to the literature, the amygdala appears to play a key role in giving rise to the apneic response. Our findings on neuroimaging data support what has already been demonstrated about the involvement of the basolateral complex ipsilateral to the EZ, also suggesting that the volume increase of this specific amygdalae subregion could be a distinctive hallmark of ICA in patients with epilepsy. The identification of valuable biomarkers of ictal autonomic manifestations is needed for a more accurate stratification of the SUDEP risk.

Chapter 4

Spatial patterns of gray and white matter compromise relate to age of seizure onset in temporal lobe epilepsy

Alice Ballerini[1,2], Donatello Arienzo[2,3], Alena Stasenko[2,3], Adam Schadler[2,3], Anna Elisabetta Vaudano[1,4], Stefano Meletti[1,4], Erik Kaestner[2,3,‡], Carrie R. McDonald[2,3,‡]

[1]*Department of Biomedical, Metabolic and Neural Science, University of Modena and Reggio Emilia, Modena, Italy*

[2]*Department of Psychiatry, University of California, San Diego, USA*

[3]*Center for Multimodal Imaging and Genetics, University of California, San Diego, USA*

[4]*Neurology Unit, OCB Hospital, AOU Modena, Italy*

‡ Both authors contributed equally as senior authors

4.1. Introduction

Temporal Lobe Epilepsy (TLE) is often a debilitating disorder, affecting both gray matter (GM) and white matter (WM) networks throughout the brain (Hatton et al., 2020; Whelan et al., 2018). These pathological changes can be progressive and are intricately linked to clinical outcomes and cognitive comorbidities (Kaestner et al., 2019; Reyes et al., 2020; Stasenko et al., 2022). Thus, it is important to understand the origins and the disease mechanisms that contribute to GM and WM pathology in TLE.

TLE can begin at any point in life and lead to abnormalities in brain structure and function. However, the brain is particularly vulnerable to the effects of epilepsy during childhood (Beghi, 2020). As a result, age of seizure onset has important implications for understanding patterns of GM and WM pathology and how they relate to one another. In particular, recurrent seizures early in life, during a period of heightened plasticity and brain development, may disrupt WM myelination and/or interfere with synaptic pruning in neocortex leading to structural abnormalities in the WM and GM, respectively (Bencurova et al., 2022; Blümcke et al., 2013; B. Hermann et al., 2002). These changes may occur globally, or they may be more pronounced proximal to the seizure focus. Conversely, when seizures begin in adulthood, they may lead to different patterns of GM and WM vulnerability because of decreases in brain plasticity in the fully developed brain (Doucet et al., 2015).

Despite accumulating evidence for the presence of broad cortical thinning (Larivière et al., 2020; C. R. McDonald, Hagler, et al., 2008), subcortical volume loss (Whelan et al., 2018), and WM compromise in TLE (Hatton et al., 2020; Stasenko et al., 2022), studies investigating how GM and

WM pathologies are related to one another are limited (Chang et al., 2019; Liu et al., 2016; Winston et al., 2020). Neocortical GM appears to follow a widespread multi-lobar and bilateral pattern of atrophy in TLE (Galovic et al., 2019; Larivière et al., 2020; C. R. McDonald, Hagler, et al., 2008). Conversely, there is some evidence that limbic WM damage is more pronounced in the ipsilateral hemisphere and is greatest close to the seizure focus (Hatton et al., 2020; Urquia-Osorio et al., 2022). However, because GM and WM developmental trajectories differ markedly early in life (Bethlehem et al., 2022), associations between the two may differ as a function of when seizures begin. Indeed, WM pathology has been shown to be more pronounced in those with an early seizure onset (Nagy et al., 2016), and there is evidence that injury to the WM sub-adjacent to the neocortex (i.e., the superficial white matter; SWM) is related to hippocampal sclerosis (HS) (Liu et al., 2016) — another feature associated with early seizure onset in TLE. However, the presence of HS has also been associated with broad patterns of cortical thinning, suggesting a relationship between hippocampal and cortical damage in TLE (Bonilha et al., 2010; Mueller et al., 2009). To date, studies that have investigated the spatial patterns of atrophy in cortical thickness and SWM (Chang et al., 2019; Liu et al., 2016; Winston et al., 2020) hint that different biological processes are likely driving these two types of injury in TLE. However, these studies did not directly explore the role of the age of seizure onset and test how the age at which seizures begin influences cortical-subcortical GM atrophy relationships with WM disruption.

Our study aims to extend knowledge about the processes underlying GM and WM atrophy across the developmental spectrum using structural and diffusion MRI. First, we examine patterns of subcortical and cortical GM atrophy and WM microstructural loss in a large group of individuals with drug-resistant TLE compared to healthy controls. Next, we characterize how these pathologies spatially correlate in TLE. Finally, we explore how GM and WM atrophy relationships vary across different ages of seizure onset. We test this by measuring changes not only in neocortical thinning and subcortical GM, but also in both the SWM and deep WM tracts, leading to a comprehensive analysis of neuroanatomical relationships in TLE.

4.2. Methods and Materials

4.2.1. Participants

Eighty-two patients with focal TLE [mean age 35.85(±12.95), 44 females] and 59 healthy controls [mean age 36.95(±13.72), 36 females] were enrolled from the UC San Diego and UC San Francisco Epilepsy Centers. The TLE diagnoses were established by board-certified neurologists with

expertise in epileptology, according to the criteria defined by International League Against Epilepsy (ILAE, (Fisher et al., 2017; Scheffer et al., 2017)). Forty-three out of 82 patients were classified as left TLE (L-TLE), and 39 were classified as right TLE (R-TLE) based on video-EEG telemetry, clinical history, seizure semiology, and neuroimaging evaluation. The MRI images were visually inspected by a board-certified neuroradiologist with expertise in epileptology, in order to detect the presence of HS. Patients with and without HS were enrolled in this study, however we excluded patients with space-occupying lesions (e.g., focal cortical dysplasia, tumors).

4.2.2. Image acquisition

MRI sequences were performed on a General Electric Discovery MR750 3T scanner with an 8-channel phased-array head coil at either UCSD or UCSF. Both centers used a prospectively harmonized and identical MRI acquisition that included a conventional three-plane localizer, GE calibration scan, a T1-weighted 3D structural scan (TR=8.08 ms, TE=3.16 ms, TI=600 ms, flip angle=8°, FOV=256 mm, matrix=256×192, slice thickness=1 mm), and for diffusion, a single-shot pulsed-field gradient spin-echo EPI sequence (TE/TR=80.4 ms/8 s; FOV=240 mm, matrix=128×128×53; axial). Diffusion-weighted images were acquired with b=0 and b=1000 mm^2/s with 30 diffusion gradient directions. Two additional b=0 volumes were acquired with either forward or reverse phase-encode polarity for use in B0 correction. Both T1w and DWI data were preprocessed using a multimodal imaging processing pipeline developed for the *Adolescent Brain Cognitive Development* study, according to Hagler et al., 2019 (Hagler et al., 2019).

4.2.3. Image processing

4.2.3.1. T_1-weighted image processing

Automatic segmentation of T1-weighted images was performed with FreeSurfer (v7.1.1, (Fischl, 2012)). From the structural MRI, 16 subcortical volumes were segmented and 68 cortical regions of interest (ROIs) were parcellated and cortical thickness was derived based on the Desikan-Killiany atlas (Desikan et al., 2006). Visual inspections of morphometric segmentations were conducted following standardized FreeSurfer protocols.

4.2.3.2. Diffusion-weighted imaging processing

The diffusion MRI images were corrected for spatial and intensity distortions due to B0 magnetic field inhomogeneities, eddy current distortion, gradient nonlinearity distortion, and head motion using FSL's TOPUP (Andersson et al., 2003; S. M. Smith et al., 2004). The reverse gradient method was used to correct B0 distortion (Holland et al., 2010). A method using least squares inverse and iterative conjugate gradient descent was used to correct for eddy currents (Zhuang et al., 2006). Distortions due to gradient nonlinearity were corrected for each frame of the diffusion data (Jovicich et al., 2006). Head motion was corrected by registering each frame to the parameters obtained through diffusion tensor fitting, accounting for variation in image contrast across diffusion orientations (Hagler et al., 2009). DMRI-derived fractional anisotropy (FA) and mean diffusivity (MD) were calculated based on a tensor fit to the b=1.000 data.

Fiber tract FA and MD values were analyzed for three bilateral fiber tracts of interest [i.e., uncinate fasciculus (UNC), parahippocampal cingulum (PHC) and fornix (FX)]. These three tracts were selected due to their connectivity with the hippocampus/medial temporal lobe (MTL) and evidence that they are particularly affected in TLE (Hatton et al., 2020; Stasenko et al., 2022). FA and MD for each track was extracted using AtlasTrack, a probabilistic diffusion tensor atlas validated in healthy controls and TLE patients (Hagler et al., 2009). For each participant, the T1-weighted structural images were nonlinearly registered to a common space and the respective diffusion tensor orientation estimates were compared to the atlas. This resulted in a map of the relative probability that a voxel belongs to a particular tract given its location and similarity of diffusion orientation. Voxels identified with Freesurfer (v7.1.1) as cerebrospinal fluid or GM were excluded from the fiber ROIs. Average of the diffusion parameters was calculated for each fiber ROI, weighted by fiber probability, so that voxels with low probability of belonging to a given fiber contributed minimally to average values.

SWM FA and MD were collected for the same 68 Desikan-Killiany ROIs as was obtained for the cortical thickness. FA and MD for SWM were calculated at each vertex using seven samples in 0.2 mm increments along the vector normal to the GM/WM boundary surface, from 0.8 mm to 2 mm inwards into peri-cortical white matter. Multiple samples were collected to account for passing through multiple voxels with varying properties. In order to minimize the effects of partial voluming and regional variations, we calculated weighted averages of FA and MD based on the proportion of GM or WM in each voxel using Tukey's bi-square weight function (Beaton & Tukey, 1974) to down weight the contribution of voxels with a low proportion of the tissue of interest. Average FA and MD

measured in the WM directly beneath GM ROIs in each individual's native space (Elman et al., 2017). The method is described in detail in Elman et al., 2017 (Elman et al., 2017).

4.2.4. Statistical analysis

4.2.4.1. Demographic and clinical variables

One-way ANOVAs and Chi-square tests were conducted to explore differences between TLE and controls, and between L-TLE and R-TLE, in demographic and clinical variables' distribution. Statistical significance for all tests was set at $p<.05$.

4.2.4.2. Ipsilateral versus contralateral hemisphere

After inspection of the spatial maps to ensure similar SWM, cortical, and subcortical patterns in patients with L-TLE and R-TLE, the cortical and subcortical ROIs for the R-TLEs were flipped, thus ipsilateral structural and diffusion data were projected on the left hemisphere and contralateral data are projected on the right hemisphere for all patients. This procedure allowed us to maximize power and consider ipsi- and contralateral differences as our primary variables. Thus, all the following analyses are reported as ipsi- or contralateral with respect to the seizure focus. Of note, the flipping was performed after each feature was z-scored relative to control values for each respective hemisphere, accordingly to the literature (Horsley et al., 2022; Larivière et al., 2022; Winston et al., 2020) and ensuring that there were no hemispheric asymmetries for cortical thickness, subcortical volumes, SWM (FA/MD), and WM tracts (FA/MD) in the control population.

4.2.4.3. Topography of grey and white matter structures

All brain measures were converted into z-scores based on the mean and the standard deviation of the control cohort. In order to control for differences in brain size, subcortical volumes were divided by total intracranial volume (ICV) for each subject. An inspection of brain asymmetry in controls was performed by a paired sample t-test. All analyses that follow were performed using SPSS software 28 (IBM, Chicago, IL) or R-package software, and statistical significance for all tests was set at $p<.05$. Significant p-values were considered those that survived a 5% FDR correction (Benjamini & Hochberg, 1995). Whole brain differences between TLE and controls were examined in GM (i.e., cortical thickness and subcortical volumes) and WM (i.e., SWM and deep WM tracts) using multivariate analyses of covariance (MANCOVAs) models with age and sex included as covariates in all comparisons (Whelan et al., 2018).

4.2.4.4. Relationship between GM and SWM

To assess the relationships among cortical thinning, hippocampal volume, and SWM damage, partial Pearson correlations were performed for each ROI with age and sex as covariates.

4.2.4.5. Effects of age of seizure onset

To test the association between age of seizure onset and regional GM-SWM atrophy associations, we performed a series of sliding window correlations (Schulz & Huston, 2002). This procedure involves computing correlations in overlapping successive windows across a clinical variable distribution (e.g., across age of the seizure onset), revealing fluctuations in the degree, and direction of the correlation. We ranked participants according to their clinical variable (e.g., from lowest age of seizure onset to highest). The correlation was computed for successive samples of 25 participants at a time, starting from the first 25, and then proceeding up the variable level rank order, always including the next patient and excluding the first patient of the previous interval. Additionally, we applied this approach to a random rank order of values to ensure that the correlation values obtained in the prior analyses were not due to chance. This approach has much in common with bootstrapping and clustering approaches (E. A. Allen et al., 2014; Shakil et al., 2018). Finally, we considered a window significant if three consecutive windows produced a significant effect. With this approach, we also explored the relationship between the ipsilateral SWM FA/MD and ipsilateral hippocampal volume. All plots were smoothed with the 'zoo' package in R, using a moving average value of five and a step of one.

To avoid overfitting due to the high number of ROIs in the Desikan-Killiany atlas, for this analysis we clustered the 68 cortical ROIs into three major groups: (I) MTL, including the entorhinal cortex, parahippocampal cortex, and the fusiform gyrus; (II) lateral temporal lobe (LTL), including the inferior, the middle, and the superior temporal gyri, banks of superior temporal sulcus, and transverse temporal gyrus; (III) extra-temporal regions, which included all the ROIs within the frontal, parietal, and occipital lobes.

4.3. Results

4.3.1. Demographic and clinical variables

Controls and patients with TLE did not significantly differ in age, sex, and ICV. Patients had significantly lower education compared to controls ($p<.001$). Forty-seven out of 82 patients had HS,

whereas the rest had a normal MRI. Most of the patients were on polytherapy (82%). We did not find any significant differences between L-TLE and R-TLE patients in the clinical and demographic variables. All results are summarized in **Table 4.1**.

As noted, the patterns of ipsilateral and contralateral cortical, subcortical and diffusion alterations were similar for L-TLE and R-TLE, which justified our combining of the patients into one group to maximize power.

Table 4.1. Clinical and demographic variables in TLE and controls populations.

	TLE (N=82)	**Controls (N=59)**	**Stat.**	**Sig.**
Age	35.85(±12.95)	36.95(±13.72)	.234[F]	.630
Sex (f/m)	44/38	36/23	.757[X]	.384
Education (y)	13.30(±2)	16.03(±2.27)	56.986[F]	.000***
ICV (mm^3)	990814.46(±114529.56)	1024829.31(±97008.95)	3.431[F]	.066
HS (y/n)	47/35	-	1.756[X]	.185
Age of epilepsy onset (y)	20.72(±14.30)	-		
Epilepsy duration (y)	15.13(±14.21)	-		
ASMs (mono/poly)	15/67	-		

Data are presented in means (±standard deviations). ICV: intracranial volume, HS: hippocampal sclerosis, ASM: anti-seizure medication. [F]: ANOVA, [X]: Chi-squared test, ***: p<.001.

4.3.2. Topography of grey and white matter structures

There were no differences in brain asymmetry (i.e., cortical thickness, subcortical volumes, SWM FA/MD, WM tracts FA/MD) in the control population between the left and right hemispheres. Whole brain cortical thickness comparison between TLE patients and controls is shown in **Figure 4.1A**. Significantly thinner cortex for patients was found in posterior brain regions, particularly the bilateral precuneus [Ipsi: ($F_{(1,140)}$=18.928, p_{FDR}=.001, η^2=.121), Contra: ($F_{(1,140)}$=17.267, p_{FDR}=.001, η^2=.112)], the pre-central [Ipsi: ($F_{(1,140)}$=8.908, p_{FDR}=.013, η^2=.061), Contra: ($F_{(1,140)}$=9.486, p_{FDR}=.011, η^2=.065)] and the post-central [Ipsi: ($F_{(1,140)}$=11.338, p_{FDR}=.007, η^2=.076), Contra: ($F_{(1,140)}$=11.108, p_{FDR}=.007, η^2=.074)] gyri. Cortical thinning in the superior temporal gyrus was observed bilaterally [Ipsi: ($F_{(1,140)}$=9.905, p_{FDR}=.010, η^2=.068), Contra: ($F_{(1,140)}$=5.800, p_{FDR}=.045, η^2=.041)], while the middle temporal gyri was thinner only ipsilaterally ($F_{(1,140)}$=6.696, p_{FDR}=.032, η^2=.047). The MTL did not show any significant differences in TLE compared to controls. As expected, the ipsilateral hippocampal volume was lower in TLEs compared to controls ($F_{(1,140)}$=19.878, p_{FDR}<.001, η^2=.127) (**Figure 4.1A**).

Figure 4.1B display the whole brain SWM comparison between TLE patients and controls, and the significant results are summarized in **Table 4.2**. The SWM showed a spatially different pattern of alterations compared to the cortical thickness; decreased FA and increased MD was observed in TLE patients in the ipsilateral hemisphere only, with significant reductions in FA in the ipsilateral medial and inferior temporal lobe. This pattern of ipsilateral SWM loss was more extensive for MD, with increased MD that extended beyond the temporal lobe into the orbitofrontal, cingulate and insular SWM.

Finally, **Figure 4.1C** and **Table 4.2** displays FA and MD standardized values for the three bilateral tracts and comparisons between patients and controls. The PHC and UNC showed a lower FA in both hemispheres, but more pronounced decreases in FA in each ipsilateral tract. All three fiber tracts showed increased MD in the ipsilateral tract compared to controls.

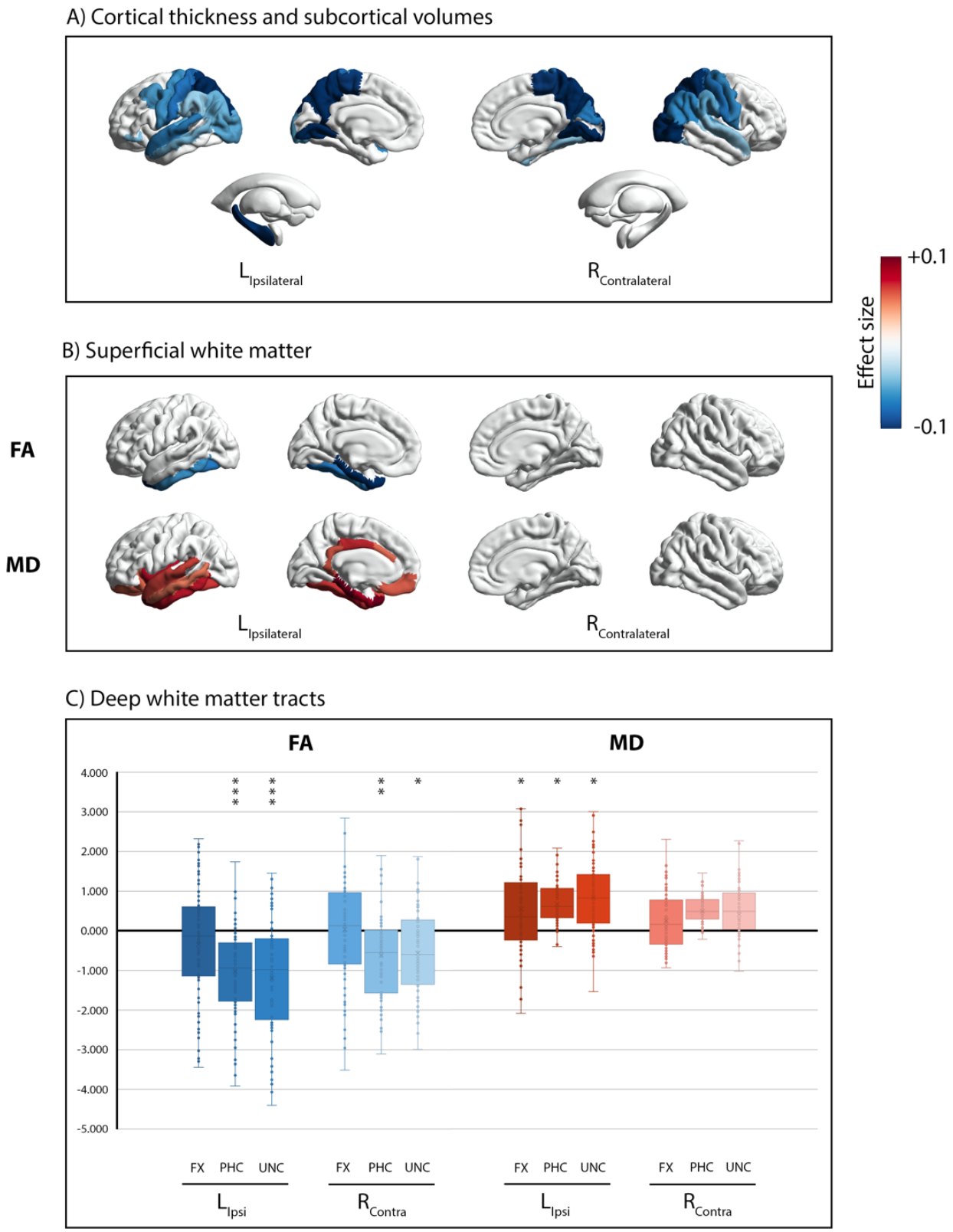

Figure 4.1. Whole brain comparison between TLE and controls. Panel A) visualizes significant group differences in cortical thickness and subcortical volume. Panel B) shows significant group differences of superficial white matter fractional anisotropy (FA) above, and mean diffusivity (MD) below. Data for each comparison are presented as effect size

(Partial Eta Squared). Blue colors (-0.1) represent the regions where TLE showed atrophy, or lower FA values, compared to controls; red colors (+0.1) represent the regions where TLE showed hypertrophy, or higher MD values, compared to controls. Only effect sizes associated with p-values that survived FDR correction (i.e., $p_{FDR}<.05$) are presented in panels a) and b). Finally, panel C) shows box-and-whisker plots of deep white matter tracts, standardized relative to controls. The central horizontal line of the boxes marks the median of the sample, the upper and lower edges of the box (the hinges) mark the 25th and 75th percentiles (the central 50% of the values fall within the box). The open circles represent individual patients. The "x" in the middle of each box marks the mean values for each fasciculus. The black line on value 0 designates the mean volume of controls. The "*" on the box indicates the significant results of the MANCOVA analysis (*: $p_{FDR}<.05$, **: $p_{FDR}<.01$, ***: $p_{FDR}<.001$). FX: fornix fasciculus, PHC: parahippocampal cingulum bundle, UNC: uncinate fasciculus. Brain maps in panel A) and B) were created by using the ENIGMA-Toolbox(Larivière, Paquola, et al., 2021).

Table 4.2. Group comparisons between TLE and controls in superficial and deep white matter.

	TLE	**Controls**	**F**	**Sig.$_{FDR}$**	**η^2**
Superficial white matter					
Ipsilateral superior temporal$_{MD}$	.806(±.069)	.772(±.032)	9.797	.016*	.068
Ipsilateral middle temporal$_{MD}$	.810(±.062)	.782(±.029)	7.538	.033*	.053
Ipsilateral inferior temporal$_{FA}$	.237(±.045)	.254(±.032)	8.987	.037*	.062
Ipsilateral inferior temporal$_{MD}$	.825(±.057)	.791(±.026)	11.645	.010*	.079
Ipsilateral entorhinal cortex$_{FA}$	.219(±.052)	.259(±.060)	17.472	.001**	.115
Ipsilateral entorhinal cortex$_{MD}$	.907(±.114)	.832(±.113)	12.271	.015*	.083
Ipsilateral fusiform$_{FA}$	.233(±.048)	.256(±.036)	10.736	.018*	.074
Ipsilateral fusiform$_{MD}$	.795(±.053)	.771(±.029)	10.465	.013*	.072
Ipsilateral parahippocampal cortex$_{FA}$	.257(±.061)	.299(±.047)	20.278	<.001***	.131
Ipsilateral parahippocampal cortex$_{MD}$	.864(±.095)	.796(±.081)	21.996	<.001***	.140
Ipsilateral temporal pole$_{FA}$	.212(±.041)	.240(±.035)	22.075	<.001***	.141
Ipsilateral temporal pole$_{MD}$	.906(±.075)	.856(±.041)	23.710	<.001***	.149
Deep white matter					
Ipsilateral FX$_{FA}$	.335(±.040)	.344(±.028)	3.221	.087	.023
Ipsilateral FX$_{MD}$	1.156(±.213)	1.067(±.156)	8.612	.034*	.060
Contralateral FX$_{FA}$	.346(±.041)	.346(±.028)	.002	.967	.000
Contralateral FX$_{MD}$	1.105(±.193)	1.064(±.170)	2.160	.158	.016
Ipsilateral PHC$_{FA}$	.337(±.049)	.375(±.032)	24.405	<.001***	.153
Ipsilateral PHC$_{MD}$	.850(±135)	.777(±.089)	11.746	.014*	.080
Contralateral PHC$_{FA}$	.353(±.050)	.379(±.049)	9.479	.010*	.066
Contralateral PHC$_{MD}$	.826(±.124)	.769(±.140)	6.747	.052	.048
Ipsilateral UNC$_{FA}$	.393(±.037)	.424(±.023)	28.200	<.001***	.173
Ipsilateral UNC$_{MD}$	.828(±.074)	.788(±.42)	11.934	.026*	.081
Contralateral UNC$_{FA}$	.407(±.032)	.414(±.051)	7.498	.018*	.053
Contralateral UNC$_{MD}$	.807(±.070)	.787(±.058)	4.004	.083	.027

Data are presented in means (±standard deviations). FA: fractional anisotropy, MD: mean diffusivity, FX: fornix, PHC: parahippocampal cingulum, UNC: uncinate. *: $p_{FDR}<.05$, **: $p_{FDR}<.01$, ***: $p_{FDR}<.001$.

4.3.3. Relationship between grey matter and SWM

Because the deep WM tract FA/MD values mirrored those of the SWM but are not in spatial alignment with the cortical ROIs, we limited our correlational analysis to GM-SWM associations. We did not find any significant linear correlations between cortical thickness and SWM FA/MD for any ROI in patients. However, SWCs across the age of epilepsy onset and the years of the illness duration revealed a more complex pattern. Lower hippocampal volumes were associated with higher SWM MD across all ROIs in those TLE with an early ASO (**Figure 4.2A**). There was no association between hippocampal volumes and cortical thinning. Conversely, decreases in cortical thickness were associated with increases in SWM MD in the ipsilateral MTL only (**Figure 4.2B**), but only in patients with a later ASO (i.e., >20 years old). This relationship was not found in the other regions. In the contralateral lobe, extra-temporal cortical thinning was associated with higher SWM MD in a restricted time window those with a very early onset (**Figure 4.2C**).

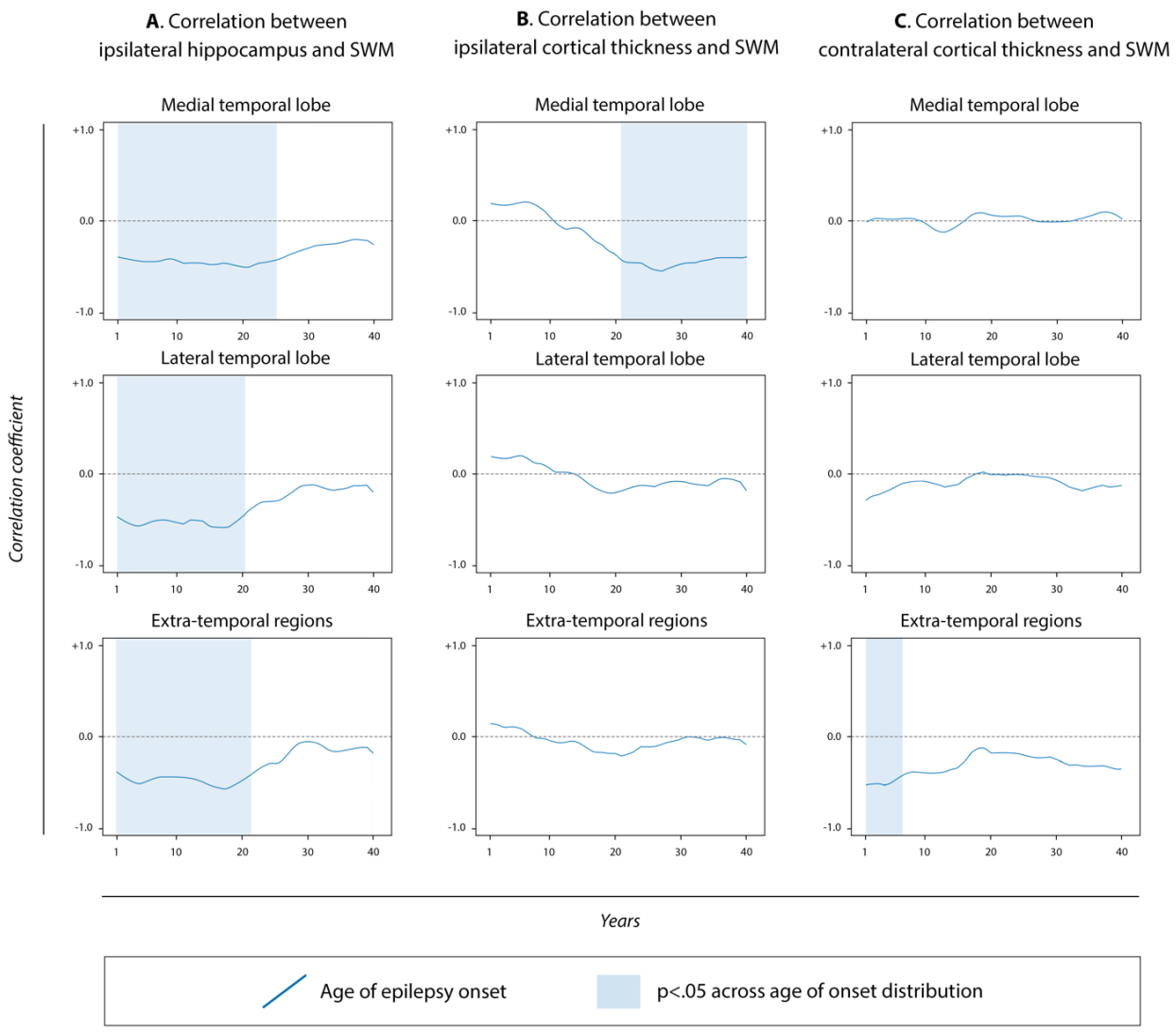

Figure 4.2. Sliding window correlations between brain measures in the TLE population as a function of the age of epilepsy onset. Panel A) shows the non-linear correlation between SWM-MD and hippocampal volume in the ipsilateral hemisphere. Panel B) shows the non-linear correlation between ipsilateral cortical thickness and SWM-MD for the three main groups of regions. Panel C) shows the same correlation between contralateral cortical thickness and SWM-MD for the same groups of regions. The blue lines display the correlation coefficients' fluctuation value across age of epilepsy onset, and the blue shading indicates when the relation is significant ($p<.05$).

4.3.3.1. Effects of early and late age of epilepsy onset

Because associations between GM and WM atrophy in TLE appear to depend on the ASO, we performed a posthoc analysis to investigate whether patients with an onset during childhood/adolescence differed in clinical characteristics from those with onset during adulthood. To accomplish this, we divided the patients in two groups; a childhood-onset TLE group (C-TLE) composed of patients who developed epilepsy on or before 18 years old based on the ILAE guidelines

(Wirrell et al., 2022), and an adult-onset group (A-TLE) characterized by those who developed seizures after age 18. In the full sample, age, age of epilepsy onset, and years of epilepsy duration were strongly related to each other. C-TLE were characterized by a younger age, and a longer disease duration compared to A-TLE. Moreover, C-TLE patients showed a higher frequency of HS compared to the A-TLE group. Conversely, the A-TLE were characterized by an older age, and a shorter disease duration. There were no group differences in sex, education, ICV, and number of ASMs. All the results are summarized in **Table 4.3**.

Table 4.3. Clinical and demographic variables in C-TLE and A-TLE.

	C-TLE (N=37)	**A-TLE (N=45)**	**Stat.**	**Sig.**
Age	32.46(±13.617)	38.64(±11.798)	4.855[F]	.030*
Sex (f/m)	24/13	20/25	3.405[X]	.065
Education (y)	12.97(±1.724)	13.58(±2.179)	1.881[F]	.174
ICV (mm^3)	979131.730(±113650.017)	1000420.270(±115629.576)	.699[F]	.406
HS (y/n)	27/10	20/25	6.755[X]	.009**
Age of epilepsy onset (y)	8.30(±6.235)	30.93(±10.391)	135.325[F]	<.001***
Epilepsy duration (y)	24.16(±15.645)	7.71(±6.808)	40.517[F]	<.001***
ASMs (mono/poly)	2.30(±0.909)	2.31(±0.925)	.005[F]	.946

Data are presented in means (±standard deviations). HS: hippocampal sclerosis, ASM: anti-seizure medication. [F]: ANOVA, [X]: Chi-squared test, *: p<.05, **: p<.01, ***: p<.001.

Due to group differences in some patient characteristics, we performed a secondary analysis between the groups, correcting for age, sex, and HS status. This secondary analysis supported our original SWC observations. In C-TLE, ipsilateral hippocampal volume loss was associated with increased ipsilateral SWM MD across the whole brain (r=-.496, p=.002, **Figure 4.3A**), in the temporal lobe (MTL: r=-.488, p=.003; LTL: r=-.501, p=.002), and in extra-temporal regions (r=-.423, p=.011). As expected, there was no association between cortical thinning and SWM MD in the C-TLE group. On the other hand, in patients with A-TLE, cortical thinning was associated with greater SWM MD in the ipsilateral MTL (r=-.374, p=.015), but there were no correlations in extra-temporal lobe regions, or between SWM MD and hippocampal atrophy (r=-.125, p=.431, **Figure 4.3B**). Finally, these findings seemed to be related to TLE pathology as these associations were not found in controls (**Figure 4.3**).

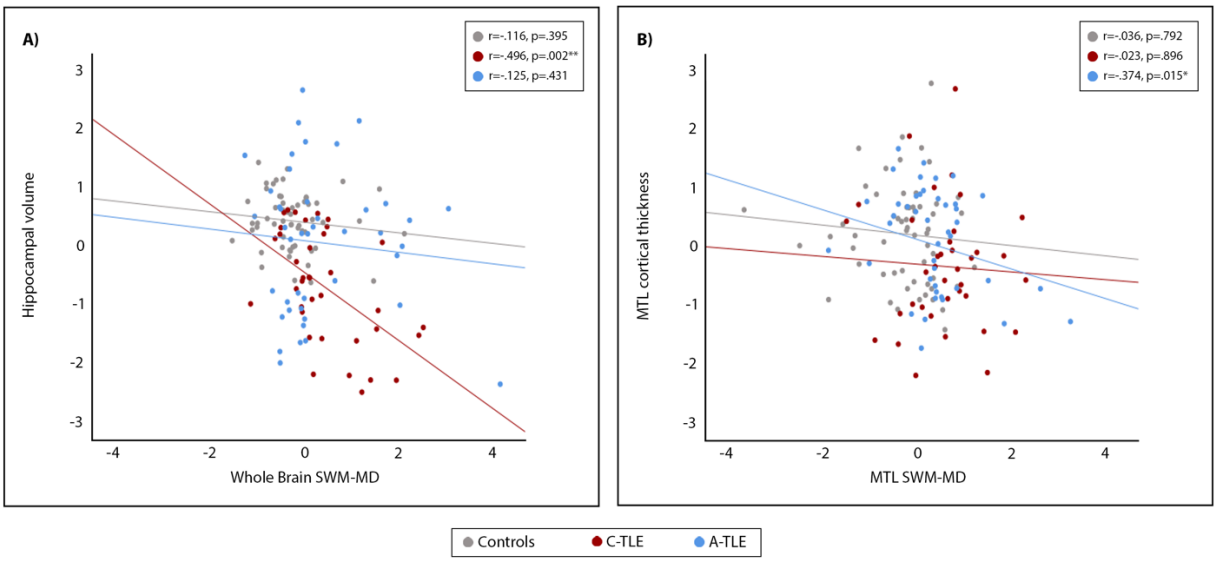

Figure 4.3. Partial correlations in controls, C-TLE (childhood onset TLE) and A-TLE (adult-onset TLE) population. Plot A) shows the correlation between hippocampal volume and whole brain SWM-MD. Plot B) shows the correlation between MTL cortical thickness and MTL SWM-MD. The scatterplots represent partial correlations between the brain measures corrected for age and sex. Thus, the data are presented as standardized residuals. Grey dots and line are used to represent controls, red dots and line represent C-TLE, and blue dots and line represent A-TLE. SWM: superficial white matter, MD: mean diffusivity, MTL: medial temporal lobe.

4.4. Discussion

The present study extends the literature by providing a comprehensive analysis of neocortical and subcortical GM and WM atrophy profiles in TLE and demonstrating how these patterns relate to one another and to the seizure focus. At the whole group level, GM and WM atrophy patterns in TLE were spatially distinct. Cortical atrophy was observed to be widespread and bilateral, and most prominent in centro-parietal regions. Conversely, WM atrophy was mostly ipsilateral and temporo-limbic, following a similar pattern for both SWM and deep WM tracts. However, unique relationships emerged between GM and SWM pathology when groups were stratified by age of seizure onset, suggesting that different GM and WM structures are differentially impacted by TLE as a function of when seizures begin in life.

4.4.1. The diffuse and widespread structural pathologies of TLE

TLE is a focal epilepsy syndrome that nonetheless is associated with widespread and diffuse structural and microstructural damage (Hatton et al., 2020; Larivière et al., 2020; B. Park et al., 2022; Whelan et al., 2018) and abnormal connectivity patterns across most of the brain (Bernhardt et al., 2019; Liu et al., 2014; Tavakol et al., 2019). Much of the previous literature has focused on cortical thickness, hippocampal volumes, and deep WM tracts (Hatton et al., 2020; Larivière et al., 2020; B.

Park et al., 2022; Whelan et al., 2018). However, despite their proximity, our findings complement previous reports (Chang et al., 2019; Liu et al., 2016) and highlight that cortical atrophy and SWM disruption appear to follow different spatial patterns of injury in TLE. Here, cortical thinning was widespread and bilateral, involving mostly of the posterior neocortex including the bilateral parietal and occipital lobes, especially in the bilateral precuneus, somatosensory and motor cortices. Furthermore, the ipsilateral MTL did not show prominent cortical thinning, which is also in line with previous reports (Larivière et al., 2020). This widespread multi-lobar cortical atrophy was instead characterized by a non-limbic and non-lateralized predominance (Larivière et al., 2020; C. R. McDonald, Hagler, et al., 2008; Whelan et al., 2018) suggesting that it arises from processes independent of the seizure focus. This broad pattern of atrophy is supported by literature demonstrating similar patterns of cortical thinning across very different epilepsy syndromes, indicating that this may reflect a more general epilepsy-related phenomenon (Whelan et al., 2018). One recent study proposed that this spatial distribution of cortical atrophy could occur in those brain regions structurally connected with the hippocampus (i.e., pre and post central gyri, precuneus, lateral and medial temporal lobe) (Galovic et al., 2019). Nevertheless, this would not explain the full pattern observed in our study and requires replication in future studies.

In contrast to the cortical GM, the SWM showed a temporo-limbic pattern of atrophy that was mostly restricted to the ipsilateral hemisphere. Although FA was reduced in the inferomedial MTL only, MD anomalies extended to the ipsilateral orbitofrontal cortex, insula, and cingulate WM. This pattern of highly lateralized WM pathology was mirrored in the deep WM temporo-limbic tracts of the UNC, PHC, and FX where FA reductions were greater and MD increases were only observed in the ipsilateral fibers. These findings are supported by prior reports demonstrating an association between the seizure focus and proximal WM injury (Concha et al., 2012; Hatton et al., 2020; Urquia-Osorio et al., 2022). Our findings extend the literature by demonstrating that this pattern exists for both the SWM and deep WM association tracts.

4.4.2. Structural pathology and the developmental trajectory

Our results demonstrate spatially distinct patterns of neocortical and WM atrophy in TLE patients in most brain regions, suggesting that different biological processes are likely driving these two types of injury. Data from animal models provide support for this, demonstrating that GM and WM are impacted along different timelines (Luna-Munguia et al., 2021; Roch et al., 2002b, 2002a), with cortical GM affected more acutely and WM affected over a longer time period following seizure

onset. In addition, WM damage in chronic TLE models supports the idea of co-occurring damage in WM and hippocampal volume (Luna-Munguia et al., 2021). Additionally, research on TLE patients has reported SWM anomalies that were mediated by hippocampal atrophy (Liu et al., 2016). However, our results suggest that a more complex relationship may exist between cortical thinning, SWM loss, and hippocampal injury, which may be driven by the period of life during which seizures began. Indeed, SWM injury and hippocampal volume loss were highly related, but only for individuals with an early age of seizure onset. This relationship was maintained even after controlling for group imbalance in HS, suggesting that the WM damage was not merely a by-product of HS. Although WM and subcortical GM maturation reach their peak at different ages, changes in both are maximal between mid-gestation to adolescence (Bethlehem et al., 2022). Thus, the onset of seizures during this period could interfere with brain maturation, leading to concurrent hippocampal injury and disruption of WM development (Liu et al., 2016).

On the other hand, developing TLE in adulthood was associated with co-occurring cortical thinning and SWM injury, but only in the ipsilateral MTL. While cortical thinning begins in childhood and shows a relatively linear decrease across the lifespan in healthy individuals, SWM microstructure follows a similar pattern to the deep WM association tracts with an increase in FA and decrease in MD that accelerates during adolescence, reaching a peak between 20-35 years of age (Bethlehem et al., 2022; Lebel et al., 2012; Schilling et al., 2022). In adulthood, SWM FA/MD levels off and then declines during late-adulthood (Schilling et al., 2022). Our results suggest that when TLE begins in adulthood, after the period of SWM peak development, it leads to co-occurring and age-accelerated cortical and WM injury proximal to the epileptogenic zone. Interestingly, this is observed in TLE patients with a relatively short disease duration (**Supplementary Figure 2**), suggesting that these pathological changes may occur quite rapidly in drug-resistant adults and could underlie the progressive cognitive decline observed in many of these patients (Costa et al., 2019; Fernandes et al., 2022). Finally, all the results from the non-linear correlations highlighted effects only with respect to SWM MD, with no significant results found for FA. MD abnormalities refer to an overall tissue barrier impairment and degree of water diffusion within a voxel, with no orientation (Basser et al., 2000; Beaulieu, 2002). Thus, because of the convergence of deep and peripheral fibers with the SWM with less anisotropy than long WM bundles, MD may be a more sensitive marker of SWM microstructural disruption (Urquia-Osorio et al., 2022).

4.4.3. Limitations and Future Directions

Despite our novel findings, several limitations of our study should be addressed. First, we lack a cohort of older adults with TLE, preventing us from evaluating the impact of epilepsy on brain pathology across the adult lifespan. In particular, late onset epilepsy is defined as seizures that begin after the age of 55, often having a temporal lobe predominance, greater levels of MTL atrophy than observed in our current study, and often no clear etiology (Kaestner et al., 2021). Future studies should explore whether the pattern of structural pathology and its relationship across tissue types is affected by this very late age of seizure onset, and how these relationships may be related to cognitive decline and risk for dementia. Although our sample size is larger than many prior studies (Chang et al., 2019; Liu et al., 2016), a larger multi-center cohort would allow us to stratify patients by additional clinical and brain-related characteristics. First, this would enable us to better disentangle the roles of the age of seizure onset from the years of epilepsy duration. Age of seizure onset and duration of epilepsy were co-linear, and our analyses were cross-sectional, therefore limiting our ability to tease apart the unique effects of these two variables or understand the causality of the relationships. Moreover, a longitudinal study with a large cohort of patients who are heterogeneous in clinical characteristics would allow for a more enriched understanding of the mechanisms underlying TLE-related pathology. It is well known that FA, MD, cortical thickness, and volume have different maturation peaks during the lifespan (Bethlehem et al., 2022). In our secondary analysis, we clustered our sample into those with a pediatric vs adult age of seizure onset (i.e., before or after 18 years old), according to ILAE guidelines (Wirrell et al., 2022). A larger multi-center cohort would allow us to stratify our sample according to a range of brain maturation peaks and test our GM and WM relationships across various peaks. Finally, although we purport to replicate prior findings in our initial analysis of discordant GM and SWM patterns, it is of note that we used different methods for both extracting and summarizing our variables. However, we consider this a strength and believe that it provides evidence that these findings are robust to the methods employed.

4.5. Conclusion

Our data provide compelling evidence of a complex relationship between cortico-subcortical GM loss and WM injury in TLE; our findings suggest spatially unique patterns of cortical, hippocampal, and WM atrophy. The age at which the seizures begin appears to influence the way in which these features are related to one another. Whereas the co-occurrence of hippocampal injury and WM damage in the ipsilateral hemisphere may be linked to neurodevelopmental factors, the onset of

seizures in adulthood could set off a cascade of neurodegenerative changes, dominated by cortical atrophy and subcortical WM injury close to the epileptogenic zone.

Conclusion

The purpose of this doctoral thesis was to contribute to a better knowledge of the morphological cortico-subcortical patterns underlying Temporal Lobe Epilepsy (TLE) to better understand and characterize this pathological condition.

In the present work, the first aim was to explore the role of the amygdala subnuclei in TLE, highlighting the central role of this subcortical structure in the epileptogenic network of the disease. Specifically, our results reported different morphometric behaviors in the amygdala's nuclei with respect to the epileptic etiology. As reported in Chapter 2, HS seems to affect the ipsilateral basolateral amygdala causing a reduction in its volume. Conversely, in those patients with the absence of obvious epileptogenic lesions, the medial portion of the amygdala exhibited isolated hypertrophy ipsilateral to the seizure focus. These results supported and confirmed the involvement of the amygdala in TLE, moreover, our findings expanded previous knowledge of the amygdala as a possible morphological biomarker of patients with TLE with or without detectable lesions at the MRI investigation. The importance of studying the role of the amygdala in the complexity of the disease is a future goal of our research group. In the future, we aim to better understand how the different amygdala substructures could be involved in specific cognitive-behavioral characteristics, due to the frequent psychiatric comorbidity and neuropsychological impairment associated with TLE. In Chapter 3 we applied the same subnuclear morphometric methodology to study epileptic patients with Ictal Central Apnea (ICA) manifestations. Our findings reported the involvement of the ipsilateral basolateral amygdala, showing an increase in volume as a distinctive hallmark of ICA in patients with epilepsy. The identification of valuable biomarkers of ictal autonomic manifestations is needed for a more accurate stratification and prevention of the sudden unexpected death in epilepsy (SUDEP) risk.

Finally, in Chapter 4 our investigation focused on the processes underlying cortical grey and white matter compromise in TLE patients. Although there is already evidence that cortical atrophy and superficial white matter (SWM) microstructural damage follow different spatial patterns in TLE, we trying to characterize how these pathologies spatially correlate across tissue types and with respect to clinical-related variables. Our findings provide compelling evidence of a complex relationship between cortico-subcortical grey matter loss and white matter injury in TLE. Despite cortical, hippocampal and SWM atrophy patterns appear spatially unique, the relationship among these features depends on the age at which seizures begin. Whereas neurodevelopmental aspects of TLE may result

in co-occurring white matter and hippocampal injury near the epileptogenic zone, the onset of seizures in adulthood may set off a cascade of SWM and cortical atrophy of a neurodegenerative nature. Thank to our collaboration with the ENIGMA-Epilepsy consortium, this study is going to be extended to a large, heterogeneous, and geographically diverse population of epileptic patients across the lifespan, to better understand the influence of the age of seizure onset and the effect of the years of disease duration in both patients with focal and generalized epilepsies.

Appendices

A) Exploring the relationship between amygdala subnuclei volumes and cognitive performance in left-lateralized temporal lobe epilepsy with and without hippocampal sclerosis

Alice Ballerini[1], Francesca Talami[1,2], Maria Angela Molinari[3], Elisa Micalizzi[4,5], Simona Scolastico[1,3], Niccolò Biagioli[1,3], Niccolò Orlandi[1,3], Matteo Pugnaghi[3], Giada Giovannini[3], Stefano Meletti[1,3], Anna Elisabetta Vaudano[1,3]

[1] *Department of Biomedical, Metabolic and Neural Sciences, University of Modena and Reggio Emilia, Modena, Italy*

[2] *Italian National Research Council (CNR), Institute of Neuroscience, Parma, Italy*

[3] *Neurology Unit, OCB Hospital, AOU Modena, Modena, Italy*

[4] *PhD Program in Clinical and Experimental Medicine, University of Modena and Reggio Emilia, Modena, Italy*

[5] *Neurophysiology Unit, Epilepsy Center, IRCCS San Martino Hospital, Genoa, Italy*

Introduction: Temporal lobe epilepsy (TLE) is recognized as a network disorder characterized by patterns of cortico-subcortical atrophy (Whelan et al., 2018). The most common histopathologic and radiological abnormality in TLE is hippocampal sclerosis (HS). Cognitive dysfunctions are highly prevalent and a debilitating comorbidity in this condition. Several studies have identifying different cognitive phenotypes affecting TLE patients and the morphometric networks underlying these categories (B. Hermann et al., 2020; Reyes et al., 2019, 2020). Recently, the amygdala is receiving attention as key structure in the TLE epileptogenic network, and the engagement of its nuclei was documented to be different in TLE with HS compared to non-lesional TLE (Ballerini et al., 2022). These evidence, however, did not explore the relationships between cognitive performances and amygdala morphometric measures. We aim to fill this gap, by correlating the volumes of amygdala subnuclei and the cognitive profile of a population of left-lateralized TLE, with respect to the etiology of the epilepsy.

Methods: We retrospectively reviewed a cohort of consecutive left TLE admitted at our hospital for presurgical evaluation. This cohort is part of an already published study (for more details see: **Chapter 2**). The inclusion criteria were (I) age > 18 years, (II) execution of formal neuropsychological assessment, and (III) a brain MRI protocol encompassing a 3D T1-weighted (T1-3D) sequence no

longer that 12 months distant from the neuropsychological evaluation. TLE patients were clustered into those with a negative MRI (TLE-MRIneg), if no focal lesions were observed, and TLE-HS if clinical MRI had shown a focal alteration consistent with hippocampal sclerosis (HS). Diagnosis and lateralization were determined by board-certified neurologists with expertise in epileptology (SM and AEV) and in accordance with criteria defined by the International League Against Epilepsy (ILAE; (Fisher et al., 2017)). From each patient recruited we collected clinical information regarding age, sex, handedness, age of seizure onset, years of epilepsy, number of antiseizure medication (ASM) at the MRI scan, and drug-resistance status. Finally, we collected age and sex-matched healthy controls population. MRI was performed on two different 3T scanners (i.e., Philips Intera and GE Healthcare) adopting an epilepsy-dedicated protocol. The automatic FreeSurfer (v6.0) segmentation was performed on 3D-T1 sequences. Subsequentially, the dedicated pipeline for the automatic parcellation of the hippocampus and the amygdala was performed with FreeSurfer dev version. The measurements obtained were harmonized across the different scanners using the "neuroCombat" package for R. A detailed description of the MRI pre and post processing is provided elsewhere (for more details see: **Chapter 2**). The hippocampus was parceled into three subfields for each hemisphere (Saygin et al., 2017): head, body, and tail. The amygdala was segmented into nine nuclei (Saygin et al., 2017): anterior amygdaloid area (AAA), cortico-amygdaloid transition area (CAT), basal, lateral, accessory-basal, central, cortical, medial, and paralaminar nuclei. Based on their cytoarchitectonics, histochemistry, and connections and according to previous approach by our group (Ballerini et al., 2022), the nuclei of the amygdala were clustered into three main regions or complexes: (I) the basolateral complex (BLA), which includes the lateral, basal, accessory-basal, and paralaminar nuclei; (II) the cortical complex, which include the cortical nucleus; (III) and the central-medial complex composed by the medial and the central nuclei. All TLEs underwent a complete cognitive assessment, and raw scores from the following domains were collected: (I) language (Category and Letter fluency), (II) verbal memory (Babcock Short Story Recall test, and Verbal Paired Associates test), (III) attention and processing speed (Attention Matrices, Trail Making Test part A, and Stroop Color/Word Interference Test), and (IV) executive functions (Trail Making Test part B, number of errors at Stroop Color/Word Interference Test, Frontal Assessment Battery, and Time and Weight estimation). Chi-squared tests and one-way ANOVAs were used to test for differences in demographic and clinical variables among the TLE groups and between patients and controls. TLE subgroups' cognitive performances differences were tested with a MANCOVA with age, sex, years of education, and handedness as covariates. Group differences for the subcortical parcellations were examined using a MANCOVA

with age, sex, and estimated total intracranial volume (eTIV) as covariates. The analysis was performed using SPSS software 28 (IBM, Chicago, IL) and statistical significance was set at $p<.05$. Significant p-values were considered if survived a 5% FDR correction. Finally, linear regressions were performed between hippocampus-amygdala substructures and the raw score for each cognitive domain within the TLE-HS and TLE-MRIneg populations separately. The analysis was performed using SPSS software 28; in TLE patients, the models were regressed out for confounding factors as age, sex, years of education and handedness. Statistical significance for all tests was set at $p<.05$.

Results: Controls and patients were not significantly different in age, sex, and eTIV. TLE-HS did not differ from TLE-MRIneg in years of education, age of onset, drug-resistance, and eTIV. Conversely, TLE-HS showed a longer duration and a higher number of ASMs compared to TLE-MRIneg. All results are summarized in **Table A1**. Of note, all subjects were right-handed but one TLE-HS patient.

Table A1. Clinical and demographic variables across TLE populations and controls.

	TLE-HS	TLE-MRIneg	Controls	Stat.	Sig.
N	14	15	30		
Age (y)	40.50(±11.654)	38.60(±15.268)	35.27(±5.825)	1.362^{F}	.264
Sex (f/m)	8/6	9/6	19/11	$.163^{X}$	.922
eTIV	$1.46^{E+06}(\pm1.65^{E+05})$	$1.39^{E+06}(\pm1.57^{E+05})$	$1.46^{E+06}(\pm2.13^{E+05})$	$.691^{F}$	.505
Education (y)	11.29(±3.338)	11.47(±3.603)	-	$.020^{F}$	.890
Age of onset (y)	21.07(±14.025)	29.27(±17.010)	-	1.987^{F}	.170
Epilepsy duration (y)	19.57(±13.013)	9.40(±9.583)	-	5.801^{F}	.023*
N° ASMs	2.50(±.650)	1.87(±.915)	-	4.551^{F}	.042*
Drug-resistance (y/n)	8/6	6/9	-	$.852^{X}$	.356

Data are presented in means (±standard deviations). y: years, eTIV: estimated intracranial volume, ASM: anti-seizure medication. ^{F}*: ANOVA,* ^{X}*: Chi-squared test, *: p<.05.*

The analysis of subcortical volumes highlighted ipsilateral atrophy of the whole hippocampus in TLE-HS compared to controls ($F_{(1,77)}=14.853$, $p_{FDR}<.001$), as well as all the subfields explored [head: $F_{(1,77)}=15.191$, $p_{FDR}<.001$; body: $F_{(1,77)}=10.139$, $p_{FDR}<.001$; tail: $F_{(1,77)}=4.871$, $p_{FDR}<.001$]. No differences were found in TLE-MRIneg hippocampus with respect to controls. Regarding the amygdala, a global atrophy was found in TLE-HS for the whole ipsilateral amygdala ($F_{(1,77)}=4.466$, $p_{FDR}=.021$), particularly in its basolateral portion ($F_{(1,77)}=4.608$, $p_{FDR}=.027$). In addition, a modest atrophy was found even in the contralateral amygdala ($F_{(1,77)}=2.341$, $p_{FDR}=.046$). The TLE-MRIneg showed isolated hypertrophy involving the ipsilateral medial nucleus ($F_{(1,77)}=4.260$, $p_{FDR}=.014$).

We did not find any significant differences in the cognitive performances between TLE-HS and TLE-MRIneg. Linear regressions in the TLE-HS population revelated that left hippocampal atrophy was related to poorer verbal memory scores (**Fig. A1**). The same association has been found between verbal memory performances and the volume of the accessory-basal and cortical nuclei of the left amygdala (**Fig. A1**). Thus, the greatest is the atrophy in those amygdala nuclei, the worst the memory performances. We did not find any correlation between verbal memory scores and hippocampal/amygdala volume in TLE-MRIneg. However, greater volume in the whole left amygdala particularly in its basolateral and cortical portions was related to worst scores in attentional and processing speed tasks (**Fig. A1**).

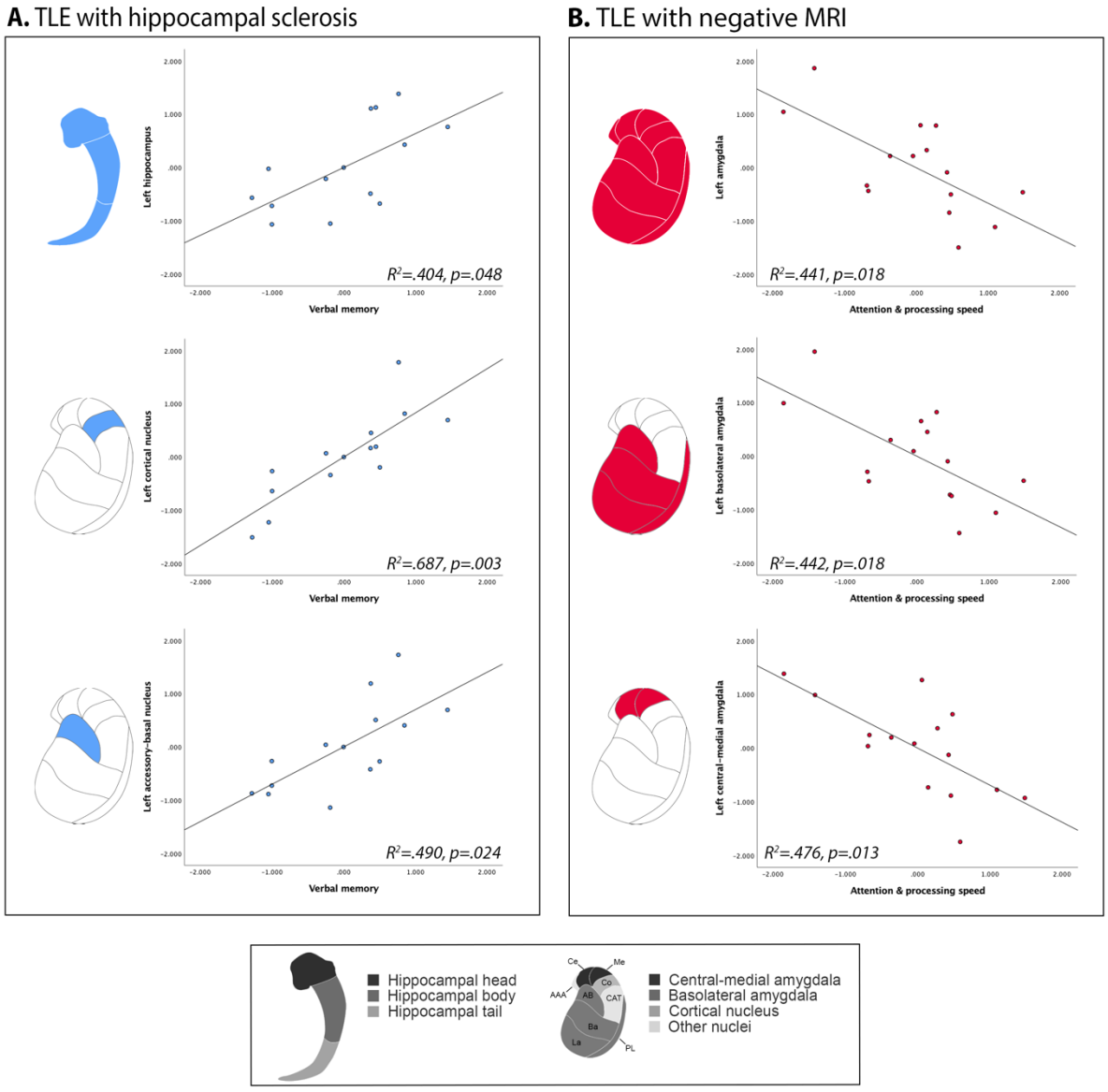

Figure A1. Association between subcortical volumes and cognitive scores in TLE patients.
Panel A) shows the positive association between verbal memory performance and the total ipsilateral hippocampal volume (top), the ipsilateral cortical nucleus volume (middle), and the ipsilateral accessory-basal volume (bottom). Blue colors refer to the positive association between these regions and the verbal memory tasks. Panel B) shows the negative association between attention and processing speed and the total ipsilateral amygdala volume (top), and specifically, in the ipsilateral basolateral amygdala (middle) and the ipsilateral central-medial amygdala (bottom). Red colors refer to the negative association between these regions and the attention and processing speed tasks. Of note, the scatterplots represent partial correlations between the hippocampal and amygdalae volumes (on the y-axes) and the raw cognitive data (on the x-axes), both corrected for age, sex, years of education, and handedness. Thus, the data are presented as standardized residuals. Finally, only the ipsilateral subcortical structures are presented. La: lateral nucleus, Ba: basal nucleus, AB: accessory basal nucleus, PL: paralaminar nucleus, Ce: central nucleus, Me: medial nucleus, Co: cortical nucleus, AAA: anterior amygdaloid area, CAT: corticoamygdaloid transition area.

Discussion: This study revealed a role of the amygdala substructures in the cognitive networks of a population of left TLE with and without HS. TLE is recognized to be a heterogenous disorder, reflecting different etiologies with the common feature of involvement of one or more of the temporal-limbic structures (Thom & Bertram, 2012). The involvement of the amygdala in the TLE epileptogenic network has been reported. Previous studies have shown different morphometric patterns of the amygdala in TLE with or without symptomatic HS (Ballerini et al., 2022; Coan, Morita, de Campos, et al., 2013; Reyes et al., 2017). Specifically, amygdala enlargement (AE) has been proposed as a morphological biomarker of a subtype of TLE patients without MRI abnormalities (Coan, Morita, de Campos, et al., 2013; Reyes et al., 2017). Herein, as well as in our previous study (6), we showed that TLE-MRIneg present an isolated increase volume of the ipsilateral medial nucleus, while TLE-HS demonstrate a global amygdala atrophy, particularly of the BLA. So far, no study explored the correlation between amygdala volumes and cognitive profiles of TLE patients. The present findings expand and complete the previous data by providing for the first time evidence of a different amygdala involvement in cognitive performances of TLE patients. We reported that ipsilateral amygdala atrophy relates to worst scores in verbal memory tasks in TLE-HS. As expected, this pattern was confirmed also with respect to the ipsilateral hippocampal atrophy. Conversely and intriguingly, TLE patients with a negative MRI showed a completely different pattern. Worst scores in attention and processing speed tasks were indeed related to amygdala hypertrophy ipsilateral to the side of the epileptogenic focus. Our findings support previous speculations considering TLE-HS and TLE-MRIneg different entities (Ballerini et al., 2022), as reflected not only by morphometric biomarkers but even by neuropsychological profiles. Furthermore, the results of present analyses highlight the importance to consider the volume of amygdala and its substructures as a biomarker for a correct TLE patients' classification. Amygdala has always been reported associated with impairments in emotion recognition in TLE (Monti & Meletti, 2015). However, our findings are in line with previous connectivity studies, its involvement also in memory and other cognitive functions.

Verbal memory is the most common impaired cognitive domain in TLE (C. R. McDonald et al., 2014). While the hippocampus is widely recognized to have a central role, several studies demonstrated that a more complex network is involved in memory performances. Volume loss in entorhinal cortex (Alessio et al., 2006), reduced functional connectivity in medial temporal lobe (TL), as well as microstructural damages within white matter fasciculi adjacent to TL contributes to poorer VM in TLE (Alessio et al., 2006; C. R. McDonald et al., 2014). Our study adds compelling evidence of amygdala involvement in this network. Volume loss in accessory-basal (AB) and cortical nuclei

ipsilateral to the HS are associated with worst scores. The AB nucleus is part of BLA, a complex strongly connected with the hippocampus and the entorhinal cortex (Benarroch, 2015), which role in memory function has been well documented (Paré, 2003). Conversely, there is a lack of evidence of human cortical amygdala (CoA) functions, even in healthy subjects. However, a recent study reported the CoA as functionally connected with the posterior hippocampus and the middle temporal gyrus, supporting its role in learning and memory (Noto et al., 2021).

Despite memory and language impairments are the commonest cognitive comorbidity in TLE, attentional deficits and cognitive slowing has been often reported (Piazzini et al., 2006). We provide evidence of the morphometric counterpart of these neuropsychological alterations. Indeed, as reported by ours and other groups, AE in TLE-MRIneg is not innocuous rather is associated with a disruption of attentional functions and processing speed. Amygdala involvement in top-down processes critical for guiding spatial attention has been reported (Jacobs et al., 2012). Specifically, the amygdala seems to play a role in learning the features that are relevant for a given task and then guiding attention and orientation behaviors.

This study has some limitations. Firstly, it lacks neuropsychological assessment in the control group, preventing from mapping the amygdala behavior in a healthy population and performing a comparison between patients and controls. Secondly, we recognize the limited sample size of TLE population. Of note, we adopted strict inclusion criteria; particularly, we rigidly selected only those patients with a time window not longer than 12 months between MRI and NPS. Finally, as preliminary study, we focused only on left TLE patients. Future studies are warranted to confirm our observations, exploring the role of amygdala subnuclei in right-side TLE and on larger and heterogenous populations of epilepsy patients.

Conclusion: Our findings suggested different amygdala behaviors across different TLE etiologies and contribute to extend our knowledge of amygdala involvement in TLE cognition. In left TLE-HS population amygdala atrophy was related to poor scores in verbal memory, conversely, in TLE-MRIneg poorer performances in attention and processing speed were associated with amygdala hypertrophy. Amygdala morphometric measures may serve as useful disease biomarker in TLE.

B) Ictal apnea: A prospective monocentric study in patients with epilepsy

Elisa Micalizzi[1,2], Anna Elisabetta Vaudano[2,3], Alice Ballerini[3], Francesca Talami[3], Giada Giovannini[1,2], Giulia Turchi[2], Maria Cristina Cioclu[2,3], Leandra Giunta[2], Stefano Meletti[2,3]

[1]Clinical and Experimental Medicine PhD Program, University of Modena and Reggio Emilia, Modena, Italy

[2]Neurology Unit, Civil Hospital of Baggiovara, Modena Academic Hospital, Modena, Italy

[3]Department of Biomedical, Metabolic, and Neural Science, University of Modena and Reggio Emilia, Modena, Italy

Introduction: Ictal respiratory disturbances have increasingly been reported, in both generalized and focal seizures, especially involving the temporal lobe. Recognition of ictal breathing impairment has gained importance for the risk of sudden unexpected death in epilepsy (SUDEP). The aim of this study was to evaluate the incidence of ictal apnea (IA) and related hypoxemia during seizures.

Methods: We collected and analyzed electroclinical data from consecutive patients undergoing long-term video-electroencephalographic (video-EEG) monitoring with cardiorespiratory polygraphy. Patients were recruited at the epilepsy monitoring unit (EMU) of the Civil Hospital of Baggiovara, Modena Academic Hospital, from April 2020 to February 2022.

Results: A total of 552 seizures were recorded in 63 patients. IA was observed in 57 of 552 (10.3%) seizures in 16 of 63 (25.4%) patients. Thirteen (81.2%) patients had focal seizures, and 11 of 16 patients showing IA had a diagnosis of temporal lobe epilepsy; two had a diagnosis of frontal lobe epilepsy and three of epileptic encephalopathy. Apnea agnosia was reported in all seizure types. Hypoxemia was observed in 25 of 57 (43.9%) seizures with IA, and the severity of hypoxemia was related to apnea duration. Apnea duration was significantly associated with epilepsy of unknown etiology (magnetic resonance imaging negative) and with older age at epilepsy onset ($p < 0.001$).

Conclusions: Ictal respiratory changes are a frequent clinical phenomenon, more likely to occur in focal epilepsies, although detected even in patients with epileptic encephalopathy. Our findings emphasize the need for respiratory polygraphy during long-term video-EEG monitoring for diagnostic and prognostic purposes, as well as in relation to the potential link of ictal apnea with the SUDEP risk.

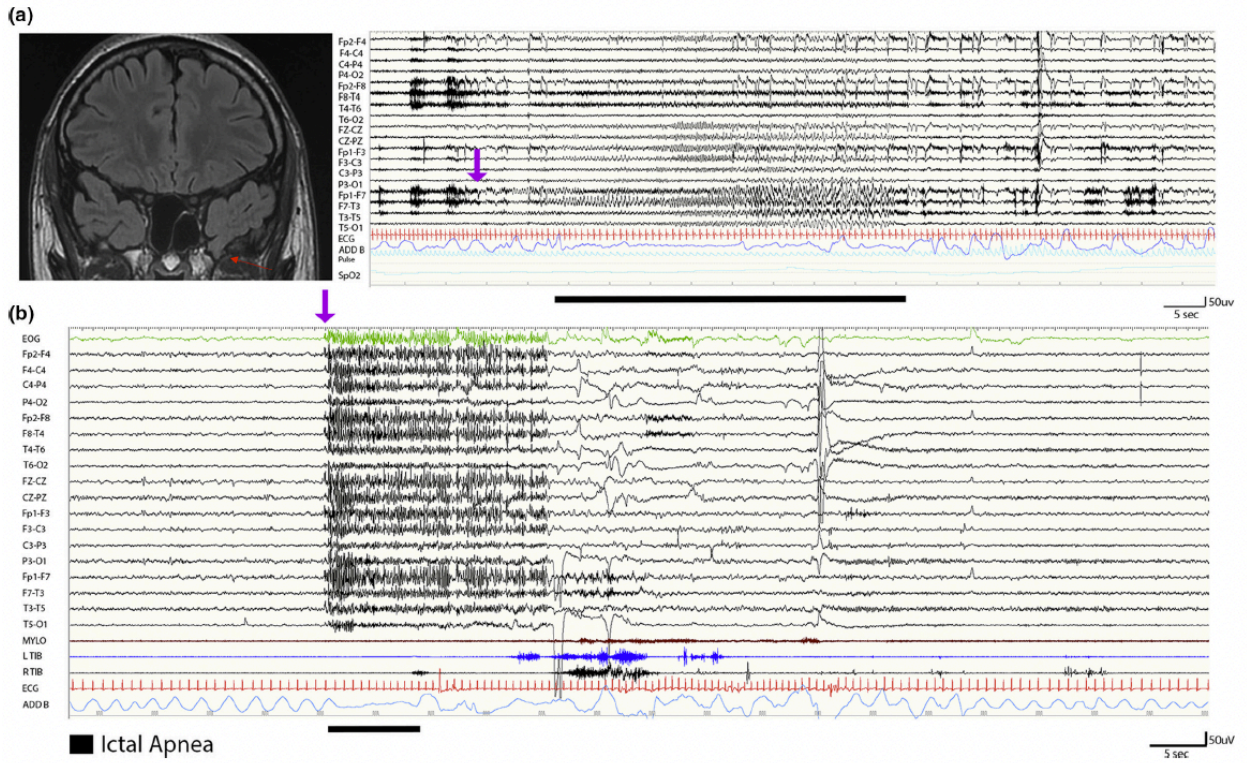

Figure A2. Apnea observed in focal and generalized seizures.
(a) A 20-year-old male with ictal apnea seizures. On the left, a coronal T2 fluid-attenuated inversion recovery magnetic resonance imaging scan shows the presence of a left temporopolar encephalocele (red arrow). On the right, the electroencephalogram (EEG; 120 s) shows a left temporal seizure arising from the frontotemporal channels (Fp1-F7, F7-T3), rapidly involving the ipsilateral and contralateral frontal regions including the anterior vertex. The ictal discharge (indicated by the purple arrow) is characterized by low-voltage fast rhythms evolving in sharply contoured theta and then delta rhythmic activity with diffuse abrupt termination. Ictal apnea starts during the ictal phase in association with bradycardia. Ictal apnea duration is indicated by the black bar. Red channel: electrocardiogram; blue channel: thoracoabdominal respirogram.
(b) A 14-year-old male patient with Lennox–Gastaut epileptic encephalopathy. During non-rapid eye movement sleep, the EEG shows abrupt diffuse fast activity (as indicated by the purple arrow) predominant over the frontocentral and vertex regions for 20 s, followed by slow activity. The polygraphy shows ictal tachycardia (red channel) and flattening of the thoracoabdominal respirogram (light blue channel; indicated by the black bar). No significant muscle activity was recorded (mylohyoid and left and right tibialis anterior muscles) during the epileptic discharge.

For more details, see: Micalizzi, et al. (2022). *European Journal of Neurology*, 29(12), 3701-3710. https://doi.org/10.1111/ene.15547

Bibliography

Aggleton, J. P., Burton, M. J., & Passingham, R. E. (1980). Cortical and subcortical afferents to the amygdala of the rhesus monkey (Macaca mulatta). *Brain Research*, *190*(2), 347–368. https://doi.org/10.1016/0006-8993(80)90279-6

Aghamohammadi-Sereshki, A., Coupland, N. J., Silverstone, P. H., Huang, Y., Hegadoren, K. M., Carter, R., Seres, P., & Malykhin, N. V. (2021). Effects of childhood adversity on the volumes of the amygdala subnuclei and hippocampal subfields in individuals with major depressive disorder. *Journal of Psychiatry and Neuroscience*, *46*(1), E186–E195. https://doi.org/10.1503/jpn.200034

Ahmadi, M. E., Hagler, D. J., McDonald, C. R., Tecoma, E. S., Iragui, V. J., Dale, A. M., & Halgren, E. (2009). Side Matters: Diffusion Tensor Imaging Tractography in Left and Right Temporal Lobe Epilepsy. *AJNR: American Journal of Neuroradiology*, *30*(9), 1740–1747. https://doi.org/10.3174/ajnr.A1650

Alessio, A., Bonilha, L., Rorden, C., Kobayashi, E., Min, L. L., Damasceno, B. P., & Cendes, F. (2006). Memory and language impairments and their relationships to hippocampal and perirhinal cortex damage in patients with medial temporal lobe epilepsy. *Epilepsy & Behavior: E&B*, *8*(3), 593–600. https://doi.org/10.1016/j.yebeh.2006.01.007

Alexander-Bloch, A., Giedd, J. N., & Bullmore, E. (2013). Imaging structural co-variance between human brain regions. *Nature Reviews Neuroscience*, *14*(5), Article 5. https://doi.org/10.1038/nrn3465

Aliashkevich, A. F., Yilmazer-Hanke, D., Van Roost, D., Mundhenk, B., Schramm, J., & Blümcke, I. (2003). Cellular pathology of amygdala neurons in human temporal lobe epilepsy. *Acta Neuropathologica*, *106*(2), 99–106. https://doi.org/10.1007/s00401-003-0707-0

Allen, E. A., Damaraju, E., Plis, S. M., Erhardt, E. B., Eichele, T., & Calhoun, V. D. (2014). Tracking Whole-Brain Connectivity Dynamics in the Resting State. *Cerebral Cortex (New York, NY)*, *24*(3), 663–676. https://doi.org/10.1093/cercor/bhs352

Allen, L. A., Harper, R. M., Lhatoo, S., Lemieux, L., & Diehl, B. (2019). Neuroimaging of Sudden Unexpected Death in Epilepsy (SUDEP): Insights From Structural and Resting-State Functional MRI Studies. *Frontiers in Neurology*, *10*, 185. https://doi.org/10.3389/fneur.2019.00185

Allen, L. A., Vos, S. B., Kumar, R., Ogren, J. A., Harper, R. K., Winston, G. P., Balestrini, S., Wandschneider, B., Scott, C. A., Ourselin, S., Duncan, J. S., Lhatoo, S. D., Harper, R. M., & Diehl, B. (2019). Cerebellar, limbic and midbrain volume alterations in sudden unexpected death in epilepsy (SUDEP). *Epilepsia*, *60*(4), 718–729. https://doi.org/10.1111/epi.14689

Andersson, J. L. R., Skare, S., & Ashburner, J. (2003). How to correct susceptibility distortions in spin-echo echo-planar images: Application to diffusion tensor imaging. *NeuroImage*, *20*(2), 870–888. https://doi.org/10.1016/S1053-8119(03)00336-7

Armio, R.-L., Laurikainen, H., Ilonen, T., Walta, M., Salokangas, R. K. R., Koutsouleris, N., Hietala, J., & Tuominen, L. (2020). Amygdala subnucleus volumes in psychosis high-risk state and first-episode psychosis. *Schizophrenia Research*, *215*, 284–292. https://doi.org/10.1016/j.schres.2019.10.014

Arruda, F., Cendes, F., Andermann, F., Dubeau, F., Villemure, J. G., Jones-Gotman, M., Poulin, N., Arnold, D. L., & Olivier, A. (1996). Mesial atrophy and outcome after amygdalohippocampectomy or temporal lobe removal. *Annals of Neurology*, *40*(3), 446–450. https://doi.org/10.1002/ana.410400314

Asadi-Pooya, A. A., & Rostami, C. (2017). History of surgery for temporal lobe epilepsy. *Epilepsy & Behavior*, *70*, 57–60. https://doi.org/10.1016/j.yebeh.2017.02.020

Asami, T., Nakamura, R., Takaishi, M., Yoshida, H., Yoshimi, A., Whitford, T. J., & Hirayasu, Y. (2018). Smaller volumes in the lateral and basal nuclei of the amygdala in patients with panic disorder. *PLOS ONE*, *13*(11), e0207163. https://doi.org/10.1371/journal.pone.0207163

Ashburner, J. (2009). Computational anatomy with the SPM software. *Magnetic Resonance Imaging*, *27*(8), 1163–1174. https://doi.org/10.1016/j.mri.2009.01.006

Ashburner, J., & Friston, K. J. (2000). Voxel-Based Morphometry—The Methods. *NeuroImage*, *11*(6), 805–821. https://doi.org/10.1006/nimg.2000.0582

Atkinson, A. J., Colburn, W. A., DeGruttola, V. G., DeMets, D. L., Downing, G. J., Hoth, D. F., Oates, J. A., Peck, C. C., Schooley, R. T., Spilker, B. A., Woodcock, J., & Zeger, S. L. (2001). Biomarkers and surrogate endpoints: Preferred definitions and conceptual framework. *Clinical Pharmacology & Therapeutics*, *69*(3), 89–95. https://doi.org/10.1067/mcp.2001.113989

Backhausen, L. L., Herting, M. M., Buse, J., Roessner, V., Smolka, M. N., & Vetter, N. C. (2016). Quality Control of Structural MRI Images Applied Using FreeSurfer—A Hands-On Workflow to Rate Motion Artifacts. *Frontiers in Neuroscience*, *10*. https://doi.org/10.3389/fnins.2016.00558

Bailey, P., & Sweet, W. H. (1940). Effects on respiration, blood pressure and gastric motility of stimulation of orbital surface of frontal lobe. *Journal of Neurophysiology*, *3*(3), 276–281. https://doi.org/10.1152/jn.1940.3.3.276

Ballerini, A., Tondelli, M., Talami, F., Molinari, M. A., Micalizzi, E., Giovannini, G., Turchi, G., Malagoli, M., Genovese, M., Meletti, S., & Vaudano, A. E. (2022). Amygdala subnuclear volumes in temporal lobe epilepsy with hippocampal sclerosis and in non-lesional patients. *Brain Communications*, *4*(5), fcac225. https://doi.org/10.1093/braincomms/fcac225

Barron, D. S., Eickhoff, S. B., Clos, M., & Fox, P. T. (2015). Human pulvinar functional organization and connectivity. *Human Brain Mapping*, *36*(7), 2417–2431. https://doi.org/10.1002/hbm.22781

Basser, P. J., Pajevic, S., Pierpaoli, C., Duda, J., & Aldroubi, A. (2000). In vivo fiber tractography using DT-MRI data. *Magnetic Resonance in Medicine*, *44*(4), 625–632. https://doi.org/10.1002/1522-2594(200010)44:4<625::AID-MRM17>3.0.CO;2-O

Baxendale, S., & Thompson, P. (2010). Beyond localization: The role of traditional neuropsychological tests in an age of imaging. *Epilepsia*, *51*(11), 2225–2230. https://doi.org/10.1111/j.1528-1167.2010.02710.x

Beaton, A. E., & Tukey, J. W. (1974). The Fitting of Power Series, Meaning Polynomials, Illustrated on Band-Spectroscopic Data. *Technometrics*, *16*(2), 147–185. https://doi.org/10.1080/00401706.1974.10489171

Beaulieu, C. (2002). The basis of anisotropic water diffusion in the nervous system – a technical review. *NMR in Biomedicine*, *15*(7–8), 435–455. https://doi.org/10.1002/nbm.782

Beghi, E. (2020). The Epidemiology of Epilepsy. *Neuroepidemiology*, *54*(2), 185–191. https://doi.org/10.1159/000503831

Beh, S. M. J., Cook, M. J., & D'Souza, W. J. (2016). Isolated amygdala enlargement in temporal lobe epilepsy: A systematic review. *Epilepsy & Behavior*, *60*, 33–41. https://doi.org/10.1016/j.yebeh.2016.04.015

Bell, B., Lin, J. J., Seidenberg, M., & Hermann, B. (2011). The neurobiology of cognitive disorders in temporal lobe epilepsy. *Nature Reviews. Neurology*, *7*(3), 10.1038/nrneurol.2011.3. https://doi.org/10.1038/nrneurol.2011.3

Bell, G. S., Neligan, A., & Sander, J. W. (2014). An unknown quantity—The worldwide prevalence of epilepsy. *Epilepsia*, *55*(7), 958–962. https://doi.org/10.1111/epi.12605

Benarroch, E. E. (2015). The amygdala: Functional organization and involvement in neurologic disorders. *Neurology*, *84*(3), 313–324. https://doi.org/10.1212/WNL.0000000000001171

Bencurova, P., Laakso, H., Salo, R. A., Paasonen, E., Manninen, E., Paasonen, J., Michaeli, S., Mangia, S., Bares, M., Brazdil, M., Kubova, H., & Gröhn, O. (2022). Infantile status epilepticus disrupts myelin development. *Neurobiology of Disease*, *162*, 105566. https://doi.org/10.1016/j.nbd.2021.105566

Benjamini, Y., & Hochberg, Y. (1995). Controlling the False Discovery Rate: A Practical and Powerful Approach to Multiple Testing. *Journal of the Royal Statistical Society: Series B (Methodological)*, *57*(1), 289–300. https://doi.org/10.1111/j.2517-6161.1995.tb02031.x

Berg, A. T., Berkovic, S. F., Brodie, M. J., Buchhalter, J., Cross, J. H., Van Emde Boas, W., Engel, J., French, J., Glauser, T. A., Mathern, G. W., Moshé, S. L., Nordli, D., Plouin, P., & Scheffer, I. E. (2010). Revised terminology and concepts for organization of seizures and epilepsies: Report of the ILAE Commission on Classification and Terminology, 2005–2009. *Epilepsia*, *51*(4), 676–685. https://doi.org/10.1111/j.1528-1167.2010.02522.x

Bernasconi, A., Cendes, F., Theodore, W. H., Gill, R. S., Koepp, M. J., Hogan, R. E., Jackson, G. D., Federico, P., Labate, A., Vaudano, A. E., Blümcke, I., Ryvlin, P., & Bernasconi, N. (2019). Recommendations for the use of structural magnetic resonance imaging in the care of patients with epilepsy: A consensus report from the International League Against Epilepsy Neuroimaging Task Force. *Epilepsia*, epi.15612. https://doi.org/10.1111/epi.15612

Bernasconi, N. (2003). Mesial temporal damage in temporal lobe epilepsy: A volumetric MRI study of the hippocampus, amygdala and parahippocampal region. *Brain*, *126*(2), 462–469. https://doi.org/10.1093/brain/awg034

Bernasconi, N. (2016). Is epilepsy a curable neurodegenerative disease? *Brain*, *139*(9), 2336–2337. https://doi.org/10.1093/brain/aww202

Bernhardt, B. C., Bonilha, L., & Gross, D. W. (2015). Network analysis for a network disorder: The emerging role of graph theory in the study of epilepsy. *Epilepsy & Behavior*, *50*, 162–170. https://doi.org/10.1016/j.yebeh.2015.06.005

Bernhardt, B. C., Fadaie, F., Liu, M., Caldairou, B., Gu, S., Jefferies, E., Smallwood, J., Bassett, D. S., Bernasconi, A., & Bernasconi, N. (2019). Temporal lobe epilepsy: Hippocampal pathology modulates connectome topology and controllability. *Neurology*, *92*(19), e2209–e2220. https://doi.org/10.1212/WNL.0000000000007447

Bernhardt, B. C., Rozen, D. A., Worsley, K. J., Evans, A. C., Bernasconi, N., & Bernasconi, A. (2009). Thalamo-cortical network pathology in idiopathic generalized epilepsy: Insights from MRI-based morphometric correlation analysis. *NeuroImage*, *46*(2), 373–381. https://doi.org/10.1016/j.neuroimage.2009.01.055

Bernhardt, B. C., Worsley, K. J., Kim, H., Evans, A. C., Bernasconi, A., & Bernasconi, N. (2009). Longitudinal and cross-sectional analysis of atrophy in pharmacoresistant temporal lobe epilepsy. *Neurology*, *72*(20), 1747–1754. https://doi.org/10.1212/01.wnl.0000345969.57574.f5

Bethlehem, R. a. I., Seidlitz, J., White, S. R., Vogel, J. W., Anderson, K. M., Adamson, C., Adler, S., Alexopoulos, G. S., Anagnostou, E., Areces-Gonzalez, A., Astle, D. E., Auyeung, B., Ayub, M., Bae, J., Ball, G., Baron-Cohen, S.,

Beare, R., Bedford, S. A., Benegal, V., … Alexander-Bloch, A. F. (2022). Brain charts for the human lifespan. *Nature*, *604*(7906), Article 7906. https://doi.org/10.1038/s41586-022-04554-y

Bien, C. G., Kurthen, M., Baron, K., Lux, S., Helmstaedter, C., Schramm, J., & Elger, C. E. (2001). Long-Term Seizure Outcome and Antiepileptic Drug Treatment in Surgically Treated Temporal Lobe Epilepsy Patients: A Controlled Study. *Epilepsia*, *42*(11), 1416–1421. https://doi.org/10.1046/j.1528-1157.2001.43300.x

Blanc, F., Martinian, L., Liagkouras, I., Catarino, C., Sisodiya, S. M., & Thom, M. (2011). Investigation of widespread neocortical pathology associated with hippocampal sclerosis in epilepsy: A postmortem study. *Epilepsia*, *52*(1), 10–21. https://doi.org/10.1111/j.1528-1167.2010.02773.x

Blümcke, I., Beck, H., Suter, B., Hoffmann, D., Födisch, H. J., Wolf, H. K., Schramm, J., Elger, C. E., & Wiestler, O. D. (1999). An increase of hippocampal calretinin-immunoreactive neurons correlates with early febrile seizures in temporal lobe epilepsy. *Acta Neuropathologica*, *97*(1), 31–39. https://doi.org/10.1007/s004010050952

Blümcke, I., Coras, R., Miyata, H., & Özkara, C. (2012). Defining Clinico-Neuropathological Subtypes of Mesial Temporal Lobe Epilepsy with Hippocampal Sclerosis. *Brain Pathology*, *22*(3), 402–411. https://doi.org/10.1111/j.1750-3639.2012.00583.x

Blümcke, I., Thom, M., Aronica, E., Armstrong, D. D., Bartolomei, F., Bernasconi, A., Bernasconi, N., Bien, C. G., Cendes, F., Coras, R., Cross, J. H., Jacques, T. S., Kahane, P., Mathern, G. W., Miyata, H., Moshé, S. L., Oz, B., Özkara, Ç., Perucca, E., … Spreafico, R. (2013). International consensus classification of hippocampal sclerosis in temporal lobe epilepsy: A Task Force report from the ILAE Commission on Diagnostic Methods. *Epilepsia*, *54*(7), 1315–1329. https://doi.org/10.1111/epi.12220

Blümcke, I., Thom, M., & Wiestler, O. D. (2002). Ammon's Horn Sclerosis: A Maldevelopmental Disorder Associated with Temporal Lobe Epilepsy. *Brain Pathology*, *12*(2), 199–211. https://doi.org/10.1111/j.1750-3639.2002.tb00436.x

Boedhoe, P. S. W., Schmaal, L., Abe, Y., Alonso, P., Ameis, S. H., Anticevic, A., Arnold, P. D., Batistuzzo, M. C., Benedetti, F., Beucke, J. C., Bollettini, I., Bose, A., Brem, S., Calvo, A., Calvo, R., Cheng, Y., Cho, K. I. K., Ciullo, V., Dallaspezia, S., … ENIGMA OCD Working Group. (2018). Cortical Abnormalities Associated With Pediatric and Adult Obsessive-Compulsive Disorder: Findings From the ENIGMA Obsessive-Compulsive Disorder Working Group. *The American Journal of Psychiatry*, *175*(5), 453–462. https://doi.org/10.1176/appi.ajp.2017.17050485

Bonilha, L., Edwards, J. C., Kinsman, S. L., Morgan, P. S., Fridriksson, J., Rorden, C., Rumboldt, Z., Roberts, D. R., Eckert, M. A., & Halford, J. J. (2010). Extrahippocampal gray matter loss and hippocampal deafferentation in patients with temporal lobe epilepsy. *Epilepsia*, *51*(4), 519–528. https://doi.org/10.1111/j.1528-1167.2009.02506.x

Bonilha, L., Jensen, J. H., Baker, N., Breedlove, J., Nesland, T., Lin, J. J., Drane, D. L., Saindane, A. M., Binder, J. R., & Kuzniecky, R. I. (2015). The brain connectome as a personalized biomarker of seizure outcomes after temporal lobectomy. *Neurology*, *84*(18), 1846–1853. https://doi.org/10.1212/WNL.0000000000001548

Bonilha, L., Montenegro, M. A., Cendes, F., & Li, L. M. (2004). The role of neuroimaging in the investigation of patients with single seizures, febrile seizures, or refractory partial seizures. *Medical Science Monitor: International Medical Journal of Experimental and Clinical Research*, *10*(3), RA40-46.

Bonora, A., Benuzzi, F., Monti, G., Mirandola, L., Pugnaghi, M., Nichelli, P., & Meletti, S. (2011). Recognition of emotions from faces and voices in medial temporal lobe epilepsy. *Epilepsy & Behavior*, *20*, 648–654.

Bower, S. P. C. (2003). Amygdala volumetry in "imaging-negative" temporal lobe epilepsy. *Journal of Neurology, Neurosurgery & Psychiatry*, *74*(9), 1245–1249. https://doi.org/10.1136/jnnp.74.9.1245

Buser, N., Madan, C., & Hanson, J. (2020). *Quantifying Numerical and Spatial Reliability of Amygdala and Hippocampal Subdivisions in FreeSurfer*. https://doi.org/10.1101/2020.06.12.149203

Caligiuri, M. E., Labate, A., Cherubini, A., Mumoli, L., Ferlazzo, E., Aguglia, U., Quattrone, A., & Gambardella, A. (2016). Integrity of the corpus callosum in patients with benign temporal lobe epilepsy. *Epilepsia*, *57*(4), 590–596. https://doi.org/10.1111/epi.13339

Cavanagh, J. B., & Meyer, A. (1956). Aetiological Aspects of Ammon's Horn Sclerosis Associated with Temporal Lobe Epilepsy. *British Medical Journal*, *2*(5006), 1403–1407.

Cendes, F., Andermann, F., Gloor, P., Evans, A., Jones-Gotman, M., Watson, C., Melanson, D., Olivier, A., Peters, T., Lopes-Cendes, I., & Leroux, G. (1993). MRI volumetric measurement of amygdala and hippocampus in temporal lobe epilepsy. *Neurology*, *43*(4), 719–725.

Chang, Y. A., Marshall, A., Bahrami, N., Mathur, K., Javadi, S. S., Reyes, A., Hegde, M., Shih, J. J., Paul, B. M., Hagler, D. J., & McDonald, C. R. (2019). Differential sensitivity of structural, diffusion, and resting-state functional MRI for detecting brain alterations and verbal memory impairment in temporal lobe epilepsy. *Epilepsia*, *60*(5), 935–947. https://doi.org/10.1111/epi.14736

Clavijo Prado, C. A., Federico, P., Bernasconi, A., Bernhardt, B., Caciagli, L., Concha, L., Chinvarun, Y., Jackson, G., Morgan, V., Rampp, S., Vaudano, A. E., Wang, I., Wang, S., Zaidan, B. C., Rogerio, F., & Cendes, F. (2022). Imaging characteristics of temporopolar blurring in the context of hippocampal sclerosis. *Epileptic Disorders*, *24*(1), 1–8. https://doi.org/10.1684/epd.2021.1378

Coan, A. C., Morita, M. E., Campos, B. M., Bergo, F. P. G., Kubota, B. Y., & Cendes, F. (2013). Amygdala enlargement occurs in patients with mesial temporal lobe epilepsy and hippocampal sclerosis with early epilepsy onset. *Epilepsy & Behavior*, *29*(2), 390–394. https://doi.org/10.1016/j.yebeh.2013.08.022

Coan, A. C., Morita, M. E., de Campos, B. M., Yasuda, C. L., & Cendes, F. (2013). Amygdala Enlargement in Patients with Mesial Temporal Lobe Epilepsy without Hippocampal Sclerosis. *Frontiers in Neurology*, *4*. https://doi.org/10.3389/fneur.2013.00166

Concha, L., Kim, H., Bernasconi, A., Bernhardt, B. C., & Bernasconi, N. (2012). Spatial patterns of water diffusion along white matter tracts in temporal lobe epilepsy. *Neurology*, *79*(5), 455–462. https://doi.org/10.1212/WNL.0b013e31826170b6

Costa, B. S., Santos, M. C. V., Rosa, D. V., Schutze, M., Miranda, D. M., & Romano-Silva, M. A. (2019). Automated evaluation of hippocampal subfields volumes in mesial temporal lobe epilepsy and its relationship to the surgical outcome. *Epilepsy Research*, *154*, 152–156. https://doi.org/10.1016/j.eplepsyres.2019.05.011

Cui, D., Guo, Y., Cao, W., Gao, W., Qiu, J., Su, L., Jiao, Q., & Lu, G. (2020). Correlation Between Decreased Amygdala Subnuclei Volumes and Impaired Cognitive Functions in Pediatric Bipolar Disorder. *Frontiers in Psychiatry*, *11*, 612. https://doi.org/10.3389/fpsyt.2020.00612

Dale, A. M., Fischl, B., & Sereno, M. I. (1999). Cortical surface-based analysis. I. Segmentation and surface reconstruction. *NeuroImage*, *9*(2), 179–194. https://doi.org/10.1006/nimg.1998.0395

Davies, K. G., Hermann, B. P., Dohan, F. C., Foley, K. T., Bush, A. J., & Wyler, A. R. (1996). Relationship of hippocampal sclerosis to duration and age of onset of epilepsy, and childhood febrile seizures in temporal lobectomy patients. *Epilepsy Research*, *24*(2), 119–126. https://doi.org/10.1016/0920-1211(96)00008-3

Davis, M., Hanson, S., & Altevogt, B. (2008). *Neuroscience biomarkers and biosignatures: Converging technologies, emerging partnerships, workshop summary* (Washington, DC: The National Academies Press). Washington, DC: The National Academies Press.

de Campos, B. M., Coan, A. C., Lin Yasuda, C., Casseb, R. F., & Cendes, F. (2016). Large-scale brain networks are distinctly affected in right and left mesial temporal lobe epilepsy. *Human Brain Mapping*, *37*(9), 3137–3152. https://doi.org/10.1002/hbm.23231

De Lanerolle, N. C., Kim, J. H., Williamson, A., Spencer, S. S., Zaveri, H. P., Eid, T., & Spencer, D. D. (2003). A Retrospective Analysis of Hippocampal Pathology in Human Temporal Lobe Epilepsy: Evidence for Distinctive Patient Subcategories. *Epilepsia*, *44*(5), 677–687. https://doi.org/10.1046/j.1528-1157.2003.32701.x

Desikan, R. S., Ségonne, F., Fischl, B., Quinn, B. T., Dickerson, B. C., Blacker, D., Buckner, R. L., Dale, A. M., Maguire, R. P., Hyman, B. T., Albert, M. S., & Killiany, R. J. (2006). An automated labeling system for subdividing the human cerebral cortex on MRI scans into gyral based regions of interest. *NeuroImage*, *31*(3), 968–980. https://doi.org/10.1016/j.neuroimage.2006.01.021

Destrieux, C., Fischl, B., Dale, A., & Halgren, E. (2010). Automatic parcellation of human cortical gyri and sulci using standard anatomical nomenclature. *NeuroImage*, *53*(1), 1–15. https://doi.org/10.1016/j.neuroimage.2010.06.010

Dlouhy, B. J., Gehlbach, B. K., Kreple, C. J., Kawasaki, H., Oya, H., Buzza, C., Granner, M. A., Welsh, M. J., Howard, M. A., Wemmie, J. A., & Richerson, G. B. (2015). Breathing Inhibited When Seizures Spread to the Amygdala and upon Amygdala Stimulation. *Journal of Neuroscience*, *35*(28), 10281–10289. https://doi.org/10.1523/JNEUROSCI.0888-15.2015

Dodrill, C. B. (1992). The Role of Neuropsychology in the Assessment and Treatment of Persons with Epilepsy. *American Psychologist*.

Doucet, G. E., Sharan, A., Pustina, D., Skidmore, C., Sperling, M. R., & Tracy, J. I. (2015). Early and Late Age of Seizure Onset have a Differential Impact on Brain Resting-State Organization in Temporal Lobe Epilepsy. *Brain Topography*, *28*(1), 113–126. https://doi.org/10.1007/s10548-014-0366-6

Duncan, J. S. (2002). Seizure-induced neuronal injury: Human data. *Neurology*, *59*(9 Suppl 5), S15-20. https://doi.org/10.1212/wnl.59.9_suppl_5.s15

Dutra, J. R., Cortés, E. P., & Vonsattel, J. P. G. (2015). Update on Hippocampal Sclerosis. *Current Neurology and Neuroscience Reports*, *15*(10), 67. https://doi.org/10.1007/s11910-015-0592-7

Elman, J. A., Panizzon, M. S., Hagler, D. J., Fennema-Notestine, C., Eyler, L. T., Gillespie, N. A., Neale, M. C., Lyons, M. J., Franz, C. E., McEvoy, L. K., Dale, A. M., & Kremen, W. S. (2017). Genetic and environmental influences on cortical mean diffusivity. *NeuroImage*, *146*, 90–99. https://doi.org/10.1016/j.neuroimage.2016.11.032

Elverman, K. H., Resch, Z. J., Quasney, E. E., Sabsevitz, D. S., Binder, J. R., & Swanson, S. J. (2019). Temporal lobe epilepsy is associated with distinct cognitive phenotypes. *Epilepsy & Behavior*, *96*, 61–68. https://doi.org/10.1016/j.yebeh.2019.04.015

Engel, J. (1984). A practical guide for routine EEG studies in epilepsy. *Journal of Clinical Neurophysiology: Official Publication of the American Electroencephalographic Society*, *1*(2), 109–142. https://doi.org/10.1097/00004691-198404000-00001

Engel, J. (1993). *Surgical treatment of epilepsies* (2nd edition). Raven Press.

Engel, J., Thompson, P. M., Stern, J. M., Staba, R. J., Bragin, A., & Mody, I. (2013). Connectomics and epilepsy. *Current Opinion in Neurology*, *26*(2), 186–194. https://doi.org/10.1097/WCO.0b013e32835ee5b8

Federico, P., Ng, D. W., Bernasconi, A., Bernhardt, B., Blumenfeld, H., Cendes, F., Chinvarun, Y., Jackson, G. D., Morgan, V., Rampp, S., Vaudano, A. E., & Wang, I. (2020). ILAE Neuroimaging Task Force highlight: Review MRI scans with semiology in mind. *Epileptic Disorders : International Epilepsy Journal with Videotape*, *22*(5), 683–687. https://doi.org/10.1684/epd.2020.1202

Fernandes, M., Manfredi, N., Aluisantonio, L., Franchini, F., Chiaravalloti, A., Izzi, F., Di Santo, S., Schillaci, O., Mercuri, N. B., Placidi, F., & Liguori, C. (2022). Cognitive functioning, cerebrospinal fluid Alzheimer's disease biomarkers and cerebral glucose metabolism in late-onset epilepsy of unknown aetiology: A prospective study. *European Journal of Neuroscience*, *56*(9), 5384–5396. https://doi.org/10.1111/ejn.15734

Fischl, B. (2012). FreeSurfer. *NeuroImage*, *62*(2), 774–781. https://doi.org/10.1016/j.neuroimage.2012.01.021

Fischl, B., Sereno, M. I., & Dale, A. M. (1999). Cortical surface-based analysis. II: Inflation, flattening, and a surface-based coordinate system. *NeuroImage*, *9*(2), 195–207. https://doi.org/10.1006/nimg.1998.0396

Fisher, R. S., Boas, W. van E., Blume, W., Elger, C., Genton, P., Lee, P., & Engel Jr., J. (2005). Epileptic Seizures and Epilepsy: Definitions Proposed by the International League Against Epilepsy (ILAE) and the International Bureau for Epilepsy (IBE). *Epilepsia*, *46*(4), 470–472. https://doi.org/10.1111/j.0013-9580.2005.66104.x

Fisher, R. S., Cross, J. H., French, J. A., Higurashi, N., Hirsch, E., Jansen, F. E., Lagae, L., Moshé, S. L., Peltola, J., Roulet Perez, E., Scheffer, I. E., & Zuberi, S. M. (2017). Operational classification of seizure types by the International League Against Epilepsy: Position Paper of the ILAE Commission for Classification and Terminology. *Epilepsia*, *58*(4), 522–530. https://doi.org/10.1111/epi.13670

Florindo, I., Bisulli, F., Pittau, F., Naldi, I., Striano, P., Striano, S., Michelucci, R., Testoni, S., Baruzzi, A., & Tinuper, P. (2006). Lateralizing Value of the Auditory Aura in Partial Seizures. *Epilepsia*, *47*(s5), 68–72. https://doi.org/10.1111/j.1528-1167.2006.00881.x

Focke, N. K., Yogarajah, M., Bonelli, S. B., Bartlett, P. A., Symms, M. R., & Duncan, J. S. (2008). Voxel-based diffusion tensor imaging in patients with mesial temporal lobe epilepsy and hippocampal sclerosis. *NeuroImage*, *40*(2), 728–737. https://doi.org/10.1016/j.neuroimage.2007.12.031

Fortin, J.-P., Cullen, N., Sheline, Y. I., Taylor, W. D., Aselcioglu, I., Cook, P. A., Adams, P., Cooper, C., Fava, M., McGrath, P. J., McInnis, M., Phillips, M. L., Trivedi, M. H., Weissman, M. M., & Shinohara, R. T. (2018). Harmonization of cortical thickness measurements across scanners and sites. *NeuroImage*, *167*, 104–120. https://doi.org/10.1016/j.neuroimage.2017.11.024

Friedman, E. (2014). Epilepsy imaging in adults: Getting it right. *AJR. American Journal of Roentgenology*, *203*(5), 1093–1103. https://doi.org/10.2214/AJR.13.12035

Gaillard, W. D., Chiron, C., Helen Cross, J., Simon Harvey, A., Kuzniecky, R., Hertz-Pannier, L., & Gilbert Vezina, L. (2009). Guidelines for imaging infants and children with recent-onset epilepsy. *Epilepsia*, *50*(9), 2147–2153. https://doi.org/10.1111/j.1528-1167.2009.02075.x

Galovic, M., van Dooren, V. Q. H., Postma, T. S., Vos, S. B., Caciagli, L., Borzì, G., Cueva Rosillo, J., Vuong, K. A., de Tisi, J., Nachev, P., Duncan, J. S., & Koepp, M. J. (2019). Progressive Cortical Thinning in Patients With Focal Epilepsy. *JAMA Neurology*, *76*(10), 1230. https://doi.org/10.1001/jamaneurol.2019.1708

Gleichgerrcht, E., Munsell, B., Bhatia, S., Vandergrift, W. A., Rorden, C., McDonald, C., Edwards, J., Kuzniecky, R., & Bonilha, L. (2018). Deep learning applied to whole-brain connectome to determine seizure control after epilepsy surgery. *Epilepsia*, *59*(9), 1643–1654. https://doi.org/10.1111/epi.14528

Gloor, P., Olivier, A., Quesney, L. F., Andermann, F., & Horowitz, S. (1982). The role of the limbic system in experiential phenomena of temporal lobe epilepsy. *Annals of Neurology*, *12*(2), 129–144. https://doi.org/10.1002/ana.410120203

Goddard, G. V. (1969). Analysis of avoidance conditioning following cholinergic stimulation of amygdala in rats. *Journal of Comparative and Physiological Psychology*, *68*(2), 1–18. https://doi.org/10.1037/h0027504

Goto, M., Abe, O., Hagiwara, A., Fujita, S., Kamagata, K., Hori, M., Aoki, S., Osada, T., Konishi, S., Masutani, Y., Sakamoto, H., Sakano, Y., Kyogoku, S., & Daida, H. (2022). Advantages of Using Both Voxel- and Surface-based Morphometry in Cortical Morphology Analysis: A Review of Various Applications. *Magnetic Resonance in Medical Sciences*, *21*(1), 41–57. https://doi.org/10.2463/mrms.rev.2021-0096

Graebenitz, S., Kedo, O., Speckmann, E.-J., Gorji, A., Panneck, H., Hans, V., Palomero-Gallagher, N., Schleicher, A., Zilles, K., & Pape, H.-C. (2011). Interictal-like network activity and receptor expression in the epileptic human lateral amygdala. *Brain: A Journal of Neurology*, *134*(Pt 10), 2929–2947. https://doi.org/10.1093/brain/awr202

Greve, D. N., & Fischl, B. (2018). False Positive Rates in Surface-based Anatomical Analysis. *NeuroImage*, *171*, 6–14. https://doi.org/10.1016/j.neuroimage.2017.12.072

Guye, M., Régis, J., Tamura, M., Wendling, F., Gonigal, A. M., Chauvel, P., & Bartolomei, F. (2006). The role of corticothalamic coupling in human temporal lobe epilepsy. *Brain*, *129*(7), 1917–1928. https://doi.org/10.1093/brain/awl151

Hagler, D. J., Ahmadi, M. E., Kuperman, J., Holland, D., McDonald, C. R., Halgren, E., & Dale, A. M. (2009). Automated white-matter tractography using a probabilistic diffusion tensor atlas: Application to temporal lobe epilepsy. *Human Brain Mapping*, *30*(5), 1535–1547. https://doi.org/10.1002/hbm.20619

Hagler, D. J., Hatton, SeanN., Cornejo, M. D., Makowski, C., Fair, D. A., Dick, A. S., Sutherland, M. T., Casey, B. J., Barch, D. M., Harms, M. P., Watts, R., Bjork, J. M., Garavan, H. P., Hilmer, L., Pung, C. J., Sicat, C. S., Kuperman, J., Bartsch, H., Xue, F., … Dale, A. M. (2019). Image processing and analysis methods for the Adolescent Brain Cognitive Development Study. *NeuroImage*, *202*, 116091. https://doi.org/10.1016/j.neuroimage.2019.116091

Hansen, T. I., Brezova, V., Eikenes, L., Håberg, A., & Vangberg, T. R. (2015). How Does the Accuracy of Intracranial Volume Measurements Affect Normalized Brain Volumes? Sample Size Estimates Based on 966 Subjects from the HUNT MRI Cohort. *AJNR. American Journal of Neuroradiology*, *36*(8), 1450–1456. https://doi.org/10.3174/ajnr.A4299

Hatton, S. N., Huynh, K. H., Bonilha, L., Abela, E., Alhusaini, S., Altmann, A., Alvim, M. K. M., Balachandra, A. R., Bartolini, E., Bender, B., Bernasconi, N., Bernasconi, A., Bernhardt, B., Bargallo, N., Caldairou, B., Caligiuri, M. E., Carr, S. J. A., Cavalleri, G. L., Cendes, F., … McDonald, C. R. (2020). White matter abnormalities across different epilepsy syndromes in adults: An ENIGMA-Epilepsy study. *Brain*, *143*(8), 2454–2473. https://doi.org/10.1093/brain/awaa200

Helmstaedter, C., & Kockelmann, E. (2006). Cognitive Outcomes in Patients with Chronic Temporal Lobe Epilepsy. *Epilepsia*, *47*(s2), 96–98. https://doi.org/10.1111/j.1528-1167.2006.00702.x

Helmstaedter, C., Kurthen, M., Lux, S., Reuber, M., & Elger, C. E. (2003). Chronic epilepsy and cognition: A longitudinal study in temporal lobe epilepsy. *Annals of Neurology*, *54*(4), 425–432. https://doi.org/10.1002/ana.10692

Hermann, B., Conant, L. L., Cook, C. J., Hwang, G., Garcia-Ramos, C., Dabbs, K., Nair, V. A., Mathis, J., Bonet, C. N. R., Allen, L., Almane, D. N., Arkush, K., Birn, R., DeYoe, E. A., Felton, E., Maganti, R., Nencka, A., Raghavan, M., Shah, U., … Meyerand, M. E. (2020). Network, clinical and sociodemographic features of cognitive phenotypes in temporal lobe epilepsy. *NeuroImage: Clinical*, *27*, 102341. https://doi.org/10.1016/j.nicl.2020.102341

Hermann, B. P., Seidenberg, M., Dow, C., Jones, J., Rutecki, P., Bhattacharya, A., & Bell, B. (2006). Cognitive prognosis in chronic temporal lobe epilepsy. *Annals of Neurology*, *60*(1), 80–87. https://doi.org/10.1002/ana.20872

Hermann, B. P., Seidenberg, M., Schoenfeld, J., & Davies, K. (1997). Neuropsychological Characteristics of the Syndrome of Mesial Temporal Lobe Epilepsy. *Archives of Neurology*, *54*(4), 369–376. https://doi.org/10.1001/archneur.1997.00550160019010

Hermann, B., Seidenberg, M., Bell, B., Rutecki, P., Sheth, R., Ruggles, K., Wendt, G., O'Leary, D., & Magnotta, V. (2002). The Neurodevelopmental Impact of Childhood-onset Temporal Lobe Epilepsy on Brain Structure and Function. *Epilepsia*, *43*(9), 1062–1071. https://doi.org/10.1046/j.1528-1157.2002.49901.x

Hermann, B., Seidenberg, M., Lee, E.-J., Chan, F., & Rutecki, P. (2007). Cognitive phenotypes in temporal lobe epilepsy. *Journal of the International Neuropsychological Society*, *13*(01). https://doi.org/10.1017/S135561770707004X

Hibar, D. P., Westlye, L. T., Doan, N. T., Jahanshad, N., Cheung, J. W., Ching, C. R. K., Versace, A., Bilderbeck, A. C., Uhlmann, A., Mwangi, B., Krämer, B., Overs, B., Hartberg, C. B., Abé, C., Dima, D., Grotegerd, D., Sprooten, E., Bøen, E., Jimenez, E., … Andreassen, O. A. (2018). Cortical abnormalities in bipolar disorder: An MRI analysis of 6503 individuals from the ENIGMA Bipolar Disorder Working Group. *Molecular Psychiatry*, *23*(4), 932–942. https://doi.org/10.1038/mp.2017.73

Hoffman, B. L., & Rasmussen, T. (1953). Stimulation studies of insular cortex of macaca mulatta. *Journal of Neurophysiology*, *16*(4), 343–351. https://doi.org/10.1152/jn.1953.16.4.343

Holland, D., Kuperman, J. M., & Dale, A. M. (2010). Efficient correction of inhomogeneous static magnetic field-induced distortion in Echo Planar Imaging. *NeuroImage*, *50*(1), 175–183. https://doi.org/10.1016/j.neuroimage.2009.11.044

Hoppe, M., Wennberg, R., Tai, P., & Pohlmann-Eden, B. (2009). EEG in Epilepsy. In A. M. Lozano, P. L. Gildenberg, & R. R. Tasker (Eds.), *Textbook of Stereotactic and Functional Neurosurgery* (pp. 2575–2585). Springer. https://doi.org/10.1007/978-3-540-69960-6_153

Horsley, J. J., Schroeder, G. M., Thomas, R. H., de Tisi, J., Vos, S. B., Winston, G. P., Duncan, J. S., Wang, Y., & Taylor, P. N. (2022). Volumetric and structural connectivity abnormalities co-localise in TLE. *NeuroImage: Clinical*, *35*, 103105. https://doi.org/10.1016/j.nicl.2022.103105

Hudson, L. P., Munoz, D. G., Miller, L., McLachlan, R. S., Girvin, J. P., & Blume, W. T. (1993). Amygdaloid sclerosis in temporal lobe epilepsy. *Annals of Neurology*, *33*(6), 622–631. https://doi.org/10.1002/ana.410330611

Iglesias, J. E., Augustinack, J. C., Nguyen, K., Player, C. M., Player, A., Wright, M., Roy, N., Frosch, M. P., McKee, A. C., Wald, L. L., Fischl, B., & Van Leemput, K. (2015). A computational atlas of the hippocampal formation using ex vivo , ultra-high resolution MRI: Application to adaptive segmentation of in vivo MRI. *NeuroImage*, *115*, 117–137. https://doi.org/10.1016/j.neuroimage.2015.04.042

Iglesias, J. E., Insausti, R., Lerma-Usabiaga, G., Bocchetta, M., Van Leemput, K., Greve, D. N., van der Kouwe, A., Fischl, B., Caballero-Gaudes, C., & Paz-Alonso, P. M. (2018). A probabilistic atlas of the human thalamic nuclei combining ex vivo MRI and histology. *ArXiv:1806.08634 [Physics, q-Bio]*. http://arxiv.org/abs/1806.08634

Iglesias, J. E., Van Leemput, K., Bhatt, P., Casillas, C., Dutt, S., Schuff, N., Truran-Sacrey, D., Boxer, A., & Fischl, B. (2015). Bayesian segmentation of brainstem structures in MRI. *NeuroImage*, *113*, 184–195. https://doi.org/10.1016/j.neuroimage.2015.02.065

Jacobs, R. H. A. H., Renken, R., Aleman, A., & Cornelissen, F. W. (2012). The amygdala, top-down effects, and selective attention to features. *Neuroscience & Biobehavioral Reviews*, *36*(9), 2069–2084. https://doi.org/10.1016/j.neubiorev.2012.05.011

Janak, P. H., & Tye, K. M. (2015). From circuits to behaviour in the amygdala. *Nature*, *517*(7534), 284–292. https://doi.org/10.1038/nature14188

Janszky, J. (2004). Temporal lobe epilepsy with hippocampal sclerosis: Predictors for long-term surgical outcome. *Brain*, *128*(2), 395–404. https://doi.org/10.1093/brain/awh358

Janszky, J., Janszky, I., & Ebner, A. (2004). Age at onset in mesial temporal lobe epilepsy with a history of febrile seizures. *Neurology*, *63*(7), 1296–1298. https://doi.org/10.1212/01.WNL.0000140701.40447.88

Johnson, W. E., Li, C., & Rabinovic, A. (2007). Adjusting batch effects in microarray expression data using empirical Bayes methods. *Biostatistics*, *8*(1), 118–127. https://doi.org/10.1093/biostatistics/kxj037

Jovicich, J., Czanner, S., Greve, D., Haley, E., van der Kouwe, A., Gollub, R., Kennedy, D., Schmitt, F., Brown, G., Macfall, J., Fischl, B., & Dale, A. (2006). Reliability in multi-site structural MRI studies: Effects of gradient non-linearity correction on phantom and human data. *NeuroImage*, *30*(2), 436–443. https://doi.org/10.1016/j.neuroimage.2005.09.046

Kaada, B. R., Pribram, K. H., & Epstein, J. A. (1949). Respiratory and vascular responses in monkeys from temporal pole, insula, orbital surface and cingulate gyrus: A preliminary report. *Journal of Neurophysiology*, *12*(5), 347–356. https://doi.org/10.1152/jn.1949.12.5.347

Kaestner, E., Reyes, A., Chen, A., Rao, J., Macari, A. C., Choi, J. Y., Qiu, D., Hewitt, K., Wang, Z. I., Drane, D. L., Hermann, B., Busch, R. M., Punia, V., McDonald, C. R., & Alzheimer's Disease Neuroimaging Initiative. (2021). Atrophy and cognitive profiles in older adults with temporal lobe epilepsy are similar to mild cognitive impairment. *Brain: A Journal of Neurology*, *144*(1), 236–250. https://doi.org/10.1093/brain/awaa397

Kaestner, E., Reyes, A., Macari, A. C., Chang, Y., Paul, B. M., Hermann, B. P., & McDonald, C. R. (2019). Identifying the neural basis of a language-impaired phenotype of temporal lobe epilepsy. *Epilepsia*, *60*(8), 1627–1638. https://doi.org/10.1111/epi.16283

Kanth, K., Park, K., & Seyal, M. (2020). Severity of Peri-ictal Respiratory Dysfunction With Epilepsy Duration and Patient Age at Epilepsy Onset. *Frontiers in Neurology*, *11*, 618841. https://doi.org/10.3389/fneur.2020.618841

Kara, S., Yazici, K. M., Güleç, C., & Unsal, I. (2000). Mixed anxiety-depressive disorder and major depressive disorder: Comparison of the severity of illness and biological variables. *Psychiatry Research*, *94*(1), 59–66. https://doi.org/10.1016/s0165-1781(00)00131-1

Keller, S. S., Ahrens, T., Mohammadi, S., Möddel, G., Kugel, H., Ringelstein, E. B., & Deppe, M. (2011). Microstructural and volumetric abnormalities of the putamen in juvenile myoclonic epilepsy. *Epilepsia*, *52*(9), 1715–1724. https://doi.org/10.1111/j.1528-1167.2011.03117.x

Keller, S. S., O'Muircheartaigh, J., Traynor, C., Towgood, K., Barker, G. J., & Richardson, M. P. (2014). Thalamotemporal impairment in temporal lobe epilepsy: A combined MRI analysis of structure, integrity, and connectivity. *Epilepsia*, *55*(2), 306–315. https://doi.org/10.1111/epi.12520

Keller, S. S., Richardson, M. P., Schoene-Bake, J.-C., O'Muircheartaigh, J., Elkommos, S., Kreilkamp, B., Goh, Y. Y., Marson, A. G., Elger, C., & Weber, B. (2015). Thalamotemporal alteration and postoperative seizures in temporal lobe epilepsy. *Annals of Neurology*, *77*(5), 760–774. https://doi.org/10.1002/ana.24376

Keller, S. S., & Roberts, N. (2008). Voxel-based morphometry of temporal lobe epilepsy: An introduction and review of the literature. *Epilepsia*, *49*(5), 741–757. https://doi.org/10.1111/j.1528-1167.2007.01485.x

Kerestes, R., Chase, H. W., Phillips, M. L., Ladouceur, C. D., & Eickhoff, S. B. (2017). Multimodal evaluation of the amygdala's functional connectivity. *NeuroImage*, *148*, 219–229. https://doi.org/10.1016/j.neuroimage.2016.12.023

Kim, D. W., Lee, S. K., Chung, C. K., Koh, Y.-C., Choe, G., & Lim, S. D. (2012). Clinical features and pathological characteristics of amygdala enlargement in mesial temporal lobe epilepsy. *Journal of Clinical Neuroscience*, *19*(4), 509–512. https://doi.org/10.1016/j.jocn.2011.05.042

Kullmann, D. M. (2011). What's wrong with the amygdala in temporal lobe epilepsy? *Brain*, *134*(10), 2800–2801. https://doi.org/10.1093/brain/awr246

Kurth, F., Luders, E., & Gaser, C. (2015). Voxel-Based Morphometry. In A. W. Toga (Ed.), *Brain Mapping* (pp. 345–349). Academic Press. https://doi.org/10.1016/B978-0-12-397025-1.00304-3

Kwan, P., Arzimanoglou, A., Berg, A. T., Brodie, M. J., Allen Hauser, W., Mathern, G., Moshé, S. L., Perucca, E., Wiebe, S., & French, J. (2010). Definition of drug resistant epilepsy: Consensus proposal by the ad hoc Task Force of the ILAE Commission on Therapeutic Strategies. *Epilepsia*, *51*(6), 1069–1077. https://doi.org/10.1111/j.1528-1167.2009.02397.x

Labate, A., Cerasa, A., Aguglia, U., Mumoli, L., Quattrone, A., & Gambardella, A. (2011). Neocortical thinning in "benign" mesial temporal lobe epilepsy. *Epilepsia*, *52*(4), 712–717. https://doi.org/10.1111/j.1528-1167.2011.03038.x

Labate, A., Cherubini, A., Tripepi, G., Mumoli, L., Ferlazzo, E., Aguglia, U., Quattrone, A., & Gambardella, A. (2015). White matter abnormalities differentiate severe from benign temporal lobe epilepsy. *Epilepsia*, *56*(7), 1109–1116. https://doi.org/10.1111/epi.13027

Lacuey, N., Hampson, J. P., Harper, R. M., Miller, J. P., & Lhatoo, S. (2019). Limbic and paralimbic structures driving ictal central apnea. *Neurology*, *92*(7), e655–e669. https://doi.org/10.1212/WNL.0000000000006920

Lacuey, N., Zonjy, B., Hampson, J. P., Rani, M. R. S., Zaremba, A., Sainju, R. K., Gehlbach, B. K., Schuele, S., Friedman, D., Devinsky, O., Nei, M., Harper, R. M., Allen, L., Diehl, B., Millichap, J. J., Bateman, L., Granner, M. A., Dragon, D. N., Richerson, G. B., & Lhatoo, S. D. (2018). The incidence and significance of periictal apnea in epileptic seizures. *Epilepsia*, *59*(3), 573–582. https://doi.org/10.1111/epi.14006

Larivière, S., Federico, P., Chinvarun, Y., Jackson, G., Morgan, V., Rampp, S., Vaudano, A. E., Wang, I., Cendes, F., Boelman, C. G., Bernasconi, A., Bernasconi, N., Bernhardt, B. C., & Schrader, D. V. (2021). ILAE Neuroimaging Task Force Highlight: Harnessing optimized imaging protocols for drug-resistant childhood epilepsy. *Epileptic Disorders*, *23*(5), 675–681. https://doi.org/10.1684/epd.2021.1312

Larivière, S., Paquola, C., Park, B., Royer, J., Wang, Y., Benkarim, O., Vos de Wael, R., Valk, S. L., Thomopoulos, S. I., Kirschner, M., Lewis, L. B., Evans, A. C., Sisodiya, S. M., McDonald, C. R., Thompson, P. M., & Bernhardt, B. C. (2021). The ENIGMA Toolbox: Multiscale neural contextualization of multisite neuroimaging datasets. *Nature Methods*, *18*(7), Article 7. https://doi.org/10.1038/s41592-021-01186-4

Larivière, S., Rodríguez-Cruces, R., Royer, J., Caligiuri, M. E., Gambardella, A., Concha, L., Keller, S. S., Cendes, F., Yasuda, C., Bonilha, L., Gleichgerrcht, E., Focke, N. K., Domin, M., von Podewills, F., Langner, S., Rummel, C., Wiest, R., Martin, P., Kotikalapudi, R., … Bernhardt, B. C. (2020). Network-based atrophy modeling in the common epilepsies: A worldwide ENIGMA study. *Science Advances*, *6*(47), eabc6457. https://doi.org/10.1126/sciadv.abc6457

Larivière, S., Royer, J., Rodríguez-Cruces, R., Paquola, C., Caligiuri, M. E., Gambardella, A., Concha, L., Keller, S. S., Cendes, F., Yasuda, C. L., Bonilha, L., Gleichgerrcht, E., Focke, N. K., Domin, M., von Podewills, F., Langner, S., Rummel, C., Wiest, R., Martin, P., … Bernhardt, B. C. (2022). Structural network alterations in focal and generalized epilepsy assessed in a worldwide ENIGMA study follow axes of epilepsy risk gene expression. *Nature Communications*, *13*(1), 4320. https://doi.org/10.1038/s41467-022-31730-5

Lebel, C., Gee, M., Camicioli, R., Wieler, M., Martin, W., & Beaulieu, C. (2012). Diffusion tensor imaging of white matter tract evolution over the lifespan. *NeuroImage*, *60*(1), 340–352. https://doi.org/10.1016/j.neuroimage.2011.11.094

LeDoux, J. (2007). The amygdala. *Current Biology: CB*, *17*(20), R868-874. https://doi.org/10.1016/j.cub.2007.08.005

Lee, C.-Y., Tabesh, A., Spampinato, M. V., Helpern, J. A., Jensen, J. H., & Bonilha, L. (2014). Diffusional kurtosis imaging reveals a distinctive pattern of microstructural alternations in idiopathic generalized epilepsy. *Acta Neurologica Scandinavica*, *130*(3), 148–155. https://doi.org/10.1111/ane.12257

Lee, H.-J., Seo, S. A., & Park, K. M. (2020). Quantification of thalamic nuclei in patients diagnosed with temporal lobe epilepsy and hippocampal sclerosis. *Neuroradiology*, *62*(2), 185–195. https://doi.org/10.1007/s00234-019-02299-6

Liu, M., Bernhardt, B. C., Hong, S.-J., Caldairou, B., Bernasconi, A., & Bernasconi, N. (2016). The superficial white matter in temporal lobe epilepsy: A key link between structural and functional network disruptions. *Brain*, *139*(9), 2431–2440. https://doi.org/10.1093/brain/aww167

Liu, M., Chen, Z., Beaulieu, C., & Gross, D. W. (2014). Disrupted anatomic white matter network in left mesial temporal lobe epilepsy. *Epilepsia*, *55*(5), 674–682. https://doi.org/10.1111/epi.12581

Luna-Munguia, H., Marquez-Bravo, L., & Concha, L. (2021). Longitudinal changes in gray and white matter microstructure during epileptogenesis in pilocarpine-induced epileptic rats. *Seizure*, *90*, 130–140. https://doi.org/10.1016/j.seizure.2021.02.011

Lv, R.-J., Sun, Z.-R., Cui, T., Guan, H.-Z., Ren, H.-T., & Shao, X.-Q. (2014). Temporal lobe epilepsy with amygdala enlargement: A subtype of temporal lobe epilepsy. *BMC Neurology*, *14*(1), 194. https://doi.org/10.1186/s12883-014-0194-z

Mariajoseph, F. P., Muthusamy, S., Amukotuwa, S., & Seneviratne, U. (2021). Seizure-induced reversible MRI abnormalities in patients with single seizures: A systematic review. *Epileptic Disorders: International Epilepsy Journal with Videotape*, *23*(4), 552–562. https://doi.org/10.1684/epd.2021.1300

McDonald, A. J. (1998). Cortical pathways to the mammalian amygdala. *Progress in Neurobiology*, *55*(3), 257–332. https://doi.org/10.1016/s0301-0082(98)00003-3

McDonald, C. R., Ahmadi, M. E., Hagler, D. J., Tecoma, E. S., Iragui, V. J., Gharapetian, L., Dale, A. M., & Halgren, E. (2008). Diffusion tensor imaging correlates of memory and language impairments in temporal lobe epilepsy. *Neurology*, *71*(23), 1869–1876. https://doi.org/10.1212/01.wnl.0000327824.05348.3b

McDonald, C. R., Hagler, D. J., Ahmadi, M. E., Tecoma, E., Iragui, V., Gharapetian, L., Dale, A. M., & Halgren, E. (2008). Regional neocortical thinning in mesial temporal lobe epilepsy. *Epilepsia*, *49*(5), 794–803. https://doi.org/10.1111/j.1528-1167.2008.01539.x

McDonald, C. R., Leyden, K. M., Hagler, D. J., Kucukboyaci, N. E., Kemmotsu, N., Tecoma, E. S., & Iragui, V. J. (2014). White matter microstructure complements morphometry for predicting verbal memory in epilepsy. *Cortex*, *58*, 139–150. https://doi.org/10.1016/j.cortex.2014.05.014

Mechelli, A., Price, C., Friston, K., & Ashburner, J. (2005). Voxel-Based Morphometry of the Human Brain: Methods and Applications. *Current Medical Imaging Reviews*, *1*(2), 105–113. https://doi.org/10.2174/1573405054038726

Meletti, S., Benuzzi, F., Rubboli, G., Cantalupo, G., Stanzani Maserati, M., Nichelli, P., & Tassinari, C. A. (2003). Impaired facial emotion recognition in early-onset right mesial temporal lobe epilepsy. *Neurology*, *60*(3), 426–431. https://doi.org/10.1212/wnl.60.3.426

Memarian, N., Thompson, P. M., Engel, J., & Staba, R. J. (2013). Quantitative analysis of structural neuroimaging of mesial temporal lobe epilepsy. *Imaging in Medicine*, *5*(3), 219–235. https://doi.org/10.2217/iim.13.28

Micalizzi, E., Vaudano, A. E., Ballerini, A., Talami, F., Giovannini, G., Turchi, G., Cioclu, M. C., Giunta, L., & Meletti, S. (2022). Ictal apnea: A prospective monocentric study in patients with epilepsy. *European Journal of Neurology*, *29*(12), 3701–3710. https://doi.org/10.1111/ene.15547

Micalizzi, E., Vaudano, A. E., Giovannini, G., Turchi, G., Giunta, L., & Meletti, S. (2021). Case Report: Ictal Central Apnea as First and Overlooked Symptom in Temporal Lobe Seizures. *Frontiers in Neurology*, *12*, 753860. https://doi.org/10.3389/fneur.2021.753860

Michelucci, R., Pasini, E., & Nobile, C. (2009). Lateral temporal lobe epilepsies: Clinical and genetic features. *Epilepsia*, *50*(s5), 52–54. https://doi.org/10.1111/j.1528-1167.2009.02122.x

Mills, K. L., & Tamnes, C. K. (2014). Methods and considerations for longitudinal structural brain imaging analysis across development. *Developmental Cognitive Neuroscience*, *9*, 172–190. https://doi.org/10.1016/j.dcn.2014.04.004

Minami, N., Morino, M., Uda, T., Komori, T., Nakata, Y., Arai, N., Kohmura, E., & Nakano, I. (2015). Surgery for amygdala enlargement with mesial temporal lobe epilepsy: Pathological findings and seizure outcome. *Journal of Neurology, Neurosurgery, and Psychiatry*, *86*(8), 887–894. https://doi.org/10.1136/jnnp-2014-308383

Mitsueda-Ono, T., Ikeda, A., Inouchi, M., Takaya, S., Matsumoto, R., Hanakawa, T., Sawamoto, N., Mikuni, N., Fukuyama, H., & Takahashi, R. (2011). Amygdalar enlargement in patients with temporal lobe epilepsy. *Journal of Neurology, Neurosurgery, and Psychiatry*, *82*(6), 652–657. https://doi.org/10.1136/jnnp.2010.206342

Monti, G., & Meletti, S. (2015). Emotion recognition in temporal lobe epilepsy: A systematic review. *Neuroscience and Biobehavioral Reviews*, *55*, 280–293. https://doi.org/10.1016/j.neubiorev.2015.05.009

Morita-Sherman, M., Li, M., Joseph, B., Yasuda, C., Vegh, D., De Campos, B. M., Alvim, M. K. M., Louis, S., Bingaman, W., Najm, I., Jones, S., Wang, X., Blümcke, I., Brinkmann, B. H., Worrell, G., Cendes, F., & Jehi, L. (2021). Incorporation of quantitative MRI in a model to predict temporal lobe epilepsy surgery outcome. *Brain Communications*, *3*(3), fcab164. https://doi.org/10.1093/braincomms/fcab164

Mueller, S., Laxer, K., Barakos, J., Ian, C., Garcia, P., & Weiner, M. (2009). Widespread Neocortical Abnormalities in Temporal Lobe Epilepsy With And Without Mesial Sclerosis. *NeuroImage*, *46*(2), 353–359. https://doi.org/10.1016/j.neuroimage.2009.02.020

Na, H. K., Lee, H., Hong, S., Lee, D. H., Kim, K. M., Lee, H. W., Heo, K., & Cho, K. H. (2020). Volume change in amygdala enlargement as a prognostic factor in patients with temporal lobe epilepsy: A longitudinal study. *Epilepsia*, *61*(1), 70–80. https://doi.org/10.1111/epi.16400

Nagy, S. A., Horváth, R., Perlaki, G., Orsi, G., Barsi, P., John, F., Horváth, A., Kovács, N., Bogner, P., Ábrahám, H., Bóné, B., Gyimesi, C., Dóczi, T., & Janszky, J. (2016). Age at onset and seizure frequency affect white matter diffusion

coefficient in patients with mesial temporal lobe epilepsy. *Epilepsy & Behavior*, *61*, 14–20. https://doi.org/10.1016/j.yebeh.2016.04.019

Nelson, D. A., & Ray, C. D. (1968). Respiratory Arrest From Seizure Discharges in Limbic System: Report of Cases. *Archives of Neurology*, *19*(2), 199–207. https://doi.org/10.1001/archneur.1968.00480020085008

Nickels, K. C., Zaccariello, M. J., Hamiwka, L. D., & Wirrell, E. C. (2016). Cognitive and neurodevelopmental comorbidities in paediatric epilepsy. *Nature Reviews. Neurology*, *12*(8), 465–476. https://doi.org/10.1038/nrneurol.2016.98

Nobis, W. P., González Otárula, K. A., Templer, J. W., Gerard, E. E., VanHaerents, S., Lane, G., Zhou, G., Rosenow, J. M., Zelano, C., & Schuele, S. (2020). The effect of seizure spread to the amygdala on respiration and onset of ictal central apnea. *Journal of Neurosurgery*, *132*(5), 1313–1323. https://doi.org/10.3171/2019.1.JNS183157

Nobis, W. P., Schuele, S., Templer, J. W., Zhou, G., Lane, G., Rosenow, J. M., & Zelano, C. (2018). Amygdala-stimulation-induced apnea is attention and nasal-breathing dependent: Amygdala Stimulation and Breathing. *Annals of Neurology*, *83*(3), 460–471. https://doi.org/10.1002/ana.25178

Noto, T., Zhou, G., Yang, Q., Lane, G., & Zelano, C. (2021). Human Primary Olfactory Amygdala Subregions Form Distinct Functional Networks, Suggesting Distinct Olfactory Functions. *Frontiers in Systems Neuroscience*, *15*. https://www.frontiersin.org/articles/10.3389/fnsys.2021.752320

O'Donnell, L. J., & Westin, C.-F. (2011). An Introduction to Diffusion Tensor Image Analysis. *Neurosurgery Clinics of North America*, *22*(2), 185–196. https://doi.org/10.1016/j.nec.2010.12.004

O'Muircheartaigh, J., Vollmar, C., Barker, G. J., Kumari, V., Symms, M. R., Thompson, P., Duncan, J. S., Koepp, M. J., & Richardson, M. P. (2011). Focal structural changes and cognitive dysfunction in juvenile myoclonic epilepsy. *Neurology*, *76*(1), 34–40. https://doi.org/10.1212/WNL.0b013e318203e93d

Ono, S. E., Mader-Joaquim, M. J., de Carvalho Neto, A., de Paola, L., dos Santos, G. R., & Silvado, C. E. S. (2021). Relationship between hippocampal subfields and Verbal and Visual memory function in Mesial Temporal Lobe Epilepsy patients. *Epilepsy Research*, *175*, 106700. https://doi.org/10.1016/j.eplepsyres.2021.106700

Overvliet, G. M., Besseling, R. M. H., Jansen, J. F. A., van der Kruijs, S. J. M., Vles, J. S. H., Hofman, P. A. M., Ebus, S. C. M., de Louw, A., Aldenkamp, A. P., & Backes, W. H. (2013). Early onset of cortical thinning in children with rolandic epilepsy. *NeuroImage: Clinical*, *2*, 434–439. https://doi.org/10.1016/j.nicl.2013.03.008

Paré, D. (2003). Role of the basolateral amygdala in memory consolidation. *Progress in Neurobiology*, *70*(5), 409–420. https://doi.org/10.1016/s0301-0082(03)00104-7

Park, B., Larivière, S., Rodríguez-Cruces, R., Royer, J., Tavakol, S., Wang, Y., Caciagli, L., Caligiuri, M. E., Gambardella, A., Concha, L., Keller, S. S., Cendes, F., Alvim, M. K. M., Yasuda, C., Bonilha, L., Gleichgerrcht, E., Focke, N. K., Kreilkamp, B. A. K., Domin, M., … Bernhardt, B. C. (2022). Topographic divergence of atypical cortical asymmetry and atrophy patterns in temporal lobe epilepsy. *Brain*, *145*(4), 1285–1298. https://doi.org/10.1093/brain/awab417

Park, K. M., Kim, T. H., Mun, C. W., Shin, K. J., Ha, S. Y., Park, J., Lee, B. I., Lee, H.-J., & Kim, S. E. (2018). Reduction of ipsilateral thalamic volume in temporal lobe epilepsy with hippocampal sclerosis. *Journal of Clinical Neuroscience*, *55*, 76–81. https://doi.org/10.1016/j.jocn.2018.06.025

Peedicail, J. S., Sandy, S., Singh, S., Hader, W., Myles, T., Scott, J., Wiebe, S., & Pillay, N. (2020). Long term sequelae of amygdala enlargement in temporal lobe epilepsy. *Seizure*, *74*, 33–40. https://doi.org/10.1016/j.seizure.2019.11.015

Penfield, W., & Jasper, H. H. (1954). *Epilepsy and the functional anatomy of the human brain* ([1st ed.]). Little, Brown.

Petrulis, A. (2020). Chapter 2—Structure and function of the medial amygdala. In *Handb. Amygdala Struct. Funct.* (Vol. 29, pp. 39–61).

Piazzini, A., Turner, K., Chifari, R., Morabito, A., Canger, R., & Canevini, M. P. (2006). Attention and psychomotor speed decline in patients with temporal lobe epilepsy: A longitudinal study. *Epilepsy Research*, *72*(2–3), 89–96. https://doi.org/10.1016/j.eplepsyres.2006.04.004

Pillai, J., & Sperling, M. R. (2006). Interictal EEG and the Diagnosis of Epilepsy. *Epilepsia*, *47*(s1), 14–22. https://doi.org/10.1111/j.1528-1167.2006.00654.x

Pitkänen, A., Löscher, W., Vezzani, A., Becker, A. J., Simonato, M., Lukasiuk, K., Gröhn, O., Bankstahl, J. P., Friedman, A., Aronica, E., Gorter, J. A., Ravizza, T., Sisodiya, S. M., Kokaia, M., & Beck, H. (2016). Advances in the development of biomarkers for epilepsy. *The Lancet. Neurology*, *15*(8), 843–856. https://doi.org/10.1016/S1474-4422(16)00112-5

Price, J. L., Russchen, F. T., & Amaral, D. G. (1987). *The limbic region. II: The amygdaloid complex*. (Elsevier Sci.).

Querol Pascual, M. R. (2007). Temporal Lobe Epilepsy: Clinical Semiology and Neurophysiological Studies. *Seminars in Ultrasound, CT and MRI*, *28*(6), 416–423. https://doi.org/10.1053/j.sult.2007.09.004

Rados, M., Mouthaan, B., Barsi, P., Carmichael, D., Heckemann, R. A., Kelemen, A., Kobulashvili, T., Kuchukhidze, G., Marusic, P., Minkin, K., Tisdall, M., Trinka, E., Veersema, T., Vos, S. B., Wagner, J., Braun, K., & van Eijsden,

P. (2022). Diagnostic value of MRI in the presurgical evaluation of patients with epilepsy: Influence of field strength and sequence selection: a systematic review and meta-analysis from the E-PILEPSY Consortium. *Epileptic Disorders*, *24*(2), 323–342. https://doi.org/10.1684/epd.2021.1399

Rebsamen, M., Suter, Y., Wiest, R., Reyes, M., & Rummel, C. (2020). Brain Morphometry Estimation: From Hours to Seconds Using Deep Learning. *Frontiers in Neurology*, *11*. https://www.frontiersin.org/articles/10.3389/fneur.2020.00244

Redolfi, A., Manset, D., Barkhof, F., Wahlund, L.-O., Glatard, T., Mangin, J.-F., Frisoni, G. B., & neuGRID Consortium, for the A. D. N. I. (2015). Head-to-Head Comparison of Two Popular Cortical Thickness Extraction Algorithms: A Cross-Sectional and Longitudinal Study. *PLOS ONE*, *10*(3), e0117692. https://doi.org/10.1371/journal.pone.0117692

Reyes, A., Kaestner, E., Bahrami, N., Balachandra, A., Hegde, M., Paul, B. M., Hermann, B., & McDonald, C. R. (2019). Cognitive phenotypes in temporal lobe epilepsy are associated with distinct patterns of white matter network abnormalities. *Neurology*, *92*(17), e1957–e1968. https://doi.org/10.1212/WNL.0000000000007370

Reyes, A., Kaestner, E., Ferguson, L., Jones, J. E., Seidenberg, M., Barr, W. B., Busch, R. M., Hermann, B. P., & McDonald, C. R. (2020). Cognitive phenotypes in temporal lobe epilepsy utilizing data- and clinically driven approaches: Moving toward a new taxonomy. *Epilepsia*, *61*(6), 1211–1220. https://doi.org/10.1111/epi.16528

Reyes, A., Thesen, T., Kuzniecky, R., Devinsky, O., McDonald, C. R., Jackson, G. D., Vaughan, D. N., & Blackmon, K. (2017). Amygdala enlargement: Temporal lobe epilepsy subtype or nonspecific finding? *Epilepsy Research*, *132*, 34–40. https://doi.org/10.1016/j.eplepsyres.2017.02.019

Riederer, F., Seiger, R., Lanzenberger, R., Pataraia, E., Kasprian, G., Michels, L., Kollias, S., Czech, T., Hainfellner, J. A., Beiersdorf, J., & Baumgartner, C. (2021). Automated volumetry of hippocampal subfields in temporal lobe epilepsy. *Epilepsy Research*, *175*, 106692. https://doi.org/10.1016/j.eplepsyres.2021.106692

Righart, R., Schmidt, P., Dahnke, R., Biberacher, V., Beer, A., Buck, D., Hemmer, B., Kirschke, J. S., Zimmer, C., Gaser, C., & Mühlau, M. (2017). Volume versus surface-based cortical thickness measurements: A comparative study with healthy controls and multiple sclerosis patients. *PLOS ONE*, *12*(7), e0179590. https://doi.org/10.1371/journal.pone.0179590

Roch, C., Leroy, C., Nehlig, A., & Namer, I. J. (2002a). Magnetic Resonance Imaging in the Study of the Lithium–Pilocarpine Model of Temporal Lobe Epilepsy in Adult Rats. *Epilepsia*, *43*(4), 325–335. https://doi.org/10.1046/j.1528-1157.2002.11301.x

Roch, C., Leroy, C., Nehlig, A., & Namer, I. J. (2002b). Predictive Value of Cortical Injury for the Development of Temporal Lobe Epilepsy in 21-day-old Rats: An MRI Approach Using the Lithium-pilocarpine Model. *Epilepsia*, *43*(10), 1129–1136. https://doi.org/10.1046/j.1528-1157.2002.17802.x

Ronan, L., Alhusaini, S., Scanlon, C., Doherty, C. P., Delanty, N., & Fitzsimons, M. (2012). *Widespread cortical morphologic changes in juvenile myoclonic epilepsy: Evidence from structural MRI.* https://www.lenus.ie/handle/10147/224920

Rosenberg, D. S., Mauguière, F., Catenoix, H., Faillenot, I., & Magnin, M. (2009). Reciprocal thalamocortical connectivity of the medial pulvinar: A depth stimulation and evoked potential study in human brain. *Cerebral Cortex (New York, N.Y.: 1991)*, *19*(6), 1462–1473. https://doi.org/10.1093/cercor/bhn185

Rosenberg, D. S., Mauguière, F., Demarquay, G., Ryvlin, P., Isnard, J., Fischer, C., Guénot, M., & Magnin, M. (2006). Involvement of Medial Pulvinar Thalamic Nucleus in Human Temporal Lobe Seizures. *Epilepsia*, *47*(1), 98–107. https://doi.org/10.1111/j.1528-1167.2006.00375.x

Rudzinski, L. A., & Meador, K. J. (2013). Epilepsy and Neuropsychological Comorbidities: *CONTINUUM: Lifelong Learning in Neurology*, *19*, 682–696. https://doi.org/10.1212/01.CON.0000431382.06438.cd

Ryvlin, P., Nashef, L., Lhatoo, S. D., Bateman, L. M., Bird, J., Bleasel, A., Boon, P., Crespel, A., Dworetzky, B. A., Høgenhaven, H., Lerche, H., Maillard, L., Malter, M. P., Marchal, C., Murthy, J. M., Nitsche, M., Pataraia, E., Rabben, T., Rheims, S., … Tomson, T. (2013). Incidence and mechanisms of cardiorespiratory arrests in epilepsy monitoring units (MORTEMUS): A retrospective study. *The Lancet Neurology*, *12*(10), 966–977. https://doi.org/10.1016/S1474-4422(13)70214-X

Sadler, R. M. (2006). The syndrome of mesial temporal lobe epilepsy with hippocampal sclerosis: Clinical features and differential diagnosis. *Advances in Neurology*, *97*, 27–37.

Sah, P., Faber, E. S. L., Lopez De Armentia, M., & Power, J. (2003). The Amygdaloid Complex: Anatomy and Physiology. *Physiological Reviews*, *83*(3), 803–834. https://doi.org/10.1152/physrev.00002.2003

Saling, M. M. (2009). Verbal memory in mesial temporal lobe epilepsy: Beyond material specificity. *Brain*, *132*(3), 570–582. https://doi.org/10.1093/brain/awp012

Saygin, Z. M., Kliemann, D., Iglesias, J. E., van der Kouwe, A. J. W., Boyd, E., Reuter, M., Stevens, A., Van Leemput, K., McKee, A., Frosch, M. P., Fischl, B., & Augustinack, J. C. (2017). High-resolution magnetic resonance imaging reveals nuclei of the human amygdala: Manual segmentation to automatic atlas. *NeuroImage*, *155*, 370–382. https://doi.org/10.1016/j.neuroimage.2017.04.046

Scheffer, I. E., Berkovic, S., Capovilla, G., Connolly, M. B., French, J., Guilhoto, L., Hirsch, E., Jain, S., Mathern, G. W., Moshé, S. L., Nordli, D. R., Perucca, E., Tomson, T., Wiebe, S., Zhang, Y.-H., & Zuberi, S. M. (2017). ILAE classification of the epilepsies: Position paper of the ILAE Commission for Classification and Terminology. *Epilepsia*, *58*(4), 512–521. https://doi.org/10.1111/epi.13709

Schilling, K. G., Archer, D., Rheault, F., Lyu, I., Huo, Y., Cai, L. Y., Bunge, S. A., Weiner, K. S., Gore, J. C., Anderson, A. W., & Landman, B. A. (2022). Superficial white matter across the lifespan: Volume, thickness, change, and relationship with cortical features. *BioRxiv*, 2022.07.20.500818. https://doi.org/10.1101/2022.07.20.500818

Schmaal, L., Veltman, D. J., van Erp, T. G. M., Sämann, P. G., Frodl, T., Jahanshad, N., Loehrer, E., Tiemeier, H., Hofman, A., Niessen, W. J., Vernooij, M. W., Ikram, M. A., Wittfeld, K., Grabe, H. J., Block, A., Hegenscheid, K., Völzke, H., Hoehn, D., Czisch, M., … Hibar, D. P. (2016). Subcortical brain alterations in major depressive disorder: Findings from the ENIGMA Major Depressive Disorder working group. *Molecular Psychiatry*, *21*(6), 806–812. https://doi.org/10.1038/mp.2015.69

Schmitz-Koep, B., Zimmermann, J., Menegaux, A., Nuttall, R., Bäuml, J. G., Schneider, S. C., Daamen, M., Boecker, H., Zimmer, C., Wolke, D., Bartmann, P., Hedderich, D. M., & Sorg, C. (2021). Within amygdala: Basolateral parts are selectively impaired in premature-born adults. *NeuroImage : Clinical*, *31*, 102780. https://doi.org/10.1016/j.nicl.2021.102780

Schuele, S. U., Afshari, M., Afshari, Z. S., Macken, M. P., Asconape, J., Wolfe, L., & Gerard, E. E. (2011). Ictal central apnea as a predictor for sudden unexpected death in epilepsy. *Epilepsy & Behavior*, *22*(2), 401–403. https://doi.org/10.1016/j.yebeh.2011.06.036

Schulz, D., & Huston, J. P. (2002). The sliding window correlation procedure for detecting hidden correlations: Existence of behavioral subgroups illustrated with aged rats. *Journal of Neuroscience Methods*, *121*(2), 129–137. https://doi.org/10.1016/S0165-0270(02)00224-8

Seguin, D., Pac, S., Wang, J., Nicolson, R., Martinez-Trujillo, J., & Duerden, E. G. (n.d.). *Amygdala subnuclei development in adolescents with autism spectrum disorder: Association with social communication and repetitive behaviors*. 11.

Shakil, S., Billings, J. C., Keilholz, S. D., & Lee, C.-H. (2018). Parametric Dependencies of Sliding Window Correlation. *IEEE Transactions on Bio-Medical Engineering*, *65*(2), 254–263. https://doi.org/10.1109/TBME.2017.2762763

Sinha, S., McGovern, R. A., & Sheth, S. A. (2015). Deep brain stimulation for severe autism: From pathophysiology to procedure. *Neurosurgical Focus*, *38*(6), E3. https://doi.org/10.3171/2015.3.FOCUS1548

Sinjab, B., Martinian, L., Sisodiya, S. M., & Thom, M. (2013). Regional thalamic neuropathology in patients with hippocampal sclerosis and epilepsy: A postmortem study. *Epilepsia*, *54*(12), 2125–2133. https://doi.org/10.1111/epi.12403

Sisodiya, S. M., Whelan, C. D., Hatton, S. N., Huynh, K., Altmann, A., Ryten, M., Vezzani, A., Caligiuri, M. E., Labate, A., Gambardella, A., Ives-Deliperi, V., Meletti, S., Munsell, B. C., Bonilha, L., Tondelli, M., Rebsamen, M., Rummel, C., Vaudano, A. E., Wiest, R., … ENIGMA Consortium Epilepsy Working Group. (2020). The ENIGMA-Epilepsy working group: Mapping disease from large data sets. *Human Brain Mapping*. https://doi.org/10.1002/hbm.25037

Slinger, G., Sinke, M. R. T., Braun, K. P. J., & Otte, W. M. (2016). White matter abnormalities at a regional and voxel level in focal and generalized epilepsy: A systematic review and meta-analysis. *NeuroImage : Clinical*, *12*, 902–909. https://doi.org/10.1016/j.nicl.2016.10.025

Smith, S. (2005). EEG in the diagnosis, classification, and management of patients with epilepsy. *Journal of Neurology, Neurosurgery, and Psychiatry*, *76*(Suppl 2), ii2–ii7. https://doi.org/10.1136/jnnp.2005.069245

Smith, S. M., Jenkinson, M., Woolrich, M. W., Beckmann, C. F., Behrens, T. E. J., Johansen-Berg, H., Bannister, P. R., De Luca, M., Drobnjak, I., Flitney, D. E., Niazy, R. K., Saunders, J., Vickers, J., Zhang, Y., De Stefano, N., Brady, J. M., & Matthews, P. M. (2004). Advances in functional and structural MR image analysis and implementation as FSL. *NeuroImage*, *23 Suppl 1*, S208-219. https://doi.org/10.1016/j.neuroimage.2004.07.051

Smith, W. K. (1945). The functional significance of the rostral cingular cortex as revealed by its responses to electrical excitation. *Journal of Neurophysiology*, *8*(4), 241–255. https://doi.org/10.1152/jn.1945.8.4.241

St. Louis, E., & Frey, L. (2016). *Electroencephalography (EEG): An Introductory Text and Atlas of Normal and Abnormal Findings in Adults, Children, and Infants*. American Epilepsy Society. https://doi.org/10.5698/978-0-9979756-0-4

Stasenko, A., Lin, C., Bonilha, L., Bernhardt, B. C., & McDonald, C. R. (2022). Neurobehavioral and Clinical Comorbidities in Epilepsy: The Role of White Matter Network Disruption. *The Neuroscientist*, 10738584221076132. https://doi.org/10.1177/10738584221076133

Stein, M., Winkler, C., Kaiser, A., & Dierks, T. (2014). Structural brain changes related to bilingualism: Does immersion make a difference? *Frontiers in Psychology*, *5*, 1116. https://doi.org/10.3389/fpsyg.2014.01116

Szaflarski, J. P., Lee, S., Allendorfer, J. B., Gaston, T. E., Knowlton, R. C., Pati, S., Ver Hoef, L. W., & Deutsch, G. (2016). White Matter Abnormalities in Patients with Treatment-Resistant Genetic Generalized Epilepsies. *Medical Science*

Monitor: International Medical Journal of Experimental and Clinical Research, *22*, 1966–1975. https://doi.org/10.12659/MSM.897002

Tatum, W. O., Rubboli, G., Kaplan, P. W., Mirsatari, S. M., Radhakrishnan, K., Gloss, D., Caboclo, L. O., Drislane, F. W., Koutroumanidis, M., Schomer, D. L., Kasteleijn-Nolst Trenite, D., Cook, M., & Beniczky, S. (2018). Clinical utility of EEG in diagnosing and monitoring epilepsy in adults. *Clinical Neurophysiology*, *129*(5), 1056–1082. https://doi.org/10.1016/j.clinph.2018.01.019

Tavakol, S., Royer, J., Lowe, A. J., Bonilha, L., Tracy, J. I., Jackson, G. D., Duncan, J. S., Bernasconi, A., Bernasconi, N., & Bernhardt, B. C. (2019). Neuroimaging and connectomics of drug-resistant epilepsy at multiple scales: From focal lesions to macroscale networks. *Epilepsia*, *60*(4), 593–604. https://doi.org/10.1111/epi.14688

Tebartz Van Elst, L., Baeumer, D., Lemieux, L., Woermann, F. G., Koepp, M., Krishnamoorthy, S., Thompson, P. J., Ebert, D., & Trimble, M. R. (2002). Amygdala pathology in psychosis of epilepsy: A magnetic resonance imaging study in patients with temporal lobe epilepsy. *Brain: A Journal of Neurology*, *125*(Pt 1), 140–149. https://doi.org/10.1093/brain/awf008

Tebartz van Elst, L., Woermann, F. G., Lemieux, L., & Trimble, M. R. (1999). Amygdala enlargement in dysthymia—A volumetric study of patients with temporal lobe epilepsy. *Biological Psychiatry*, *46*(12), 1614–1623. https://doi.org/10.1016/s0006-3223(99)00212-7

Thom, M., & Bertram, E. H. (2012a). Temporal lobe epilepsy. In *Handbook of Clinical Neurology* (Vol. 107). Elsevier. https://doi.org/10.1016/B978-0-444-52898-8.00014-8

Thom, M., & Bertram, E. H. (2012b). Temporal lobe epilepsy. In *Handbook of Clinical Neurology* (Vol. 107, pp. 225–240). Elsevier. https://doi.org/10.1016/B978-0-444-52898-8.00014-8

Thompson, P. M., Jahanshad, N., Ching, C. R. K., Salminen, L. E., Thomopoulos, S. I., Bright, J., Baune, B. T., Bertolín, S., Bralten, J., Bruin, W. B., Bülow, R., Chen, J., Chye, Y., Dannlowski, U., de Kovel, C. G. F., Donohoe, G., Eyler, L. T., Faraone, S. V., Favre, P., … for the ENIGMA Consortium. (2020). ENIGMA and global neuroscience: A decade of large-scale studies of the brain in health and disease across more than 40 countries. *Translational Psychiatry*, *10*(1), 100. https://doi.org/10.1038/s41398-020-0705-1

Tio, E., Culler, G. W., Bachman, E. M., & Schuele, S. (2020). Ictal Central Apneas in Temporal Lobe Epilepsies. *Epilepsy & Behavior: E&B*, *112*, 107434. https://doi.org/10.1016/j.yebeh.2020.107434

Urquia-Osorio, H., Pimentel-Silva, L. R., Rezende, T. J. R., Almendares-Bonilla, E., Yasuda, C. L., Concha, L., & Cendes, F. (2022). Superficial and deep white matter diffusion abnormalities in focal epilepsies. *Epilepsia*, epi.17333. https://doi.org/10.1111/epi.17333

van Vliet, E. A., Dedeurwaerdere, S., Cole, A. J., Friedman, A., Koepp, M. J., Potschka, H., Immonen, R., Pitkänen, A., & Federico, P. (2017). WONOEP appraisal: Imaging biomarkers in epilepsy. *Epilepsia*, *58*(3), 315–330. https://doi.org/10.1111/epi.13621

Vaudano, A. E., Ballerini, A., Zucchini, F., Micalizzi, E., Scolastico, S., Talami, F., Giovannini, G., Pugnaghi, M., Orlandi, N., Biagioli, N., Cioclu, M. C., Vallone, S., Genovese, M., Todeschini, A., Cavalleri, F., Malagoli, M., & Meletti, S. (2023). Impact of an optimized epilepsy surgery imaging protocol for focal epilepsy: A monocentric prospective study. *Epileptic Disorders*, epd2.20050. https://doi.org/10.1002/epd2.20050

Vaughan, D. N., Rayner, G., Tailby, C., & Jackson, G. D. (2016). MRI-negative temporal lobe epilepsy: A network disorder of neocortical connectivity. *Neurology*, *87*(18), 1934–1942. https://doi.org/10.1212/WNL.0000000000003289

Vertes, R. P., Linley, S. B., & Hoover, W. B. (2015). Limbic circuitry of the midline thalamus. *Neuroscience and Biobehavioral Reviews*, *54*, 89–107. https://doi.org/10.1016/j.neubiorev.2015.01.014

Vilella, L., Lacuey, N., Hampson, J. P., Rani, M. R. S., Loparo, K., Sainju, R. K., Friedman, D., Nei, M., Strohl, K., Allen, L., Scott, C., Gehlbach, B. K., Zonjy, B., Hupp, N. J., Zaremba, A., Shafiabadi, N., Zhao, X., Reick-Mitrisin, V., Schuele, S., … Lhatoo, S. D. (2019). Incidence, Recurrence, and Risk Factors for Peri-ictal Central Apnea and Sudden Unexpected Death in Epilepsy. *Frontiers in Neurology*, *10*, 166. https://doi.org/10.3389/fneur.2019.00166

Vinti, V., Dell'Isola, G. B., Tascini, G., Mencaroni, E., Cara, G. D., Striano, P., & Verrotti, A. (2021). Temporal Lobe Epilepsy and Psychiatric Comorbidity. *Frontiers in Neurology*, *12*, 775781. https://doi.org/10.3389/fneur.2021.775781

Vlooswijk, M. C., Jansen, J. F., de Krom, M. C., Majoie, H. M., Hofman, P. A., Backes, W. H., & Aldenkamp, A. P. (2010). Functional MRI in chronic epilepsy: Associations with cognitive impairment. *The Lancet. Neurology*, *9*(10), 1018–1027. https://doi.org/10.1016/S1474-4422(10)70180-0

Voets, N. L., Hough, M. G., Douaud, G., Matthews, P. M., James, A., Winmill, L., Webster, P., & Smith, S. (2008). Evidence for abnormalities of cortical development in adolescent-onset schizophrenia. *NeuroImage*, *43*(4), 665–675. https://doi.org/10.1016/j.neuroimage.2008.08.013

Vollmar, C., O'Muircheartaigh, J., Barker, G. J., Symms, M. R., Thompson, P., Kumari, V., Duncan, J. S., Janz, D., Richardson, M. P., & Koepp, M. J. (2011). Motor system hyperconnectivity in juvenile myoclonic epilepsy: A

cognitive functional magnetic resonance imaging study. *Brain: A Journal of Neurology*, *134*(Pt 6), 1710–1719. https://doi.org/10.1093/brain/awr098

von Lehe, M., Lutz, M., Kral, T., Schramm, J., Elger, C. E., & Clusmann, H. (2006). Correlation of health-related quality of life after surgery for mesial temporal lobe epilepsy with two seizure outcome scales. *Epilepsy & Behavior*, *9*(1), 73–82. https://doi.org/10.1016/j.yebeh.2006.03.014

von Oertzen, J. (2002). Standard magnetic resonance imaging is inadequate for patients with refractory focal epilepsy. *Journal of Neurology, Neurosurgery & Psychiatry*, *73*(6), 643–647. https://doi.org/10.1136/jnnp.73.6.643

Wandschneider, B., Koepp, M., Scott, C., Micallef, C., Balestrini, S., Sisodiya, S. M., Thom, M., Harper, R. M., Sander, J. W., Vos, S. B., Duncan, J. S., Lhatoo, S., & Diehl, B. (2015). Structural imaging biomarkers of sudden unexpected death in epilepsy. *Brain*, *138*(10), 2907–2919. https://doi.org/10.1093/brain/awv233

Wellmer, J., Quesada, C. M., Rothe, L., Elger, C. E., Bien, C. G., & Urbach, H. (2013). Proposal for a magnetic resonance imaging protocol for the detection of epileptogenic lesions at early outpatient stages. *Epilepsia*, *54*(11), 1977–1987. https://doi.org/10.1111/epi.12375

Whelan, C. D., Altmann, A., Botía, J. A., Jahanshad, N., Hibar, D. P., Absil, J., Alhusaini, S., Alvim, M. K. M., Auvinen, P., Bartolini, E., Bergo, F. P. G., Bernardes, T., Blackmon, K., Braga, B., Caligiuri, M. E., Calvo, A., Carr, S. J., Chen, J., Chen, S., … Sisodiya, S. M. (2018). Structural brain abnormalities in the common epilepsies assessed in a worldwide ENIGMA study. *Brain*, *141*(2), 391–408. https://doi.org/10.1093/brain/awx341

Wiebe, S. (2000). Epidemiology of Temporal Lobe Epilepsy. *The Canadian Journal of Neurological Sciences*, *27*(01), S6–S10. https://doi.org/10.1017/S0317167100000561

Wiebe, S., Blume, W. T., Girvin, J. P., & Eliasziw, M. (2001). A Randomized, Controlled Trial of Surgery for Temporal-Lobe Epilepsy. *New England Journal of Medicine*, *345*(5), 311–318. https://doi.org/10.1056/NEJM200108023450501

Wieser, H. G., Ortega, M., Friedman, A., & Yonekawa, Y. (2003). Long-term seizure outcomes following amygdalohippocampectomy. *Journal of Neurosurgery*, *98*(4), 751–763. https://doi.org/10.3171/jns.2003.98.4.0751

Wieser, H.-G. (2004). Mesial Temporal Lobe Epilepsy with Hippocampal Sclerosis. *Epilepsia*, *45*(6), 695–714. https://doi.org/10.1111/j.0013-9580.2004.09004.x

Winkler, A. M., Kochunov, P., Blangero, J., Almasy, L., Zilles, K., Fox, P. T., Duggirala, R., & Glahn, D. C. (2010). Cortical thickness or grey matter volume? The importance of selecting the phenotype for imaging genetics studies. *NeuroImage*, *53*(3), 1135–1146. https://doi.org/10.1016/j.neuroimage.2009.12.028

Winston, G. P., Vos, S. B., Caldairou, B., Hong, S.-J., Czech, M., Wood, T. C., Wastling, S. J., Barker, G. J., Bernhardt, B. C., Bernasconi, N., Duncan, J. S., & Bernasconi, A. (2020). Microstructural imaging in temporal lobe epilepsy: Diffusion imaging changes relate to reduced neurite density. *NeuroImage: Clinical*, *26*, 102231. https://doi.org/10.1016/j.nicl.2020.102231

Wirrell, E. C., Nabbout, R., Scheffer, I. E., Alsaadi, T., Bogacz, A., French, J. A., Hirsch, E., Jain, S., Kaneko, S., Riney, K., Samia, P., Snead, O. C., Somerville, E., Specchio, N., Trinka, E., Zuberi, S. M., Balestrini, S., Wiebe, S., Cross, J. H., … Tinuper, P. (2022). Methodology for classification and definition of epilepsy syndromes with list of syndromes: Report of the ILAE Task Force on Nosology and Definitions. *Epilepsia*, *63*(6), 1333–1348. https://doi.org/10.1111/epi.17237

Woermann, F. G., Sisodiya, S. M., Free, S. L., & Duncan, J. S. (1998). Quantitative MRI in patients with idiopathic generalized epilepsy. Evidence of widespread cerebral structural changes. *Brain: A Journal of Neurology*, *121 (Pt 9)*, 1661–1667. https://doi.org/10.1093/brain/121.9.1661

Wu, D., Chang, F., Peng, D., Xie, S., Li, X., & Zheng, W. (2020). The morphological characteristics of hippocampus and thalamus in mesial temporal lobe epilepsy. *BMC Neurology*, *20*, 235. https://doi.org/10.1186/s12883-020-01817-x

Yang, Y., & Wang, J.-Z. (2017). From Structure to Behavior in Basolateral Amygdala-Hippocampus Circuits. *Frontiers in Neural Circuits*, *11*, 86. https://doi.org/10.3389/fncir.2017.00086

Yilmazer-Hanke, D. M., Wolf, H. K., Schramm, J., Elger, C. E., Wiestler, O. D., & Blümcke, I. (2000). Subregional pathology of the amygdala complex and entorhinal region in surgical specimens from patients with pharmacoresistant temporal lobe epilepsy. *Journal of Neuropathology and Experimental Neurology*, *59*(10), 907–920. https://doi.org/10.1093/jnen/59.10.907

Yogarajah, M., Focke, N. K., Bonelli, S. B., Thompson, P., Vollmar, C., McEvoy, A. W., Alexander, D. C., Symms, M. R., Koepp, M. J., & Duncan, J. S. (2010). The structural plasticity of white matter networks following anterior temporal lobe resection. *Brain: A Journal of Neurology*, *133*(Pt 8), 2348–2364. https://doi.org/10.1093/brain/awq175

Yogarajah, M., Powell, H. W. R., Parker, G. J. M., Alexander, D. C., Thompson, P. J., Symms, M. R., Boulby, P., Wheeler-Kingshott, C. A., Barker, G. J., Koepp, M. J., & Duncan, J. S. (2008). Tractography of the parahippocampal gyrus

and material specific memory impairment in unilateral temporal lobe epilepsy. *NeuroImage*, *40*(4), 1755–1764. https://doi.org/10.1016/j.neuroimage.2007.12.046

Zhang, J.-Y., Liu, T.-H., He, Y., Pan, H.-Q., Zhang, W.-H., Yin, X.-P., Tian, X.-L., Li, B.-M., Wang, X.-D., Holmes, A., Yuan, T.-F., & Pan, B.-X. (2019). Chronic Stress Remodels Synapses in an Amygdala Circuit-Specific Manner. *Biological Psychiatry*, *85*(3), 189–201. https://doi.org/10.1016/j.biopsych.2018.06.019

Zhang, L., Hu, X., Lu, L., Li, B., Hu, X., Bu, X., Li, H., Tang, S., Gao, Y., Yang, Y., Sweeney, J. A., Gong, Q., & Huang, X. (2020). Anatomic alterations across amygdala subnuclei in medication-free patients with obsessive–compulsive disorder. *Journal of Psychiatry and Neuroscience*, *45*(5), 334–343. https://doi.org/10.1503/jpn.190114

Zheng, F., Liu, Y., Yuan, Z., Gao, X., He, Y., Liu, X., Cui, D., Qi, R., Chen, T., & Qiu, J. (2019). Age-related changes in cortical and subcortical structures of healthy adult brains: A surface-based morphometry study. *Journal of Magnetic Resonance Imaging: JMRI*, *49*(1), 152–163. https://doi.org/10.1002/jmri.26037

Zhuang, J., Hrabe, J., Kangarlu, A., Xu, D., Bansal, R., Branch, C. A., & Peterson, B. S. (2006). Correction of Eddy-Current Distortions in Diffusion Tensor Images Using the Known Directions and Strengths of Diffusion Gradients. *Journal of Magnetic Resonance Imaging : JMRI*, *24*(5), 1188–1193. https://doi.org/10.1002/jmri.20727

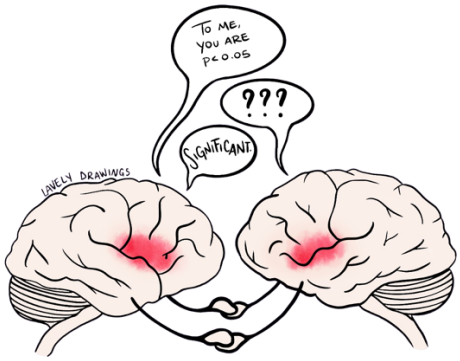

Acknowledgements

The most profound acknowledgment needs to be addressed to my mentors.
To Professor Stefano Meletti, for giving me the opportunity to start this journey, for supporting me in every decision, and for teaching me critical thinking and teamwork.
To Dr. Carrie McDonald, for welcoming me into her lab and making me feel at home from the very first day, for her constant support, and for the opportunities she gave me to grow as a researcher.
To Dr. Anna Elisabetta Vaudano, for being my guide over all these years, for her passion and commitment, for being an outstanding researcher, and a reference point for anyone lucky enough to work with her. I owe this achievement to her more than to anyone else. I owe her all my milestones, but even the dark moments because she always taught me to face them as challenges and opportunities to learn more.

This doctoral journey would not have been the same without colleagues – and friends – who made every joy even greater and could turn every setback into something to joke on. I would like to thank Dr. Simona Scolastico, Dr. Elisa Micalizzi, and Dr. Francesca Talami for walking together and supporting each other inside and outside the hospital.
Thanks to my colleagues at UCSD, for making me feel part of a great team right away. Special thanks to Dr. Erik Kaestner and Dr. Alena Stasenko. Most importantly, thanks to Dr. Donatello Arienzo; my UCSD experience wouldn't have been the same without you.

From the deepest of my heart, thanks to Dr. Jessica Sebastiani, the best roommate I could ever ask for. I will always be grateful to share my San Diego experience with you.

I would like to dedicate this thesis to my grandparents – Luciano and Natalina – because without you none of this would have been possible.

Thanks to my parents for always believing in me, even when I'm unable to do it myself. Thank you for being proud of me in every situation; I often fear that I won't be able to properly repay you for all your trust, but I hope I did it today.

Thanks to Anita, for being the best friend, sister, and supporter I could ever ask for. You know that *"there's just no one that gets me like you do"*.

Thanks to Luca, because when you met me, I wasn't the person I am today. Thank you for walking me through this journey of growth, and for helping me become the strong and independent person I am today. As always, *"when shadows try to swallow me, you're the only light I'll ever need"*.

Indeed, there would be other people to thank.

However, I would like to dedicate the end of this tiny space to someone I do not ever value enough.

I want to thank myself for getting here.

I want to thank every moment that carried me here.

Five years ago, stepping for the first time into a research lab, I was dreaming so hard to be where I am now. I never believed I could ever make it. I kept pushing and kept telling me that, at least, I had tried. So I tried, every time. And I did, every time.

Maybe that is what I do, I try.

And today I want to thank myself for never stop trying.

"No one knows what it has taken for you to arrive here. Home, with yourself.
No one knows what you have had to sacrifice or let go of for you to thrive the way you do.
No one knows the tears you have cried or the nights you have wrapped yourself in a lonely that was sometimes terrifying, sometimes comforting. Honor yourself. Honor all of your heartbreaks and all of your triumphs. Honor all of your wounds and all of your victories. Because you have carried yourself so far. Honor that."